

LE

**NASA  
Technical  
Paper  
2557**

February 1986

1253

**Low-Speed Performance  
of an Axisymmetric,  
Mixed-Compression,  
Supersonic Inlet With  
Auxiliary Inlets**

Charles J. Trefny and  
Joseph W. Wasserbauer

(NASA-TP-2557) LOW-SPEED PERFORMANCE OF AN N86-24694  
AXISYMMETRIC, MIXED-COMPRESSION, SUPERSONIC  
INLET WITH AUXILIARY INLETS (NASA) 63 p  
HC A04/MF A01 CSCL 21E Unclas  
H1/07 43068



**NASA  
Technical  
Paper  
2557**

1986

**Low-Speed Performance  
of an Axisymmetric,  
Mixed-Compression,  
Supersonic Inlet With  
Auxiliary Inlets**

Charles J. Trefny and  
Joseph W. Wasserbauer

*Lewis Research Center* ND315753  
*Cleveland, Ohio*

**NASA**

National Aeronautics  
and Space Administration

Scientific and Technical  
Information Branch



## Summary

A test program was conducted to determine the aerodynamic performance and acoustic characteristics associated with the low-speed operation of a supersonic, axisymmetric, mixed-compression inlet with auxiliary inlets. Blow-in auxiliary doors were installed on the NASA Ames "P" inlet. One door per quadrant was located on the cowl in the subsonic diffuser section of the inlet. Auxiliary inlets with areas of 20 and 40 percent of the inlet capture area were tested statically and at free-stream Mach numbers of 0.1 and 0.2. The effects of boundary layer bleed inflow were investigated. A JT8D fan simulator driven by compressed air was used to pump inlet flow and to provide a characteristic noise signature. Baseline data were obtained at static free-stream conditions with the sharp P-inlet cowl lip replaced by a blunt lip. The blunt lip prevented flow separation, thus simulating a ratio of inlet to free-stream velocity of 1.

Auxiliary inlets increased overall total pressure recovery of the order of 10 percent by reducing the Mach number at the sharp cowl lip while injecting high-pressure airflow into the duct. At ratios of cowl lip to free-stream velocity of about 1.6 or less, losses from sharp-lip flow separation were negligible at the compressor face. Losses from boundary layer bleed inflow were insignificant when either 20- or 40-percent auxiliary inlets were open.

In addition to determining the peak aerodynamic performance for each configuration, the inlet was operated with the centerbody positioned to provide high throat Mach numbers for fan noise attenuation. This operation compromised aerodynamic performance. At design airflows the maximum Mach numbers attained in the main duct were 0.68 with the 40-percent doors open and 0.96 with the 20-percent doors open. With the auxiliary doors closed, choking occurred before the design airflow was reached. The maximum Mach number with the 20-percent auxiliary doors open was obtained at the expense of a 5.5-percent loss in recovery and a 14.3-percent increase in distortion.

## Introduction

Supersonic cruise inlets generally employ sharp cowl lips, boundary layer bleed systems, and flow area contraction behind the cowl lip. These characteristics are intended to enhance the performance of the inlet system at supersonic

speeds. During low-speed, high-thrust operations such as takeoff, however, cowl lip flow separations, bleed system backflow, and a reduced capture area sized for supersonic cruise combine to degrade inlet performance to the extent that the engine may stall. Some type of auxiliary inlet system is therefore required to provide additional high-pressure flow at low aircraft speeds. This additional flow would also serve to reduce the extent of the cowl lip separation by reducing the amount of flow entering at the cowl lip station.

Acoustic analyses (refs. 1 to 3) of a supersonic cruise inlet indicate that forward-propagated fan noise is a significant component during takeoff and approach. Inlet choking techniques could be used to suppress forward-propagated fan noise at the expense of greater flow distortion. Auxiliary inlets also provide a path of noise transmission, however, and would need to be considered acoustically. Figure 1 summarizes these aerodynamic and acoustic phenomena. Variable inlet geometry can be used to relieve cowl lip flow separation by increasing the cowl lip annular area while also increasing the throat Mach number to attenuate noise. Acoustic treatment on the inlet walls could also be used to reduce the amount of noise transmission. Experimental analysis of the various aeroacoustic effects and tradeoffs is of great importance to inlet designers attempting to satisfy both aerodynamic and acoustic requirements.

Before the Supersonic Cruise Aircraft Research (SCAR) program was terminated, NASA Lewis began a project to experimentally determine the aeroacoustic performance of a representative supersonic cruise inlet. In an initial test with a supersonic cruise aircraft at ground static conditions (ref. 4), forward-propagated fan noise was significantly reduced even though the duct could not be choked. A more comprehensive test was proposed to investigate different auxiliary inlet concepts on an existing, well-instrumented, supersonic cruise inlet model. Participants in this program were NASA Lewis, NASA Langley, Boeing, Lockheed, and Douglas. Each participant (except NASA Langley) was to design, fabricate, and test a unique auxiliary inlet system. Each inlet system was to be adapted to the existing model. The model chosen as the testbed for these systems was the "P" inlet, one in a series of supersonic inlets designed at NASA Ames. The P-inlet's modular construction enables auxiliary inlet systems to be easily integrated. The inlet also incorporates centerbody and cowl boundary layer bleed systems considered representative of current supersonic transport technology. An air-driven JT8D fan simulator was chosen to pump the inlet airflow and to provide a characteristic noise signature.

Objectives of the program were to determine the effects of sharp cowl lip flow separation, bleed system reverse flow, inlet choking, and auxiliary inlet geometry and flow characteristics on the aeroacoustic performance of the inlet at speeds representative of takeoff and approach.

Testing was conducted in the NASA Lewis 9- by 15-Foot Low-Speed Anechoic Tunnel. This facility is capable of a maximum free-stream Mach number of 0.2. Figure 2 shows the model coupled to the JT8D fan simulator and mounted in the test section.

This report presents the aerodynamic results of the NASA Lewis phase of the program, previously summarized in reference 5. Extensive data are presented for each of the configurations tested. The acoustic results are summarized in reference 6.

## Symbols

$A/A_{cl}$	ratio of local area to inlet capture area
$D/H$	ratio of distance from surface to rake height
$DX/R_l$	ratio of centerbody extension to cowl lip radius
$M_{de}$	diffuser exit Mach number
$M_0$	free-stream Mach number
$N_c$	JT8D fan simulator corrected speed, percent
$R/R_l$	ratio of local radius to cowl lip radius
$P/P_{T,0}$	ratio of local total pressure to free-stream total pressure
$P_{T,2A}/P_{T,0}$	ratio of average diffuser exit total pressure to free-stream total pressure (inlet recovery)
$\frac{P_{T,2,max} - P_{T,2,min}}{P_{T,2A}}$	ratio of maximum diffuser exit probe total pressure difference to average diffuser exit total pressure
$P_{T,2,rms}/P_{T,2A}$	ratio of diffuser exit average turbulence level to average diffuser exit total pressure
$X/R_l$	ratio of distance from centerbody tip to cowl lip radius
$\alpha$	inlet angle of attack, deg

## Apparatus and Procedure

The NASA Ames P-inlet used for this investigation is an axisymmetric, mixed-compression, one-third-scale model of a representative supersonic cruise inlet. This inlet has been tested from midsubsonic to the design Mach number of 2.65. Results of these tests are reported in references 7 to 9.

Figure 3 is a cross section of the inlet model in its unmodified state. Note the multipenum bleed systems in both the centerbody and the cowl. The centerbody bleed system plenums are exhausted through slots in the centerbody support tube. These slots are placed to provide a variable bleed location depending on centerbody position. Only those plenums aligned with a slot are evacuated. Reference 8 contains a detailed description of this bleed system. Selected rows of bleed holes on both the centerbody and cowl surfaces were filled to form bleed pattern 4 of reference 8. The bleed exits, located on the outer cowl, were sealed for selected data to determine the effect of bleed system inflow on low-speed performance. Inlet area variation with centerbody position is presented in figure 4. Centerbody and cowl contour coordinates are given in tabular form (table I).

A well-instrumented JT8D fan simulator was used to pump inlet flow and to provide a source of fan noise. Reference 10 contains fan simulator design and performance details. The fan was coupled to the inlet through a transition ring. This ring was needed to match the slightly different diameters of the inlet and fan and to house the diffuser exit instrumentation described below. An inlet diffuser exit Mach number of approximately 0.6 was assumed to be the takeoff throttle condition for a typical supersonic cruise vehicle. This Mach number occurred at a JT8D fan simulator corrected speed of 80 percent. Table II correlates fan corrected speed to diffuser exit Mach number for the range of fan speeds presented in this report. A mass flowmetering device or "plug" was attached downstream of the fan to control fan pressure ratio and to keep the fan on a predetermined operating line as fan inlet total pressure (inlet recovery) varied.

The auxiliary door module used in the NASA Lewis program consisted of a cylindrical section with one auxiliary door per quadrant between the centerbody support struts. Doors were located at an axial position well downstream of the inlet throat, approximately 0.9 cowl lip radius from the compressor face. The auxiliary door assemblies eliminated ejector and overboard bypass cavities, creating a somewhat ideal flow path for the auxiliary airflow. Auxiliary doors with areas of 20 and 40 percent of the inlet capture area were tested. For configurations with closed auxiliary doors a plate was installed over each of the 40-percent doors on the outer cowl surface. Cowl and centerbody bleed systems were closed by sealing the louvered bleed exits on the outer cowl surface.

The NASA Lewis program was conducted in two phases. The phase 1 configuration, depicted in figure 5, employed a bellmouth cowl lip to eliminate sharp-cowl-lip flow separation losses and to simulate forward velocity. The auxiliary doors used with this configuration also had well-rounded corners to produce an idealized flow, providing baseline data from which real inlet effects could be evaluated. These doors provided a flow area equal to 40 percent of the inlet capture area. The inlet was also tested with the doors closed. Configurations with the centerbody and cowl bleeds both open and closed were tested with the 40-percent auxiliary doors; only the bleeds-

TABLE I.—CENTERBODY AND COWL CONTOURS

(a) Centerbody

Station $X/R_l$	$R/R_l$	Station $X/R_l$	$R/R_l$
0	0	Straight line	
.0245	.0039	(concluded)	
.0756	.0120	3.9579	0.6442
.1267	.0200	4.0090	.6464
.1778	.0282	4.0601	.6478
Straight line		4.1112	.6479
2.4765	0.3923	4.1622	.6467
2.5276	.4004	4.2133	.6444
2.5787	.4085	4.2644	.6409
2.6298	.4167	4.3155	.6367
2.6808	.4252	4.3666	.6319
2.7000	.4284	4.4177	.6269
2.7319	.4337	4.4687	.6213
2.7830	.4424	4.5198	.6159
2.8341	.4512	4.5709	.6014
2.8852	.4603	4.6220	.6051
2.9362	.4696	4.6731	.5997
2.9873	.4790	4.7242	.5943
3.0384	.4885	4.7752	.5888
3.0895	.4984	4.8263	.5823
3.1406	.5085	4.8774	.5753
3.1917	.5185	4.9285	.5675
3.2427	.5286	4.9796	.5594
3.2938	.5391	5.0306	.5507
3.3449	.5499	5.0817	.5415
3.3960	.5606	5.1328	.5317
3.4471	.5713	5.1839	.5214
3.4982	.5820	5.2350	.5101
3.5492	.5928	5.2861	.4979
3.6003	.6036	5.3371	.4844
3.6514	.6142	5.3882	.4676
3.7025	.6222	5.4393	.4474
3.7536	.6283	5.4904	.4262
3.8047	.6332	5.5415	.4061
3.8557	.6374	5.5926	.3838
3.9068	.6411	5.6436	.3627
		5.6947	.3600

(b) Cowl

Station $X/R_l$	$R/R_l$	Station $X/R_l$	$R/R_l$
2.3250	1.0000	4.3666	0.8648
2.3743	1.0013	4.4177	.8645
2.4254	1.0027	4.4687	.8645
2.4765	1.0039	4.5198	.8646
2.5276	1.0052	4.5709	.8652
2.5787	1.0063	4.6220	.8662
2.6298	1.0076	4.6730	.8672
2.6808	1.0078	4.7242	.8684
2.7319	1.0078	4.7752	.8696
2.7830	1.0078	4.8263	.8709
2.8341	1.0074	4.8774	.8722
2.8852	1.0064	4.9285	.8736
2.9362	1.0053	4.9796	.8752
2.9873	1.0037	5.0306	.8766
3.0384	1.0016	5.0817	.8782
3.0895	1.9992	5.1328	.8799
3.1406	.9962	5.1839	.8815
3.1917	.9928	5.2350	.8833
3.2427	.9889	5.2861	.8852
3.2938	.9846	5.3371	.8873
3.3449	.9797	5.3882	.8898
3.3960	.9745	5.4393	.8958
3.4471	.9687	5.4904	.9027
3.4982	.9624	5.5415	.9097
3.5492	.9556	5.5926	.9165
3.6003	.9485	5.6436	.9235
3.6514	.9413	5.6947	.9304
3.7025	.9340	5.7458	.9374
3.7536	.9266	5.7969	.9442
3.8047	.9195	5.8480	.9512
3.8557	.9120	5.8991	.9581
3.9068	.9048	5.9500	.9633
3.9579	.8973	6.0010	.9676
4.0090	.8899	6.0523	.9709
4.0600	.8825	6.1034	.9734
4.1112	.8769	6.1545	.9754
4.1622	.8736	6.2056	.9767
4.2133	.8713	6.2566	.9777
4.2644	.8689	6.3077	.9785
4.3155	.8667	6.3588	.9792

TABLE II.— DIFFUSER EXIT MACH NUMBER FOR JT8D FAN CORRECTED SPEEDS

JT8D fan simulator corrected speed, $N_c$ percent	P-inlet diffuser exit Mach number, $M_{de}$
40	0.21
50	.29
60	.37
70	.45
80	.57
90	.71

closed case was run with the auxiliary doors closed. Table III summarizes the configurations tested in both phases along with overall performance data.

The configuration tested during phase 2 of the Lewis program, shown in figure 6, had the P-inlet sharp cowl lip and more flight-like auxiliary doors. Door openings of 0, 20, and 40 percent of the inlet capture area were tested with bleeds both open and closed.

Diffuser exit weight flow, pressure recovery, distortion, and turbulence were measured with a array of 84 total pressure probes. This array consisted of 12 area-weighted rakes, 3 per quadrant, with 7 total pressure probes in each rake. Each rake also had associated with it a hub and tip static pressure tap. Three static pressure taps were also located on each side of each of the four support struts at the diffuser exit measuring

TABLE III. — PERFORMANCE SUMMARY

Cowl lip	Auxiliary doors, percent open	Bleeds	Free-stream Mach number, $M_0$	JT8D fan simulator corrected speed, $N_{c'}$ percent	Centerbody position		Recovery		Distortion		Throat Mach number		Figure
					(a)	(b)	(a)	(b)	(a)	(b)	(a)	(b)	
Blunt	0	Sealed	0	80	1.57	1.47	0.953	0.949	0.180	0.183	0.910	1.00	11
	40	Sealed	0	80	1.57	0	.988	.966	.029	.098	.436	.676	12
	40	Open	0	80	1.57	0	.983	.952	.034	.118	.471	.692	14
Sharp	0	Sealed	0	70	0.800	0.800	0.857	0.857	0.158	0.158	1.00	1.00	16
	0	Sealed	.2	70	1.20	.800	.925	.882	.135	.167	.830	1.00	17
	0	Open	.2	70	1.57	1.57	.908	.908	.172	.172	.814	.814	19
	20	Sealed	0	80	.800	.400	.923	.904	.149	.203	.832	.935	21
	20	Sealed	.2		1.20	.400	.952	.913	.087	.189	.706	.944	23
	20	Open	.2		1.57	.293	.943	.888	.106	.249	.723	.960	25
	40	Sealed	0		.800	0	.964	.951	.110	.166	.560	.673	27
	40	Sealed	.2		1.20	0	.979	.965	.036	.105	.509	.676	29
	40	Open	.2		1.57	0	.979	.956	.048	.111	.521	.673	32

<sup>a</sup>Peak recovery performance.

<sup>b</sup>Maximum throat Mach number performance.

station. One rake per quadrant was equipped with three dynamic pressure transducers. These were incorporated into the existing total pressure probes. Figure 7 depicts the diffuser exit instrumentation. The main inlet airflow was surveyed by total pressure rakes at both the cowl lip and the throat. These rakes, described in figure 8, were not installed during the first phase of the Lewis program. Main duct static pressure distributions were measured by various rows of static pressure taps located on both the centerbody and cowl surfaces along with limited dynamic transducers. This instrumentation is depicted in figure 9. Centerbody static pressure taps were not used in this investigation. The 135° and 315° auxiliary doors were instrumented with the static pressure taps depicted in figure 10.

The test was conducted in the Lewis 9- by 15-Foot Low-Speed Anechoic Wind Tunnel. The tunnel test section floor, ceiling, and walls are acoustically treated. The tunnel is capable of operation anywhere from static to Mach 0.2 at atmospheric total pressure. Tunnel details are described in reference 11. Fan pressure ratio and  $\Delta P$  were monitored in real time on a high-response analog plotter. High levels of dynamic activity or impending fan stall indicated by this instrumentation were used in determining limits of the fan speed/centerbody position envelope for a given configuration. In general, high levels of dynamic activity at the compressor face were associated with high throat Mach numbers in the inlet. Throat Mach number was monitored in near real time by the data system. The lowest cowl static pressure in the duct was the ratio to either free-stream or throat average total pressure, whichever was appropriate depending on the location in the duct of the lowest static pressure. Throat Mach number was then determined from standard one-dimensional isentropic relationships. This method determines the Mach number in the aerodynamic throat until choking occurs, at which point the method determines the maximum supersonic Mach number downstream of the

throat. Data were taken by setting first the tunnel Mach number and then the desired fan corrected speed. Fan corrected flow was adjusted with the mass flowmetering plug until the predetermined fan operating line flow was reached. Centerbody position and angle of attack were varied over the desired range while keeping corrected airflow constant with the mass flowmetering plug as recovery varied. This process continued at increasing fan speeds until impending fan stall or supersonic operation.

## Phase 1 Results (Bellmouth Cowl Lip)

### Baseline Performance (Auxiliary Doors Closed, Bleed Exits Sealed, $M_0=0$ )

Figure 11(a) presents the baseline performance of the NASA Lewis configuration at  $M_0=0$  with the bellmouth cowl lip installed, the bleed exits sealed, and the auxiliary inlets closed. Pressure recovery, throat Mach number, steady-state distortion, and average turbulence were plotted versus centerbody extension for the range of fan corrected speeds tested. Maximum recovery and minimum distortion occurred with the centerbody fully extended, providing the maximum throat area (fig. 4). If high throat Mach numbers are desired for acoustic attenuation, however, the centerbody should be fully retracted. Note that at high fan speeds the throat was choked without fully retracting the centerbody. At centerbody positions aft of the choked point data were generally not taken because performance degraded rapidly with supersonic flow in the diffuser, approaching fan stall conditions.

Figure 11(b) presents compressor face rake profiles and cowl static pressure distributions at 60-percent fan speed and  $M_0=0$ . Cowl static pressure distributions indicate that the adverse pressure gradient at a ratio of the distance from the centerbody tip to the cowl lip radius  $X/R_l$  of 4.5 increased

as the centerbody was retracted from its fully extended position. The depression in static pressure near  $X/R_I=5.4$  was due to centerbody support strut blockage. At the fully retracted centerbody position ( $DX/R_I=0$ ) compressor face rake profiles indicate separated flow at the hub surface. Centerbody bleed system recirculation may have caused or at least aggravated the separation problem. This observation was made during the Boeing program (ref. 12) when the bleed holes themselves were plugged and performance near the hub improved. The centerbody flow separation is an important loss mechanism for this configuration. Vortex generators could be used to eliminate this problem.

Reference 6 suggests that the overall sound power level can be reduced for throat Mach numbers greater than about 0.7. To demonstrate the effect of high throat Mach numbers on inlet performance, performance envelopes were constructed for each configuration. Figure 11(c) presents such an operating envelope (at static free-stream conditions) bounded by performance attained with the centerbody scheduled for peak recovery and performance attained with the centerbody scheduled for maximum throat Mach number. Thus for a given fan corrected speed (or compressor face corrected airflow), peak recovery performance (fig. 11(a)) is shown along with the performance penalty incurred by inducing a high throat Mach number for acoustic attenuation. Any point within the envelope represents a compromise between aerodynamic and acoustic performance. Centerbody extension was plotted in place of turbulence to help clarify the construction of these maps. The maximum throat Mach number curves exhibit significantly poorer performance at the lower fan speeds. This is a result of centerbody flow separation with the centerbody retracted. With increasing fan speed the centerbody was extended away from the compressor face while maintaining a choked throat.

If a diffuser exit Mach number of 0.6 (80-percent fan speed) is chosen as the design value, a recovery of 94.9 percent can be attained while choking the throat at  $DX/R_I=1.47$ . If a lesser flow is required, the centerbody must be retracted to maintain choked or maximum Mach number conditions in the throat, resulting in penalties of up to 10-percent recovery and 11-percent distortion.

#### **Effect of 40-Percent Auxiliary Flow (Bleed Exits Sealed, $M_0=0$ )**

Figure 12(a) presents bellmouth inlet performance with the 40-percent (blunt lip) auxiliary inlets open for  $M_0=0$ . As expected, all performance parameters showed marked improvement over performance with the auxiliary doors closed. The main duct could no longer be choked in the range of fan speeds and centerbody positions tested. The maximum throat Mach number occurred with the centerbody fully retracted; peak recovery occurred with the centerbody fully extended.

Figure 12(b) presents compressor face total pressure profiles and cowl and auxiliary door static pressure distributions for

the full range of centerbody positions at the design fan speed (80 percent) and  $M_0=0$ . The region of auxiliary inlet airflow is evident at the compressor face near the tip. The flow near the hub was no longer separated with the centerbody retracted, although some losses still existed. A low-energy region also existed just below the auxiliary door flow. This was attributed to the cowl boundary layer being displaced by the incoming auxiliary airflow. Auxiliary inlet static pressure distributions at  $X/R_I=6.7$  suggest that the auxiliary airflow rate increased as the centerbody was retracted. The local flow acceleration seen in the auxiliary lip static pressure profile was caused by the corner where the auxiliary lip and main duct contours merged. If free-stream total pressure was assumed, a local Mach number of approximately 0.9 was obtained at this corner. This may have attenuated some fan noise propagation through the auxiliary doors.

Figure 12(c) shows performance maps obtained by scheduling centerbody position for either peak recovery or maximum throat Mach number. At design fan speed a peak recovery of 98.8 percent was attained with 2.9-percent distortion. Operation on the maximum throat Mach number curve resulted in performance penalties of 2.2 percent in recovery and 6.9 percent in distortion.

Figure 13 compares peak recovery performance for this configuration and that with the auxiliary inlets closed for  $M_0=0$ . Recovery was increased 3.5 percent and distortion reduced 15.1 percent at design fan speed with the 40-percent auxiliary inlets.

#### **Effect of Bleed Inflow (40-Percent Auxiliary Doors, Bleed Exits Open, $M_0=0$ )**

Figure 14(a) presents bellmouth inlet performance at  $M_0=0$  with the 40-percent blunt lip auxiliary inlets and the bleed exits open. In contrast to performance with the bleed exits sealed (fig. 12), recovery was nearly equal to that with the auxiliary doors closed when the centerbody was extended but was generally lower when the centerbody was retracted.

Figure 14(b) presents cowl and auxiliary inlet static pressure distributions and compressor face total pressure profiles at design fan speed and  $M_0=0$ . Cowl static pressure distributions indicate that static pressure in the throat region decreased as the centerbody was retracted, as would be expected from the inlet area distributions. Since the external free-stream static pressure remained constant, the  $\Delta P$  driving bleed inflow and therefore the bleed flow rate increased as the centerbody was retracted. Compressor face total pressure profiles indicate that the auxiliary inlet airflow again displaced tip region losses toward the hub. Flow at the hub was not separated but displayed greater losses than with the bleed exits sealed (fig. 12(b)) because of the low-energy bleed inflow. Auxiliary inlet static pressure distributions exhibited similar characteristics whether the bleed exits were open or closed. However, decreased duct static pressure due to the lower recovery with the bleeds open caused a slight increase in auxiliary inlet airflow.

Figure 14(c) depicts performance maps for this configuration. Because of the increased bleed inflow caused by high throat Mach numbers, the penalties for operation on the maximum throat Mach number curve were slightly more severe with the bleed exits open. At design fan speed the recovery penalty was 3.1 percent with an increase in distortion of 8.4 percent. When the bleed exits were sealed, the penalties were 2.2 percent in recovery and 6.9 percent in distortion (fig. 12(c)).

Figure 15 compares peak recovery performance for the three bellmouth cowl lip configurations at  $M_0=0$ . In general, performance was greatly improved by opening the auxiliary doors, but bleed inflow had little effect with the auxiliary doors open. With the auxiliary inlets closed and bleed exits sealed at design fan speed, recovery was 95.3 percent and distortion, 18 percent. Opening the 40-percent blunt auxiliary doors increased recovery to 98.8 percent and decreased distortion to 2.9 percent. With the auxiliary doors open bleed inflow decreased recovery by only 0.5 percent and increased distortion by 0.5 percent.

## Phase 2 Results (Sharp Cowl Lip)

### Effect of Sharp Cowl Lip (Auxiliary Doors Closed, Bleed Exits Sealed, $M_0=0$ )

Figure 16(a) presents sharp-lip inlet performance at  $M_0=0$  with the bleed exits sealed and the auxiliary doors closed. In contrast to the bellmouth lip configurations a maximum now appears in the recovery curve at  $DX/R_l \approx 0.8$ . Other performance parameters also exhibited local maximums or minimums at centerbody positions between fully extended and fully retracted. At 70-percent fan speed  $DX/R_l=0.8$  was the only position that did not result in supercritical operation of the inlet.

Figure 16(b) presents inlet static pressure distributions and total pressure profiles for the complete range of centerbody positions at 60-percent fan speed and  $M_0=0$ . Comparing cowl static pressure distributions with those of the blunt cowl lip configuration (fig. 11(b)) makes evident the effect of flow separation at the sharp cowl lip. As the centerbody was extended from the fully retracted position, the flow area at the cowl lip was reduced because of the sharp-lip separation until the flow area at the cowl lip ( $X/R_l=2.5$ ) became less than the geometric throat area ( $X/R_l=4.2$ ). In general maximum recovery coincided with minimum throat Mach number, which occurred at  $DX/R_l=0.8$ . At this point static pressures at the cowl lip and geometric throat were about equal. The maximum throat Mach number for a given flow rate then occurred at the cowl lip as a result of the cowl lip flow separation with the centerbody fully extended. This Mach number, however, was that of flow in the unseparated region.

Since fan noise may propagate through the region of separated or reverse flow, choking in this manner may not

be effective in attenuating noise. Total pressure profiles at the cowl lip in figure 16(b) clearly show the flow separation. Flow at the cowl lip was separated for all centerbody positions, but the Mach numbers in the unseparated region varied significantly. Total pressure losses at the throat were proportional to this lip Mach number. The tube nearest the centerbody on the throat rake entered the centerbody boundary layer when the centerbody was fully retracted, thus the loss in total pressure at this point. Total pressure profiles at the compressor face show that the total pressure losses, generated by the sharp cowl lip at extended centerbody positions, propagated downstream to the compressor face. At retracted centerbody positions centerbody boundary layer separation was the dominant loss mechanism.

Figure 16(c) presents performance maps for this configuration at static free-stream conditions. Also included is the peak recovery curve for the bellmouth inlet with auxiliary doors closed and bleed exits sealed. For the highest fan speed at which data were obtained (70 percent), recovery was 11 percent below that of the baseline inlet and distortion was 5 percent higher.

### Effect of Free-Stream Mach Number (Auxiliary Doors Closed, Bleed Exits Sealed, $M_0=0.2$ )

Figure 17(a) presents performance of the sharp-lip inlet with the auxiliary doors closed and the bleed exits sealed at  $M_0=0.2$ . Recovery improved over that at  $M_0=0$  (fig. 16(a)) at extended centerbody positions but remained about the same with the centerbody retracted. The centerbody position at which peak recovery occurred shifted forward. The maximum throat Mach number now occurred in the geometric throat with the centerbody fully retracted for flow rates below which the throat choked. At 70-percent fan speed the throat was choked at  $DX/R_l=0.8$ .

Figure 17(b) presents cowl static pressure distributions and various total pressure profiles for the range of centerbody positions at a fan speed of 60 percent and  $M_0=0.2$ . Cowl static pressures again indicate the "double throat" caused by the sharp-cowl-lip flow separation. In contrast to the case at  $M_0=0$  (fig. 16(b)) the area restriction at the lip was much less severe at  $M_0=0.2$ . The two minimums in the static pressure distribution now became equal at  $DX/R_l \approx 1.2$ . Forward velocity reduced the extent of the cowl lip flow area restriction, allowing further extension of the centerbody before the lip static pressure equaled that of the geometric throat. Total pressure profiles at the cowl lip demonstrate that the radial extent of the flow separation was less at  $M_0=0.2$  and was eliminated completely when the centerbody was retracted at this airflow. Total pressure losses caused by a sharp cowl lip are related to the ratio of cowl lip to free-stream Mach number in the inviscid, momentum analysis of reference 13. If this ratio is less than or equal to 1, no losses are predicted. Throat rake profiles at 60-percent fan speed show almost no effect of the lip separation for centerbody positions aft of

$DX/R_l=0.4$ . At this flow rate and the cowl lip annular area at  $DX/R_l=0.4$ , the theoretical lip Mach number assuming no separation was 0.32. This resulted in a ratio of cowl lip to free-stream Mach number of 1.6, at which the aforementioned analysis predicted only a 1-percent loss.

Figure 17(c) presents performance maps for Mach 0.2 operation. At 70-percent fan speed the penalty for operation on the maximum throat Mach number curve was 4.3 percent in recovery and 3.2 percent in distortion.

Figure 18 compares peak recovery curves for the baseline inlet at  $M_0=0$  and for the sharp cowl lip inlet at  $M_0$  of 0 and 0.2, each with the bleed exits closed and the auxiliary doors sealed. For the two sharp-lip cases at 70-percent fan speed, peak recovery performance at  $M_0=0.2$  shows a 6.8-percent increase in recovery and a 2.3-percent decrease in distortion over the  $M_0=0$  case. At the lower flow rates the sharp-lip inlet performance at  $M_0=0.2$  converged to the bellmouth inlet performance (at  $M_0=0$ ) as lip separation diminished.

#### **Effect of Bleed (Auxiliary Doors Closed, Bleed Exits Open, $M_0=0.2$ )**

Figure 19(a) shows performance of the sharp-lip inlet with the auxiliary inlets closed and the bleed exits open for  $M_0=0.2$ . Recovery dropped at any centerbody position aft of fully extended. Note that peak recovery occurred with the centerbody fully extended for all fan speeds, and maximum throat Mach number occurred with the centerbody fully retracted (or retracted to the distortion/fan stall limit).

Figure 19(b) presents cowl static pressure distributions and lip, throat, and compressor face total pressure profiles at 60-percent fan speed and  $M_0=0.2$ . In contrast to the case with the bleed exits sealed (fig. 17(b)), throat rake profiles show significant losses due to cowl bleed inflow. These losses in the throat propagated back to the compressor face and thus allowed airflow near the hub to remain attached to any centerbody position despite the centerbody bleed exits also being open. Mass flow addition and losses in the throat served to slightly lower the lip Mach number. Lip rake profiles indicate that lip separation was eliminated for centerbody positions aft of  $DX/R_l=0.8$ .

Figure 20 compares the performance at peak recovery with the bleeds open or closed at  $M_0=0.2$  and with the baseline inlet at  $M_0=0$ . For the highest fan speed at which a comparison could be made (70 percent), opening the bleed exits caused a 1.7-percent decrease in recovery and a 3.7-percent increase in distortion with the sharp cowl lip. Performance with the blunt lip at  $M_0=0$  was well above performance with the sharp lip.

#### **Effect of Angle of Attack (All Configurations)**

Data at  $5^\circ$  of attack were taken for all configurations at  $M_0=0.2$ . No effect on performance was noted for any of the configurations tested; hence no data at angle of attack are presented.

#### **Effect of 20-Percent Auxiliary Doors (Bleed Exits Sealed, $M_0=0$ )**

Figure 21(a) shows sharp-lip inlet performance at  $M_0=0$  with the 20-percent auxiliary doors open. Recovery increased substantially over that with the corresponding doors-closed configuration (fig. 16(a)). Performance reductions that occurred as the centerbody was extended indicate that lip separation effects were still present. A fan speed of 90 percent was reached before choking occurred. As with the auxiliary doors closed, the lip separation area constriction caused two local maximums on the throat Mach number curve.

Figure 21(b) presents cowl and auxiliary door static pressure distributions and duct total pressure profiles at design fan speed and  $M_0=0$ . Static pressures on the cowl surface indicate that the Mach numbers at the cowl lip and geometric throat became equal between  $DX/R_l$  of 1.2 and 0.8. Auxiliary door static pressure distributions indicate that local supersonic flow occurred at design fan speed at the corner where the auxiliary door and main duct contours merged ( $X/R_l=7.1$ ). Lip separation losses at the throat were prominent until the centerbody was retracted to  $DX/R_l=0.8$ . These losses also appeared at the compressor face just below the region of high-pressure auxiliary flow. Compressor face profiles also exhibited low-energy flow near the hub when the centerbody was retracted.

Figure 21(c) presents performance maps for this configuration at  $M_0=0$ . At design fan speed a 1.9-percent reduction in recovery and a 5.4-percent increase in distortion resulted from operation on the high throat Mach number curve. The sharp reduction in distortion at high fan speeds on the high throat Mach number curve occurred as the "choke" centerbody position moved forward.

Figure 22 compares peak recovery performance of this configuration with performance with the auxiliary doors closed at  $M_0=0$  conditions. The design fan speed could not be reached with the auxiliary doors closed. At the highest fan speed at which a comparison could be made (70 percent), opening the 20-percent auxiliary doors increased recovery by 8.5 percent and decreased distortion by 7 percent.

#### **Effect of Free-Stream Mach Number (20-Percent Auxiliary Doors, Bleed Exits Sealed, $M_0=0.2$ )**

Figure 23 presents sharp-lip inlet performance with the 20-percent auxiliary doors open and the bleed exits sealed at  $M_0=0.2$ . The centerbody position for peak recovery has shifted forward slightly to  $DX/R_l \approx 1.2$ . This effect is similar to that noted with the auxiliary doors closed (fig. 17(a)). Maximum throat Mach number occurred with the centerbody retracted as far as possible, with choking in the main duct occurring at 90-percent fan speed.

Figure 23(b) presents cowl and auxiliary door static pressure distributions and duct total pressure profiles at design fan speed and  $M_0=0.2$ . Once again, the centerbody position corresponding to peak recovery exhibited nearly equal static

pressures at the cowl lip aerodynamic throat and the geometric throat. With the centerbody retracted to  $DX/R_l=0.4$  (the centerbody could not be retracted further because of fan stall and distortion limitations), the throat Mach number was 0.94. Supersonic flow at the auxiliary door corner made this an attractive condition for fan noise attenuation. Comparing lip and throat rake profiles with those at  $M_0=0$  (fig. 21(b)) makes clear the effect of free-stream Mach number. Lip separation was greatly reduced, thereby reducing the area restriction at the cowl lip. Pressure recovery at the throat was increased. At the compressor face high-pressure auxiliary airflow appeared in the tip region as well as in the shear region between the main and auxiliary duct flows.

Figure 23(c) presents performance maps for this configuration at  $M_0=0.2$ . At design fan speed operating on the maximum throat Mach number curve decreased recovery by 3.9 percent and increased distortion by 10.2 percent, on the basis of peak recovery performance.

Figure 24 shows the effect of free-stream Mach number on peak recovery performance and compares the results of this section with the results of the previous section at  $M_0=0$ . At design fan speed the recovery increased 2.9 percent but distortion decreased 6.2 percent at  $M_0=0.2$ . These performance benefits resulted from reduced sharp-lip separation.

#### **Effect of Bleed Inflow (20-Percent Auxiliary Doors, Bleed Exits Open, $M_0=0.2$ )**

Figure 25(a) presents sharp-lip inlet performance with 20-percent auxiliary doors and bleed exits open at  $M_0=0.2$ . Maximum recovery occurred with the centerbody nearly fully extended for all corrected airflows. Maximum throat Mach number occurred with the centerbody retracted as far as possible. At the maximum fan speed of 90 percent the main duct was choked by retracting the centerbody to  $DX/R_l=0.96$ .

Figure 25(b) presents cowl and auxiliary door static pressure distributions and duct total pressure profiles at design fan speed and  $M_0=0.2$ . Throat rake profiles indicate increased total pressure losses in the cowl boundary layer due to the inflow bleed. These losses occurring in the throat reduced the cowl lip Mach number and the sharp-lip losses. This effect can be demonstrated by comparing the cowl static pressure distributions and the lip rake total pressure profiles with those of the bleed-exits-closed case (fig. 23(b)). Inflow bleed clearly reduced the cowl lip Mach number for a given fan corrected flow and centerbody position. This effect, although beneficial, did not counteract the much greater losses occurring in the throat due to the low-energy mass flow addition. Auxiliary door static pressure profiles are similar to those with the bleed exits closed, with a slight overall decrease in static pressure level. This suggests that slightly more flow was entering through the auxiliary inlets with the bleed exits open, as would be expected with increased losses in the throat. Compressor

face total pressure profiles indicate the familiar auxiliary flow region, the mixing region, and centerbody separation losses near the hub. Losses near the hub, which occurred with the centerbody retracted, were more severe with the bleed exits open.

Figure 25(c) presents performance maps for this configuration at  $M_0=0.2$ . Performance decrements for operation on the high throat Mach number curve at design fan speed were a 5.5-percent reduction in recovery and a 14.3-percent increase in distortion. These decrements were more severe than those incurred with the bleed exits sealed since bleed inflow increases with increased throat Mach number.

Figure 26 compares the peak recovery performance for the bleeds-open and bleeds-closed configurations at  $M_0=0.2$ . With the 20-percent auxiliary doors open the overall effect of bleed inflow was slight, a 1-percent decrease in recovery and a 1.9-percent increase in distortion at design fan speed.

#### **Effect of 40-Percent Auxiliary Doors (Bleed Exits Sealed, $M_0=0$ )**

Figure 27(a) presents sharp-lip inlet performance with the 40-percent auxiliary doors open. Peak recovery occurred at  $DX/R_l=0.8$  for all corrected airflows. Fully retracting the centerbody resulted in the maximum throat Mach number. The highest throat Mach number attained was 0.82 at 90-percent fan speed.

Figure 27(b) presents cowl and auxiliary door static pressure distributions and duct total pressure profiles for the complete range of centerbody positions at design fan speed and  $M_0=0$ . As expected, peak recovery occurred when static pressures at the lip and throat became equal. Auxiliary flow increased slightly as recovery dropped, but Mach numbers in the auxiliary door region were still well below those of the 20-percent doors. The highest local Mach number in the 40-percent auxiliary doors at design fan speed was 0.85. Lip rake profiles show the familiar flow separation and reduction of the cowl lip Mach number as the centerbody was retracted. Comparing these profiles to those of figure 25(b), where 20-percent auxiliary doors were employed, shows a significant overall reduction in cowl lip Mach number. The results of this decrease in sharp-lip Mach number may be seen in the throat rake profiles, where total pressure losses are reduced. At the compressor face a large region of high-energy auxiliary flow was apparent, but for centerbody positions corresponding to low overall recovery or highest auxiliary airflow, the increase in auxiliary door Mach number caused a total pressure loss near the tip that increased distortion. This loss was presumed to be a separation/reattachment phenomenon due to the auxiliary door contour.

Figure 27(c) presents performance maps for the 40-percent door configuration at  $M_0=0$ . At design fan speed a 1.3-percent recovery decrement and a 6.6-percent distortion

increment were incurred by operating on the high throat Mach number curve. The distortion was caused by low-energy flow at the tip and may be reduced by more carefully designing the auxiliary doors or locating the auxiliary doors further upstream to provide a longer mixing region.

Figure 28 compares the peak performance of the three auxiliary door configurations at  $M_0=0$  with the bleed exits sealed. At design fan speed the 40-percent auxiliary doors exhibited 4.1 percent better recovery and 3.9 percent lower distortion than the 20-percent doors. The doors-closed configuration could not be operated to design speed because of distortion and fan stall limitations. Although the 40-percent auxiliary doors provided better aerodynamic characteristics, acoustic performance may have been compromised because of lower throat and auxiliary door Mach numbers.

#### **Effect of Free-Stream Mach Number (40-Percent Auxiliary Doors, Bleed Exits Sealed, $M_0=0.2$ )**

Figure 29(a) presents the performance of the sharp-lip inlet with 40-percent auxiliary doors open at  $M_0=0.2$ . The centerbody position resulting in peak recovery has shifted forward to  $DX/R_t=1.2$ . A throat Mach number of 0.8 at 90-percent fan speed was the maximum obtainable.

Figure 29(b) presents cowl and auxiliary door static pressure profiles and duct total pressure profiles at design fan speed and  $M_0=0.2$ . Static pressures at the cowl lip and throat were equal at  $DX/R_t=1.2$ . The maximum Mach number achieved with the 40-percent auxiliary doors at design fan speed was approximately 0.9. Lip and throat total pressure profiles demonstrate improvements in performance over the static free-stream case (fig. 27(b)). For centerbody positions aft of  $DX/R_t \approx 0.8$ , losses in the throat were negligible. Compressor face profiles have the familiar mixing region below the region of high-energy auxiliary flow. However, the loss at the tip above the auxiliary flow that was present at  $M_0=0$  has been eliminated at  $M_0=0.2$ . This loss did reappear, however, at 90-percent fan speed.

Figure 29(c) presents performance maps obtained with the 40-percent doors open at  $M_0=0.2$ . At design fan speed operation on the maximum throat Mach number curve incurred performance penalties of 1.4 percent in recovery and 6.9 percent in distortion.

Figure 30 shows the net effect of  $M_0=0.2$  on the peak performance of the 40-percent auxiliary door configuration with the bleed exits sealed. At design fan speed recovery improved 1.5 percent and distortion decreased 7.4 percent. The rather large distortion difference was due to the tip total pressure loss at static free-stream conditions.

Figure 31 compares performance at peak recovery of the three auxiliary door configurations tested at  $M_0=0.2$ . At design fan speed recovery ranged from 90 to 98 percent depending on the auxiliary door opening, while distortion went from 4 percent with the 40-percent-open doors to 17 percent

with the doors closed. The 40-percent doors clearly provided the best peak recovery performance, but this must be weighed against the lower internal Mach numbers and probable degradations in acoustic performance.

#### **Effect of Bleed Inflow (40-Percent Auxiliary Doors, Bleed Exits Open, $M_0=0.2$ )**

The effect of bleed inflow on the performance of the 40-percent auxiliary door configuration was similar to the effect noted with the 20-percent doors, but of an even lesser degree. Therefore only net effects are discussed here. Figure 32 presents performance maps at  $M_0=0.2$ . Performance differences between the peak recovery and maximum throat Mach number curves at design fan speed were 2.3 percent in recovery and 6.3 percent in distortion. Figure 33 compares peak recovery performance with the bleed exits both sealed and open at  $M_0=0.2$ . High throat Mach number performance was also very similar for the two configurations, as can be seen by comparing figures 29(c) and 32.

## **Summary of Results**

In a test program to determine the aerodynamic performance and acoustic characteristics associated with low-speed operation of a supersonic, axisymmetric, mixed-compression inlet with auxiliary inlets, the following results were found:

1. Peak recovery performance of the baseline inlet (bellmouth cowl lip) with the auxiliary doors closed and the bleed exits sealed at static free-stream conditions was 95.3-percent recovery and 18-percent distortion at the design fan speed of 80 percent. Opening the 40-percent, blunt-lip auxiliary doors improved recovery by 3.5 percent and reduced distortion by 15.1 percent. Opening the bleed exits to allow bleed inflow with the 40-percent auxiliary doors open decreased recovery by 0.5 percent and did not affect distortion significantly.

2. The sharp cowl lip inlet could not be operated at design fan speed with the auxiliary doors closed because of fan stall and distortion limitations. The highest fan speed attained was 70 percent with the bleed exits sealed at 0.2 free-stream Mach number. At these conditions peak performance was 92.5-percent recovery and 13.5-percent distortion.

3. The sharp-lip inlet with the 20-percent auxiliary doors open and the bleed exits sealed at the design fan speed and static free-stream conditions demonstrated peak recovery performance of 92.3-percent recovery and 14.9-percent distortion. Increasing the free-stream Mach number to 0.2 increased recovery by 2.9 percent and decreased distortion by 6.2 percent. Subsequent opening of the bleed exits caused a 1.1-percent drop in recovery and a 1.9-percent increase in distortion.

4. The sharp-lip inlet with the 40-percent doors open and the bleed exits sealed achieved peak recovery performance of 96.4-percent recovery and 11-percent distortion at static free-stream conditions and design fan speed. Increasing the free-stream Mach number to 0.2 improved recovery by 1.5 percent and decreased distortion by 7.4 percent. Inflow bleed had a negligible effect on peak recovery performance.

5. At ratios of cowl lip to free-stream Mach number of 1.6 or less, losses from sharp-lip separation were negligible at the compressor face. The design of auxiliary door systems could be based on achieving this ratio at the cowl lip.

6. Bleed inflow was not detrimental to performance if auxiliary doors were used to decrease the main duct Mach number and to energize the main duct airflow downstream of the cowl lip and throat.

7. At design fan speed a Mach number of 0.94 was attained in the main duct with the 20-percent auxiliary doors open at a centerbody position  $DX/R_l$  of 0.4. However, a region of local supersonic flow occurred just downstream of the auxiliary doors regardless of free-stream Mach number and bleed configuration. This high throat Mach number operation reduced recovery by as much as 6 percent and increased distortion by 15 percent.

8. With the 40-percent doors open the maximum throat Mach number at design fan speed was 0.68. Supersonic flow in the auxiliary door region did not occur with the 40-percent doors, although a maximum Mach number of approximately 0.85 was attained locally. At a free-stream Mach number of 0.2 performance degradations from peak recovery at these high Mach number conditions were a 1.4-percent decrease in recovery and a 6.9-percent increase in distortion.

Lewis Research Center  
National Aeronautics and Space Administration  
Cleveland, Ohio, November 4, 1985

## References

1. Technology Application Study of a Supersonic Cruise Vehicle. (MDC-J4647, McDonnell Douglas Aircraft; NASA Contract NASA-14624.) NASA CR-159276, 1980.
2. Supersonic Cruise Vehicle Technology Assessment Study of an Over/Under Engine Concept, Vol. 2. (LR-29363-Vol. 2, Lockheed-California Co.; NASA Contract NAS1-14625.) NASA CR-159247, 1980.
3. Advanced Concept Studies for Supersonic Vehicles. (D6-48864, Boeing Commercial Airplane Co.; NASA Contract NAS1-14623.) NASA CR-159244, 1980.
4. Bangert, L.H.; Burcham, F.W., Jr.; and Mackall, K.G.: YF-12 Inlet Suppression of Compressor Noise: First Results. AIAA Paper 80-0099, Jan. 1980.
5. Wasserbauer, J.F.; Cubbison, R.W.; and Trefny, C.J.: Low Speed Performance of a Supersonic Axisymmetric Mixed Compression Inlet with Auxiliary Inlets. AIAA Paper 83-1414, June 1983.
6. Woodward, R.P.; Glaser, F.W.; and Lucas, J.G.: Low Flight Speed Acoustic Results for a Supersonic Inlet with Auxiliary Inlet Doors. AIAA Paper 83-1415, June 1983.
7. Koncsek, J.L.; and Syberg, J.: Transonic and Supersonic Test of a Mach 2.65 Mixed Compression Axisymmetric Intake. NASA CR-1977, 1972.
8. Smelter, D.B.; and Sorsensen, N.E.: Analytical and Experimental Performance of Two Isentropic Mixed Compression Axisymmetric Inlets at Mach Numbers 0.8 to 2.65. NASA TN D-7320, 1973.
9. Syberg, J.; and Turner, L.: Supersonic Test of a Mixed-Compression Axisymmetric Inlet at Angles of Incidence. NASA CR-165686, 1981.
10. Moore, R.D.; Kovich, G.; and Tysl, E.R.: Aerodynamic Performance of 0.4066-Scale Model of JT8D Refan Stage. NASA TM X-3356, 1976.
11. Yuska, J.A.; Diedrich, J.H.; and Clough, N.: Lewis 9x15 ft V/STOL Wind Tunnel. NASA TM X-2305, 1971.
12. Ball, W.H.; and Pickup, N.: Low Speed Performance and Acoustic Tests of an Axisymmetric Supersonic Inlet - Phase One Tests with Auxiliary Doors Closed. (D6-52144, Boeing Commercial Airplane Co.; NASA Contract NAS1-16150.) NASA CR-172390, 1984.
13. Fradenburgh, E.A.; and Wyatt, D.D.: Theoretical Performance Characteristics of Sharp Lip Inlets at Subsonic Speeds. NACA TN-3004, 1953.

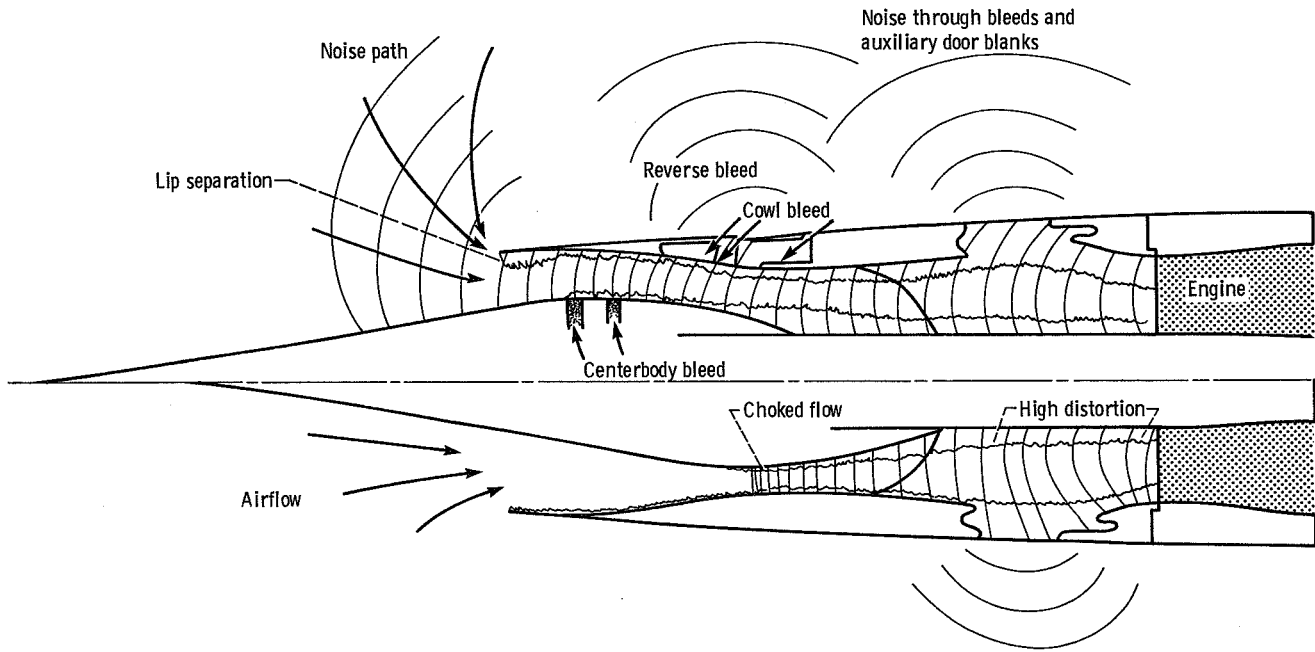


Figure 1.—Schematic of aeroacoustic phenomena.



Figure 2.—P-inlet model coupled to JT8D fan simulator and mounted in Lewis wind tunnel.

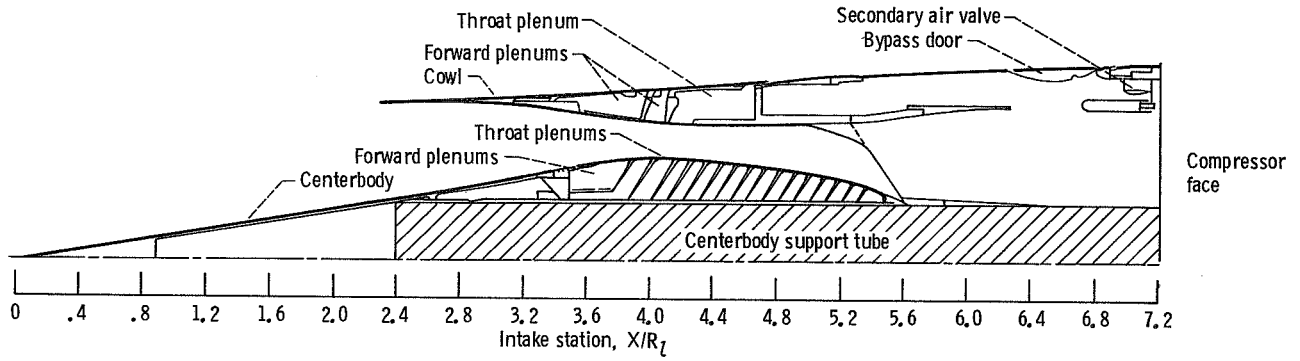


Figure 3. — Cross section of P-inlet in unmodified state.

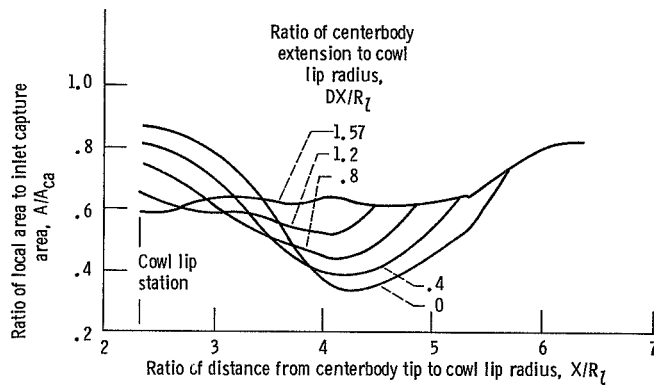


Figure 4. — Variation of P-inlet area with centerbody position.

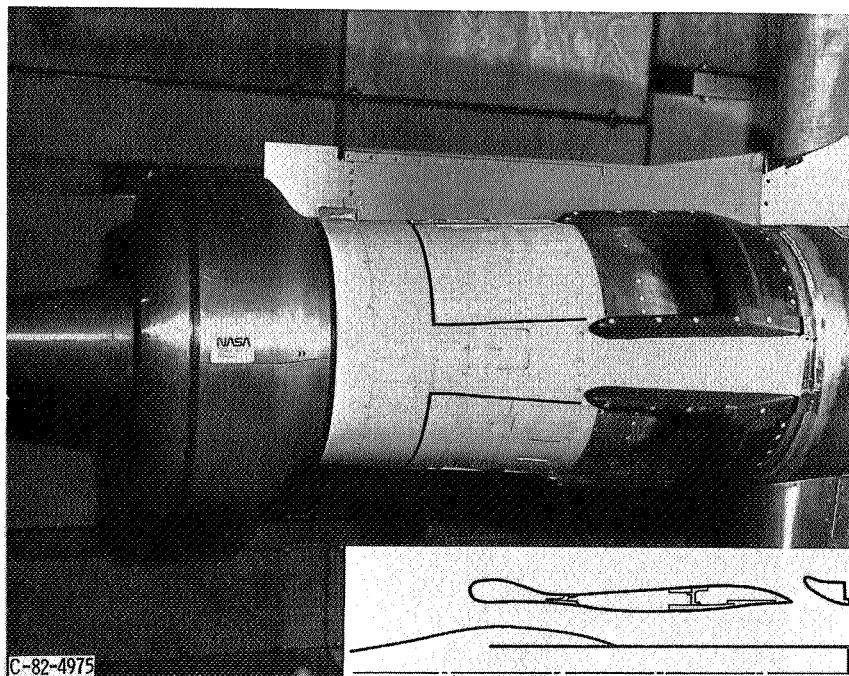


Figure 5. — Phase 1 configuration (blunt cowl lip and auxiliary doors).

ORIGINAL PAGE IS  
OF POOR QUALITY

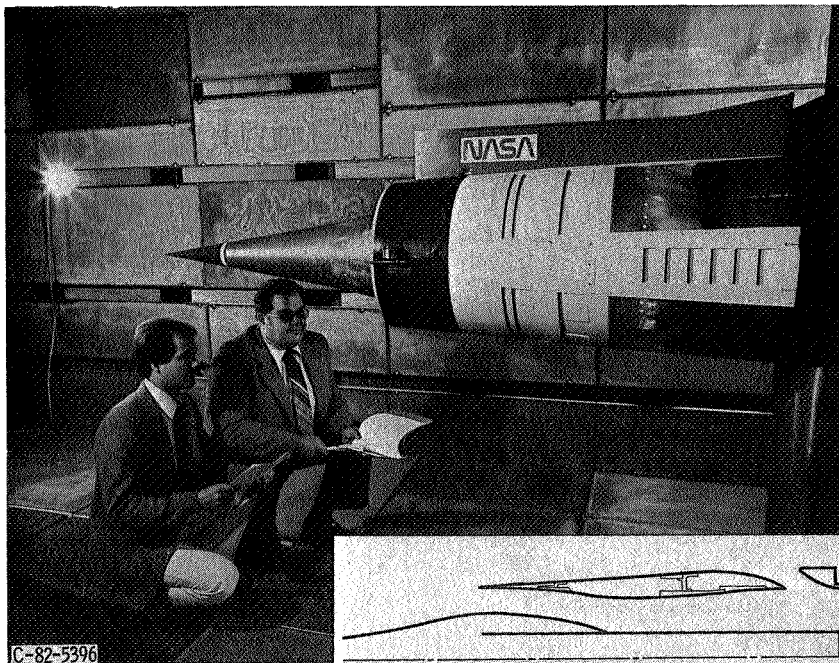


Figure 6. —Phase 2 configuration (sharp cowl lip and “flight” auxiliary doors).

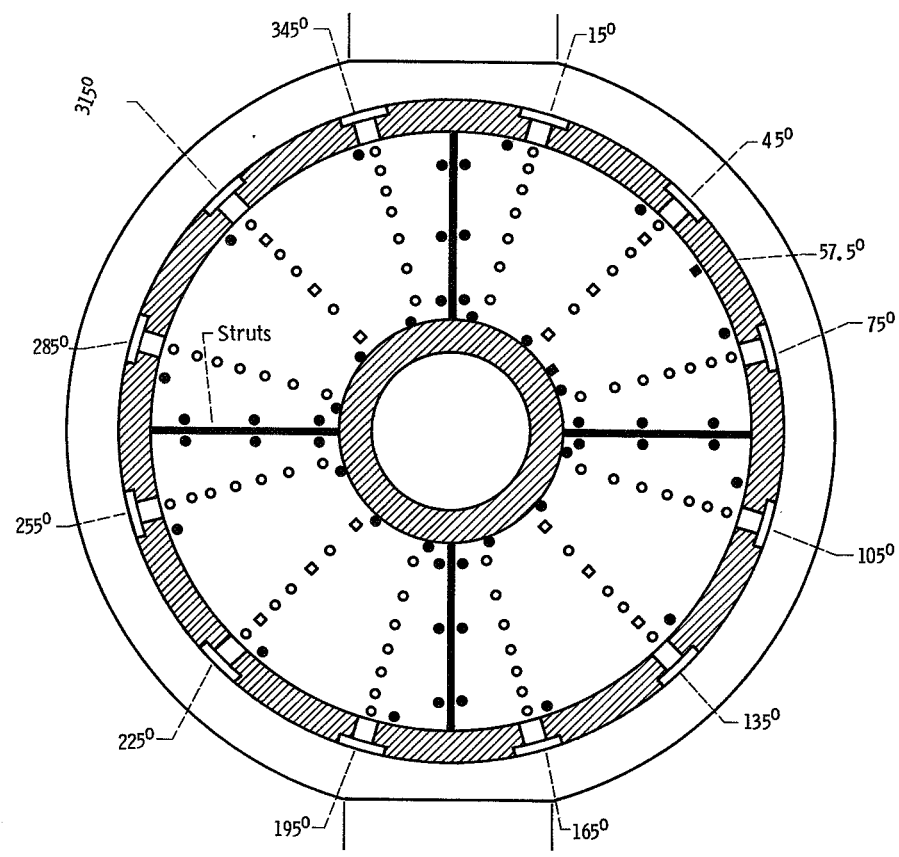
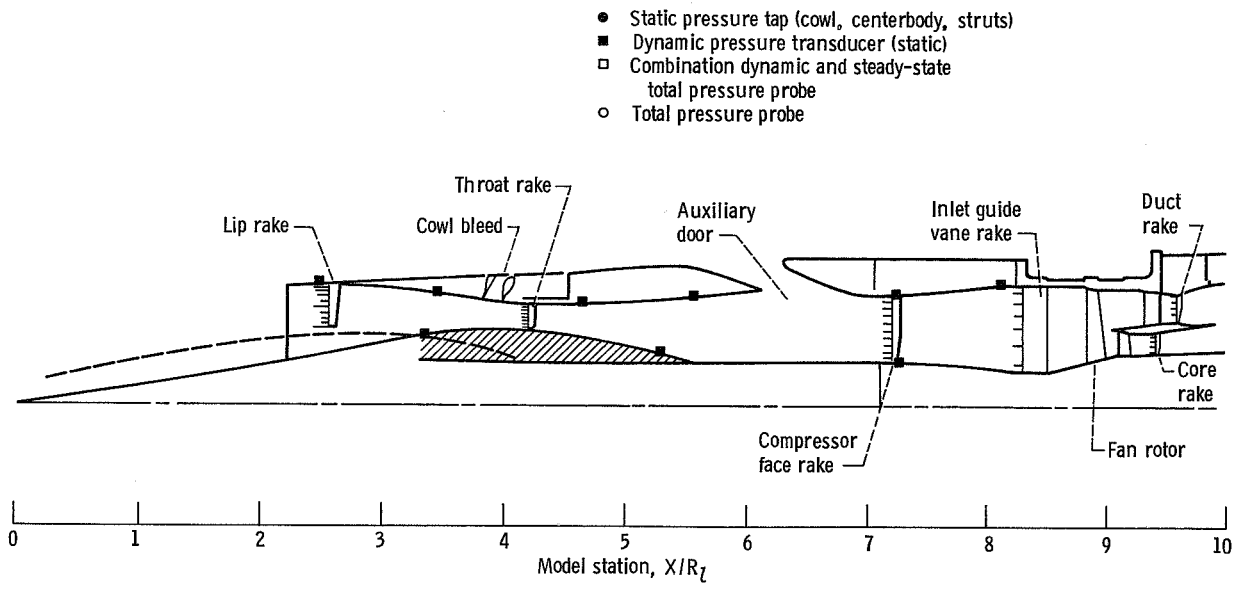


Figure 7.—Diffuser exit instrumentation.

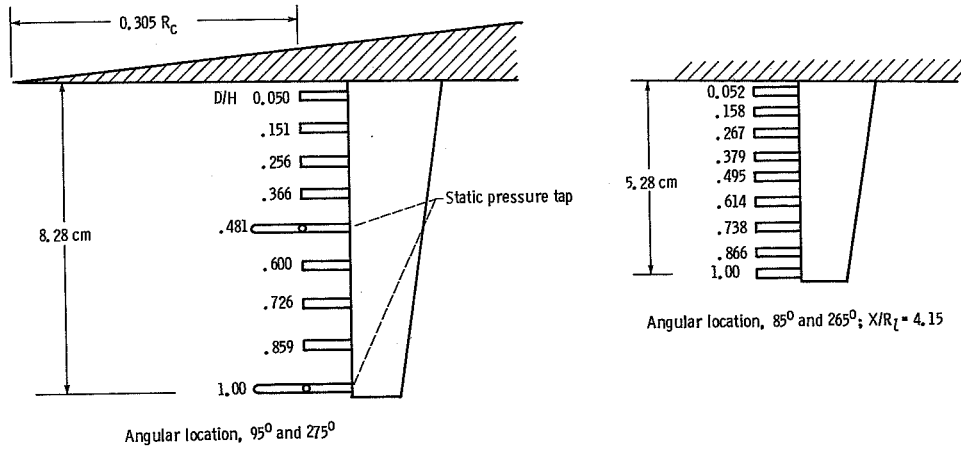


Figure 8.—Cowl lip and throat rake detail.

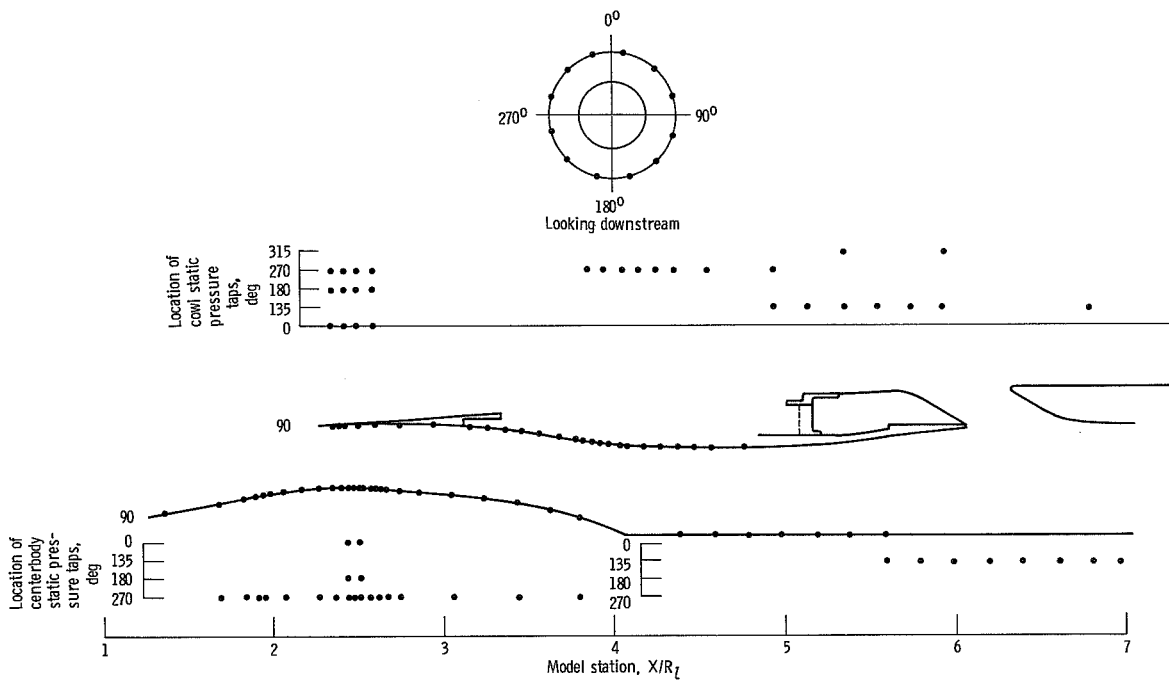


Figure 9.—Inlet static pressure instrumentation.

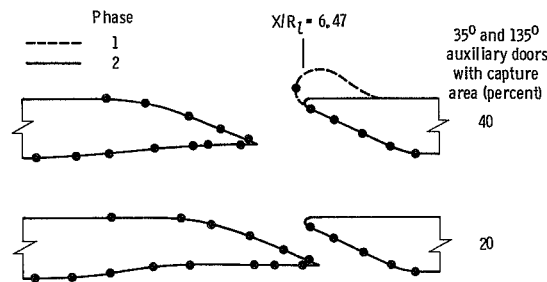
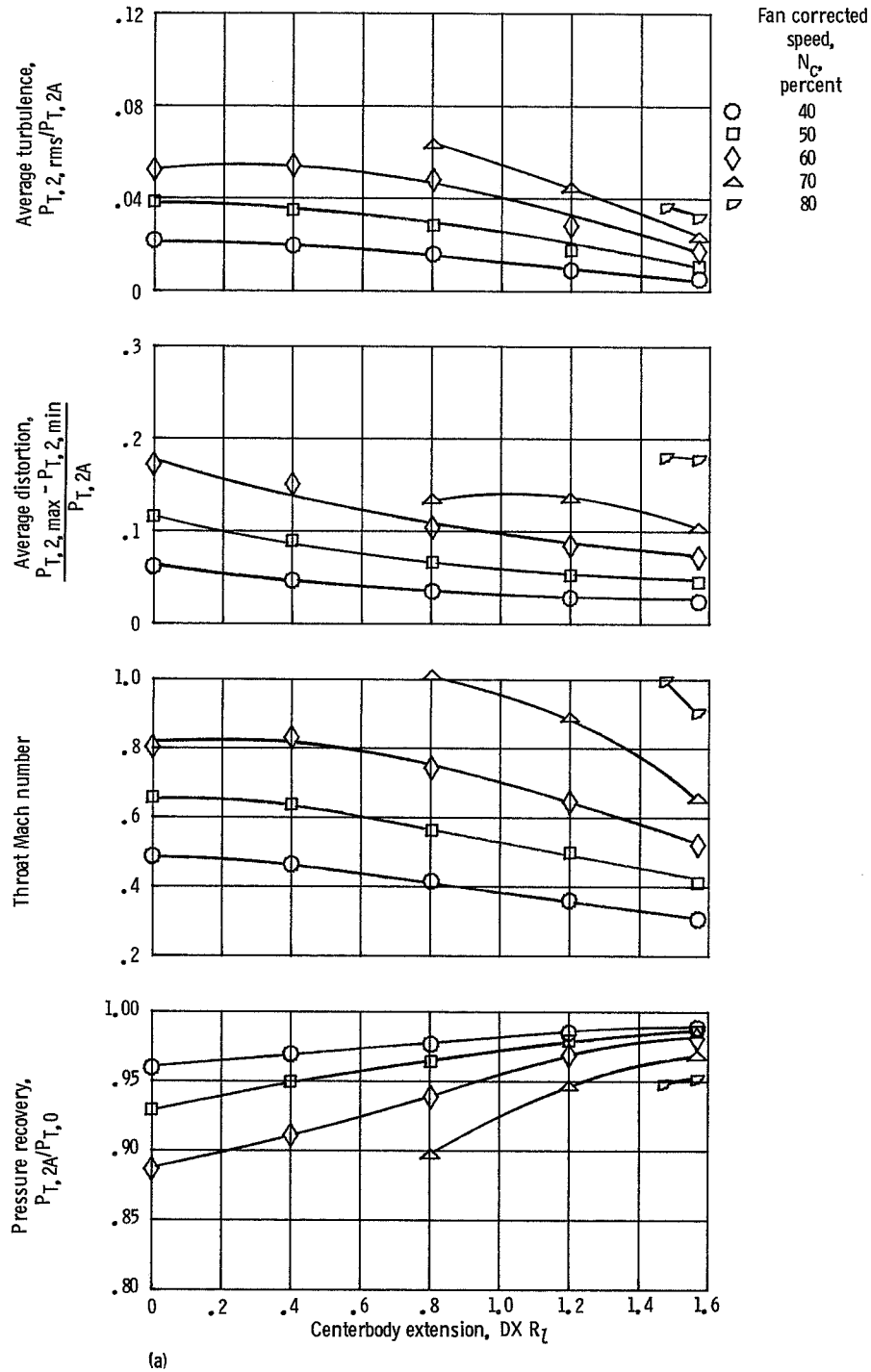
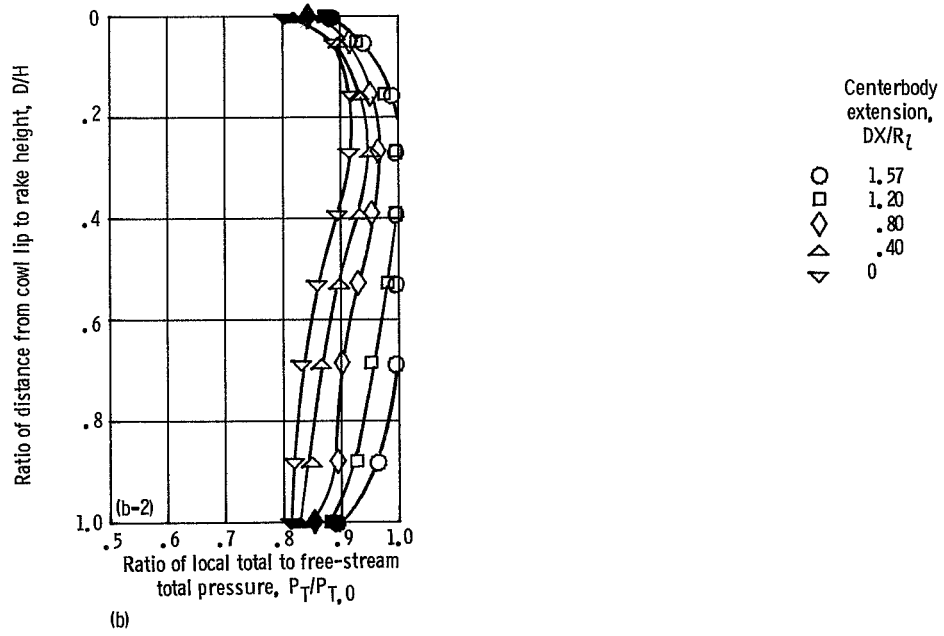
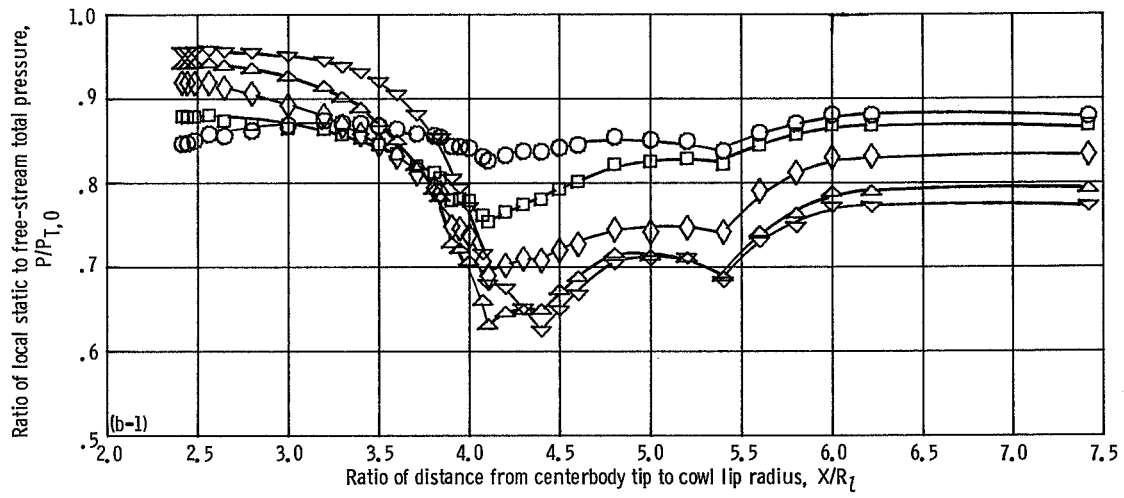


Figure 10.—Auxiliary inlet static pressure instrumentation detail.

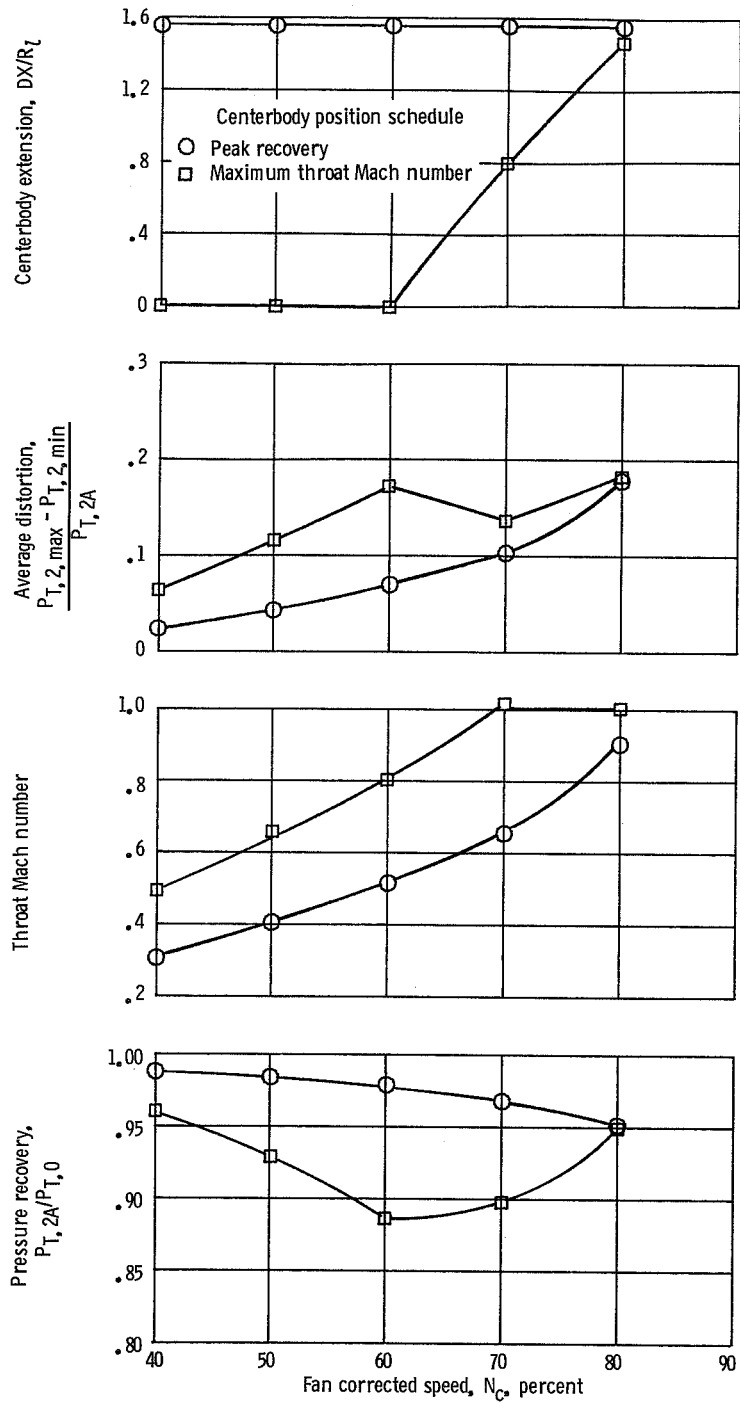


(a) Aerodynamic performance.

Figure 11.—Baseline inlet performance with bellmouth cowl lip, auxiliary doors closed,  $M_0=0$ , and bleeds closed.



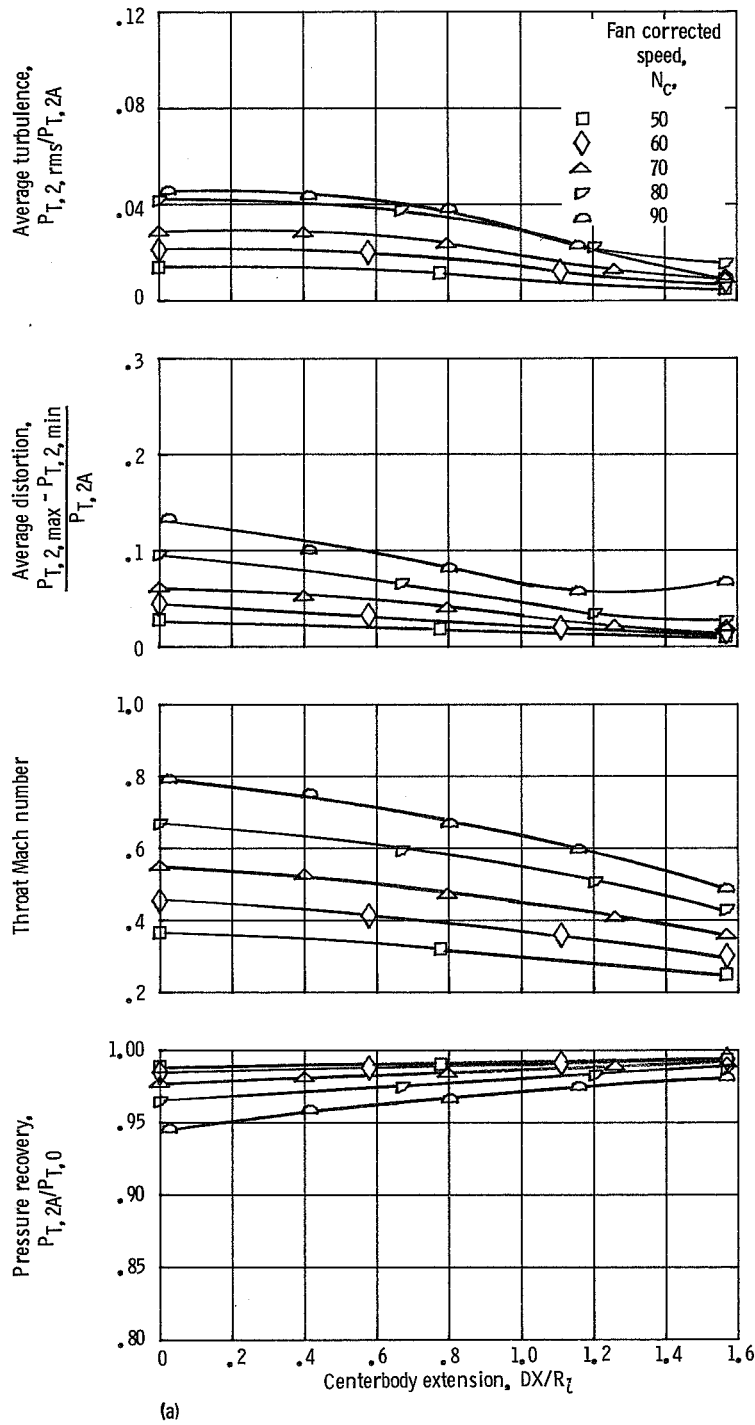
(b-1) Cowl surface.  
 (b-2) Compressor face rake ( $X/R_l=7.42$ ).  
 (b) Inlet pressure distributions. Fan speed, 60 percent. (Lip rake at  $X/R_l=2.63$  and throat rake at  $X/R_l=4.30$  not installed.)  
 Figure 11. -Continued.



(c)

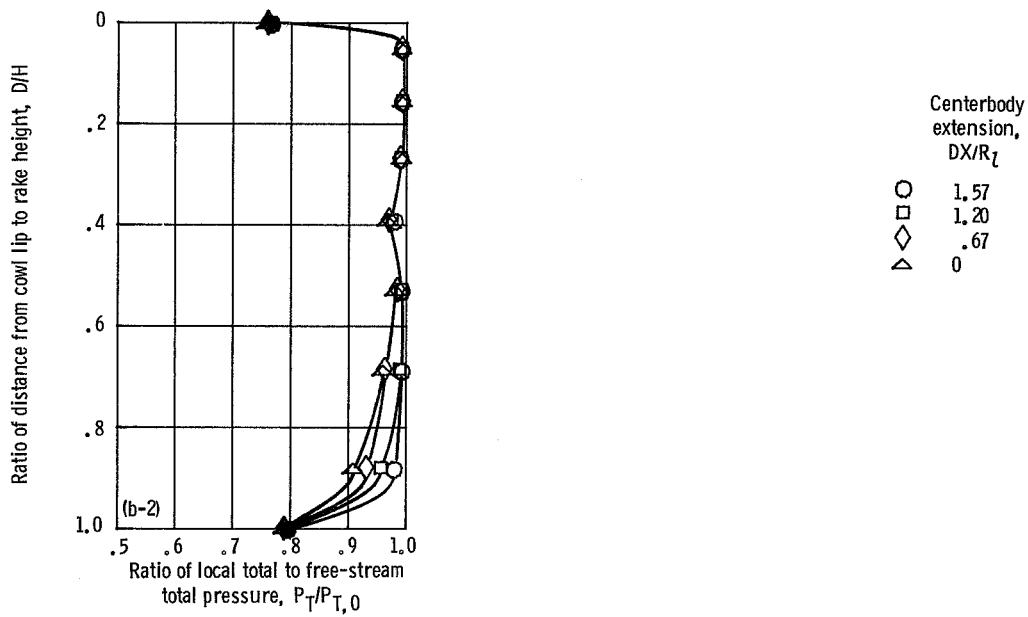
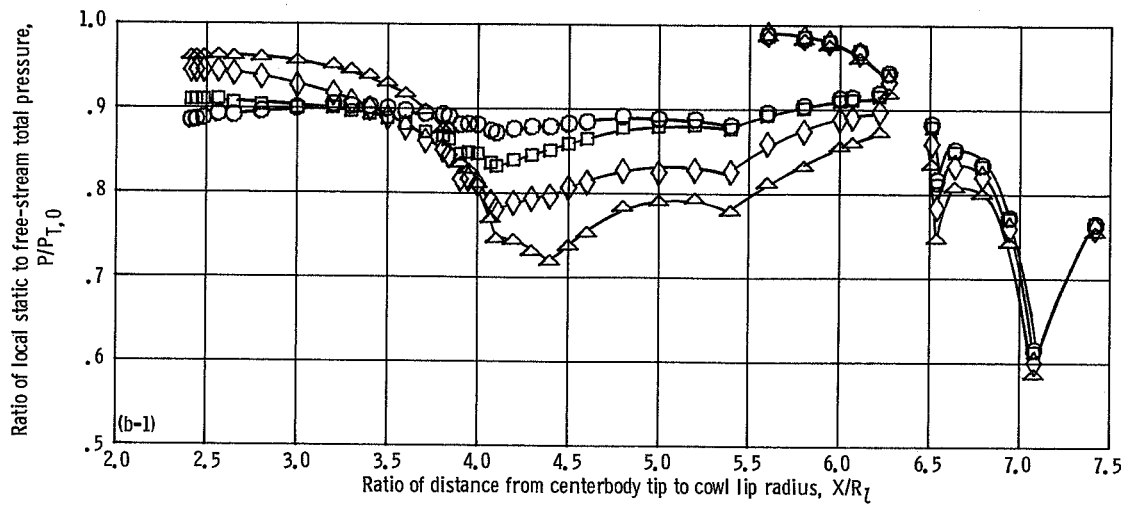
(c) Performance maps.

Figure 11.—Concluded.



(a) Aerodynamic performance.

Figure 12. - Baseline inlet performance with bellmouth cowl lip, 40-percent blunt auxiliary doors open,  $M_0=0$ , and bleeds closed.

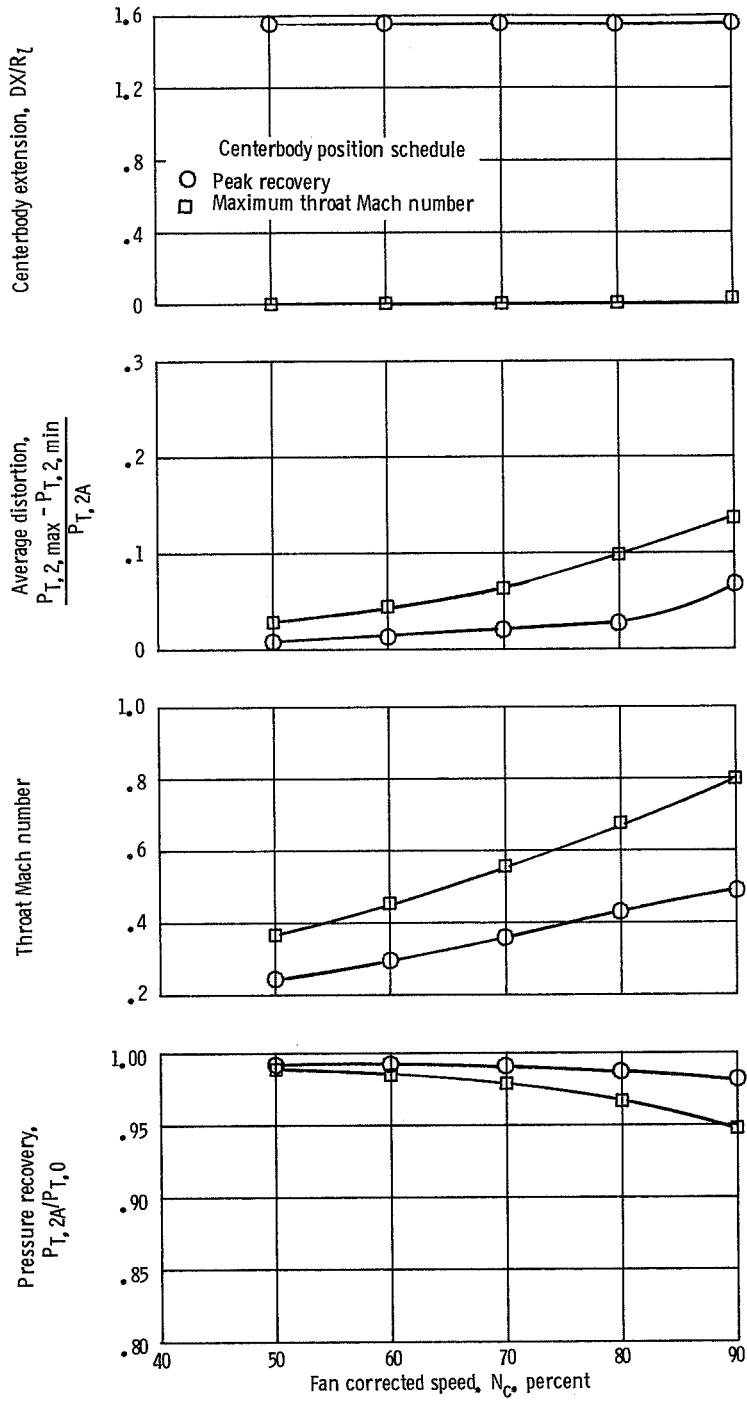


(b-1) Cowl surface.

(b-2) Compressor face rake ( $X/R_l=7.42$ ).

(b) Inlet pressure distributions. Fan speed, 80 percent. (Lip rake at  $X/R_l=2.63$  and throat rake at  $X/R_l=4.30$  not installed.)

Figure 12. - Continued.



(c)

(c) Performance maps.  
Figure 12. — Concluded.

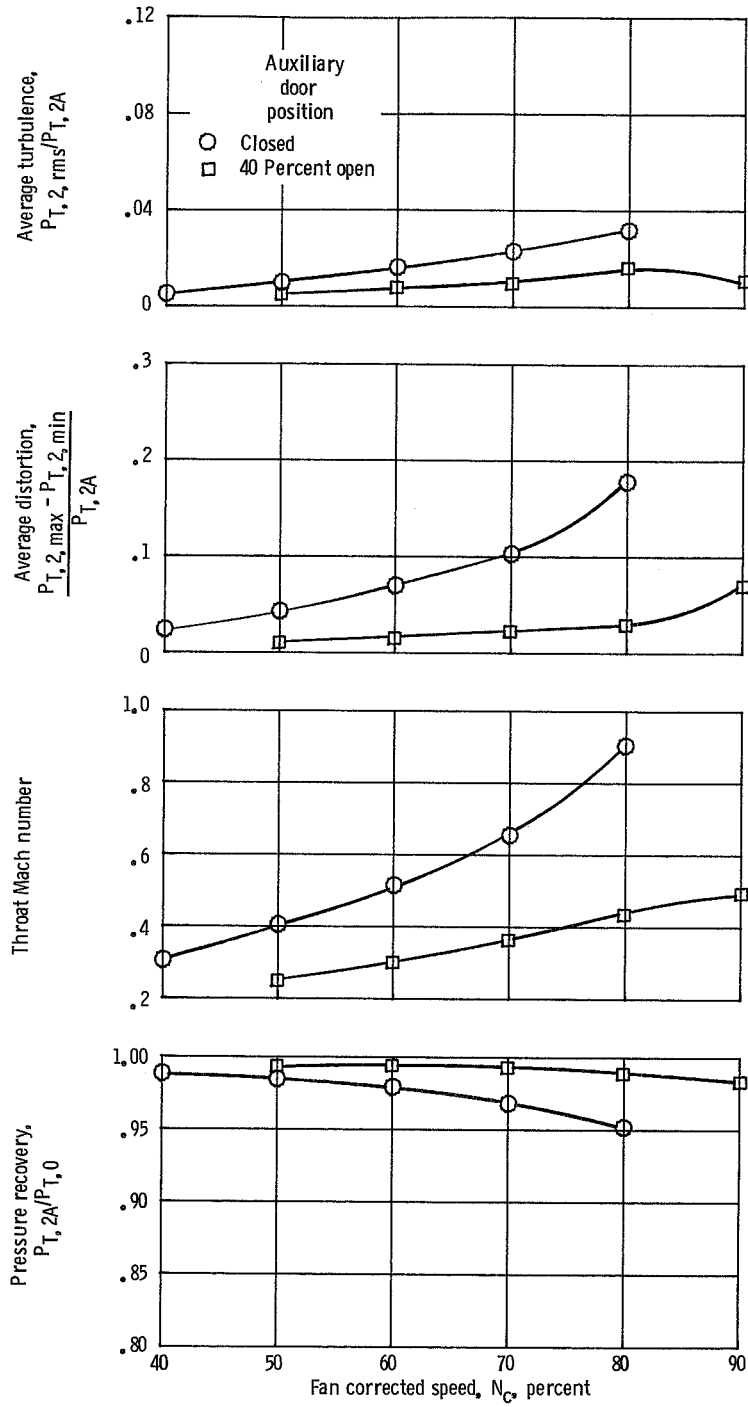
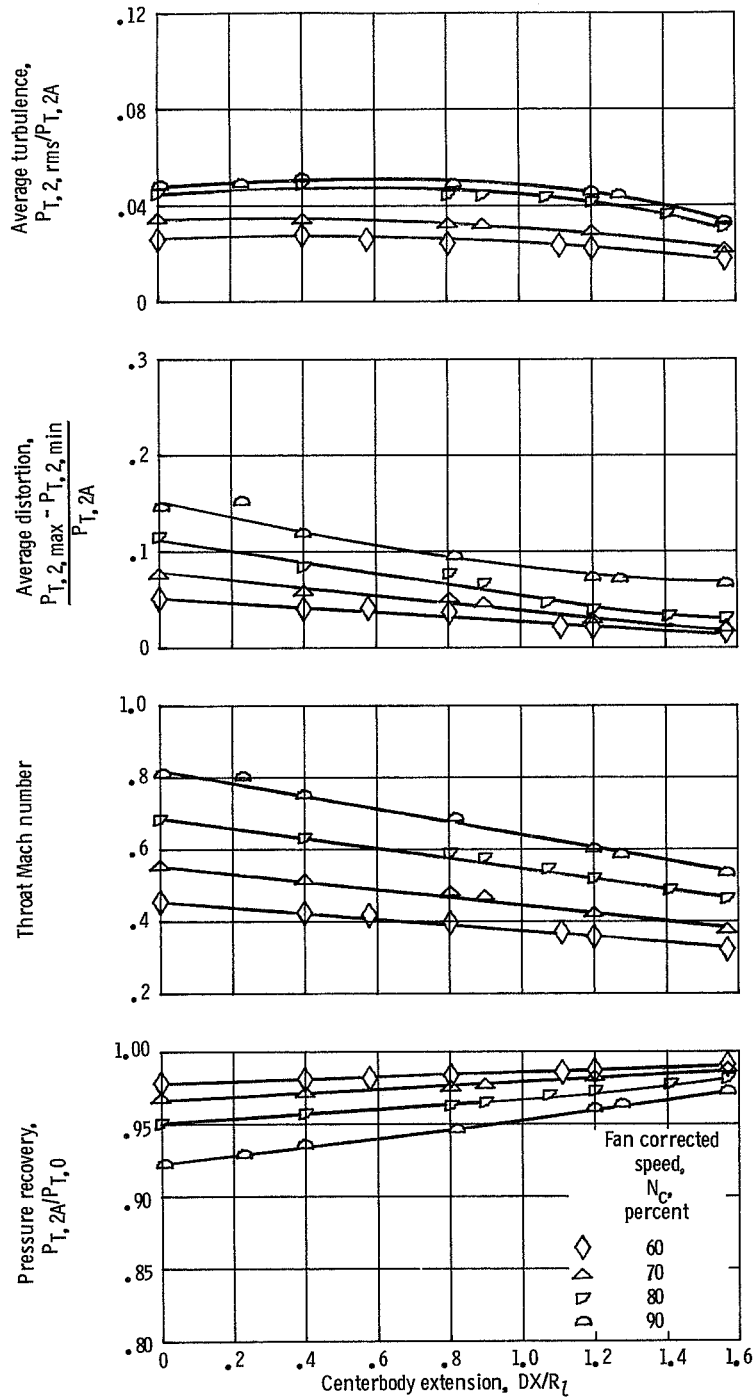


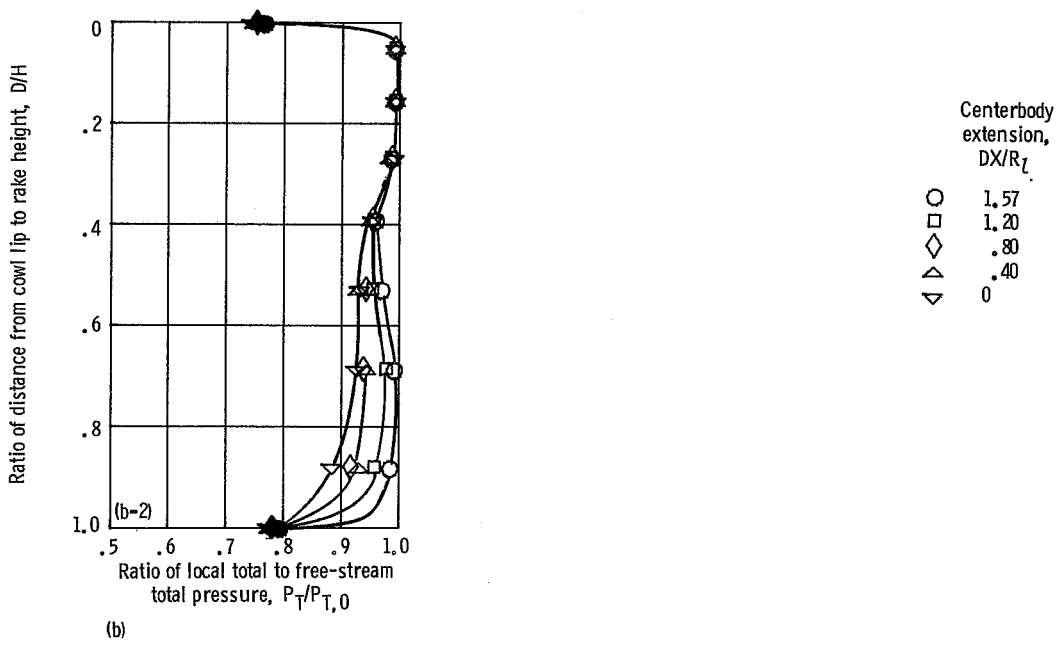
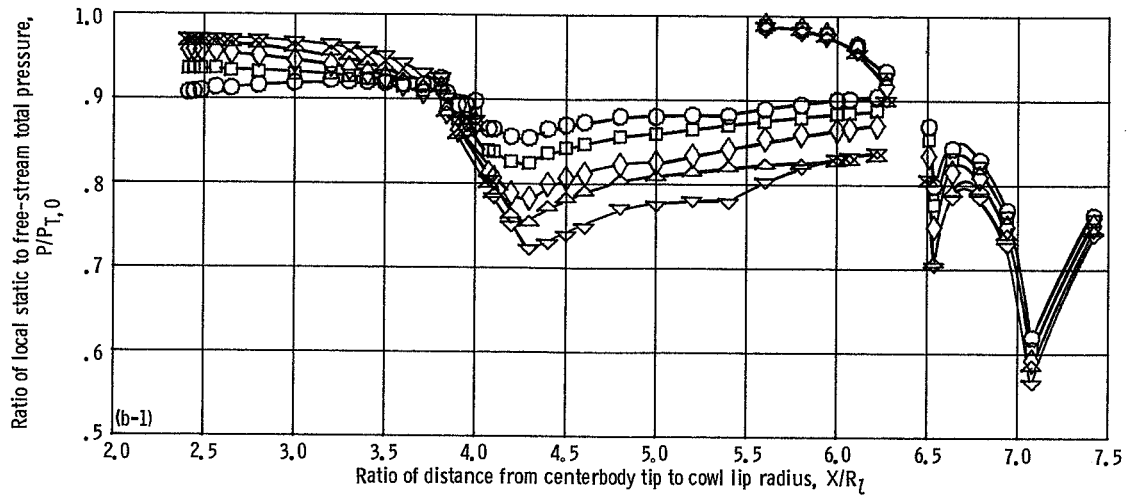
Figure 13. — Effect of 40-percent blunt auxiliary door flow on baseline inlet peak recovery performance with bellmouth cowl lip,  $M_0=0$ , and bleeds closed.



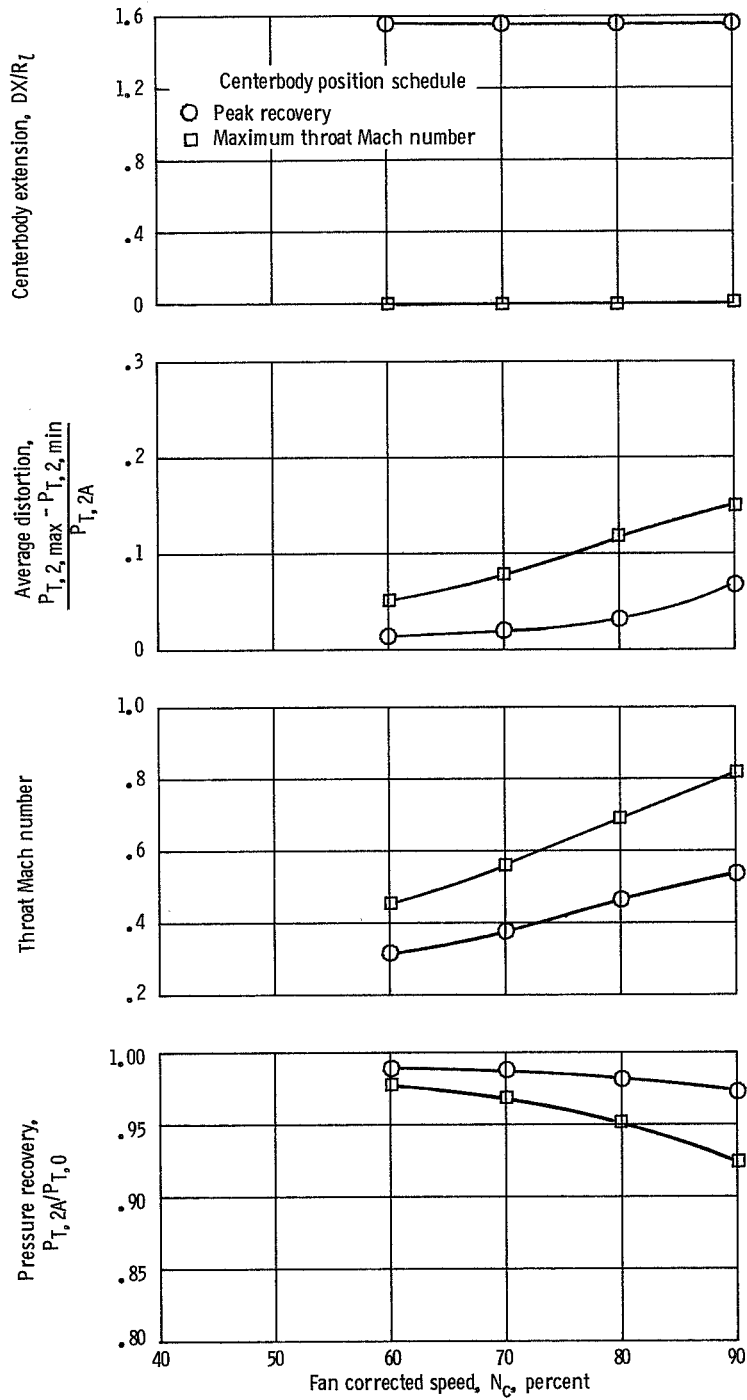
(a)

(a) Aerodynamic performance.

Figure 14. - Baseline inlet performance with bellmouth cowl lip, 40-percent blunt auxiliary doors open,  $M_0=0$ , and bleeds open.



(b-1) Cowl surface.  
 (b-2) Compressor face rake ( $X/R_L=7.42$ ).  
 (b) Inlet pressure distributions. Fan speed, 80 percent. (Lip rake at  $X/R_L=2.63$  and throat rake at  $X/R_L=4.30$  not installed.)  
 Figure 14. —Continued.



(c)

(c) Performance maps.  
 Figure 14. — Concluded.

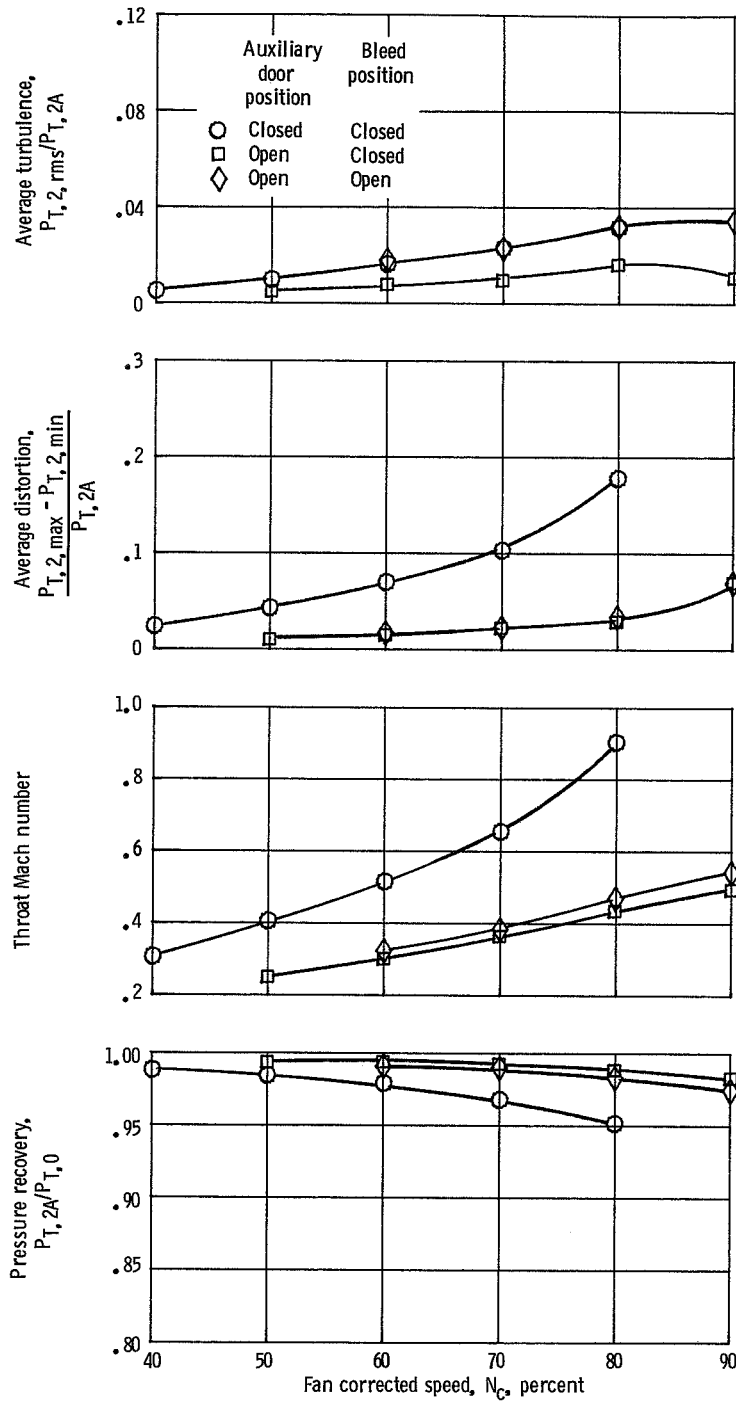
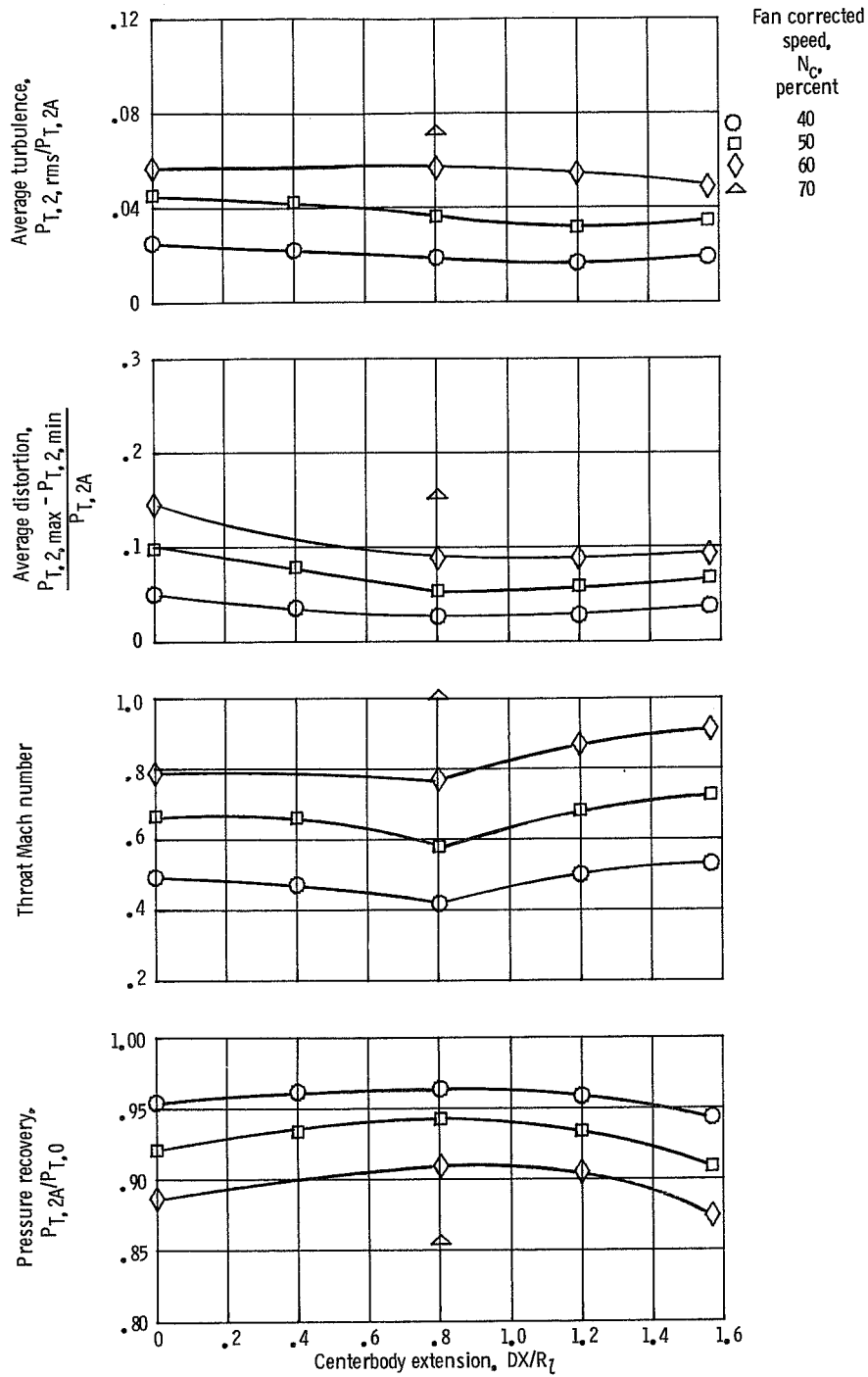


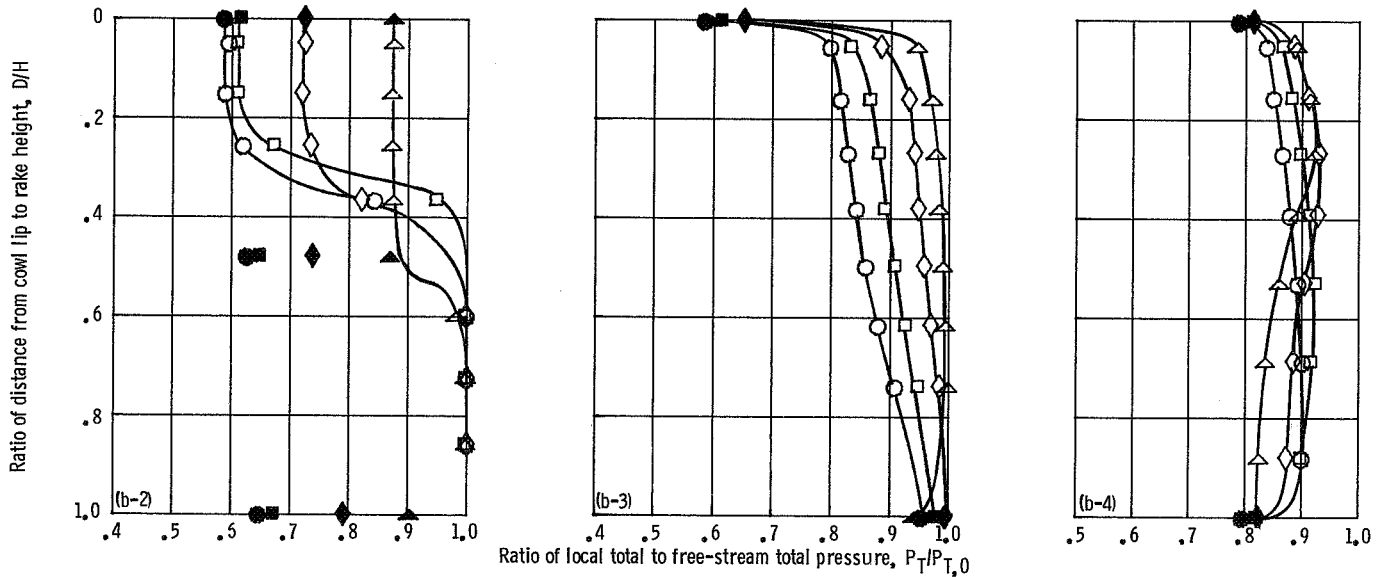
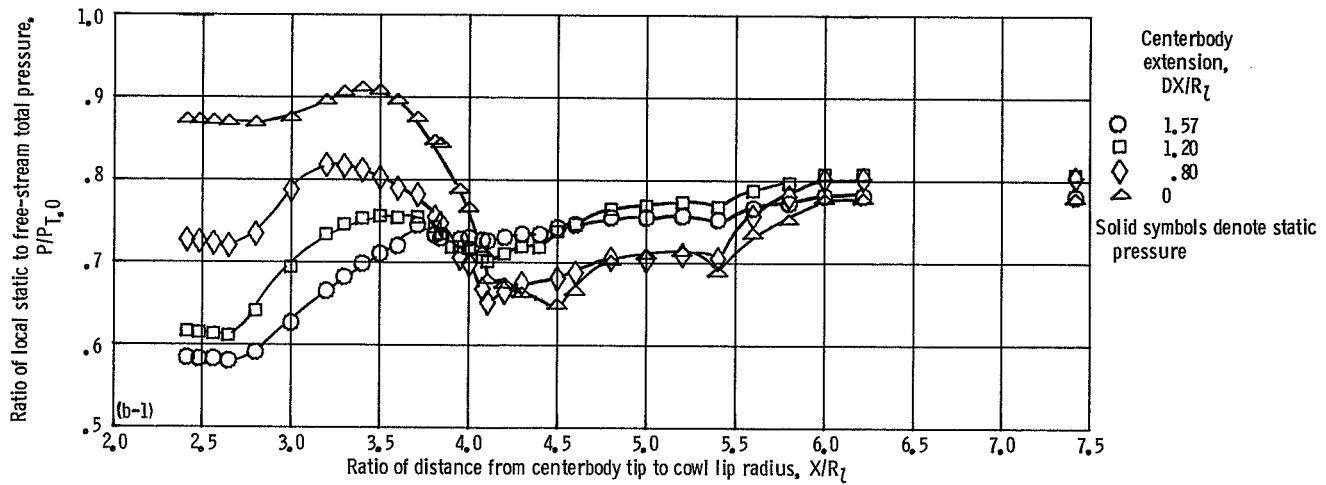
Figure 15. —Effect of bleed inflow on baseline inlet peak recovery performance for bellmouth cowl lip and  $M_0=0$ .



(a)

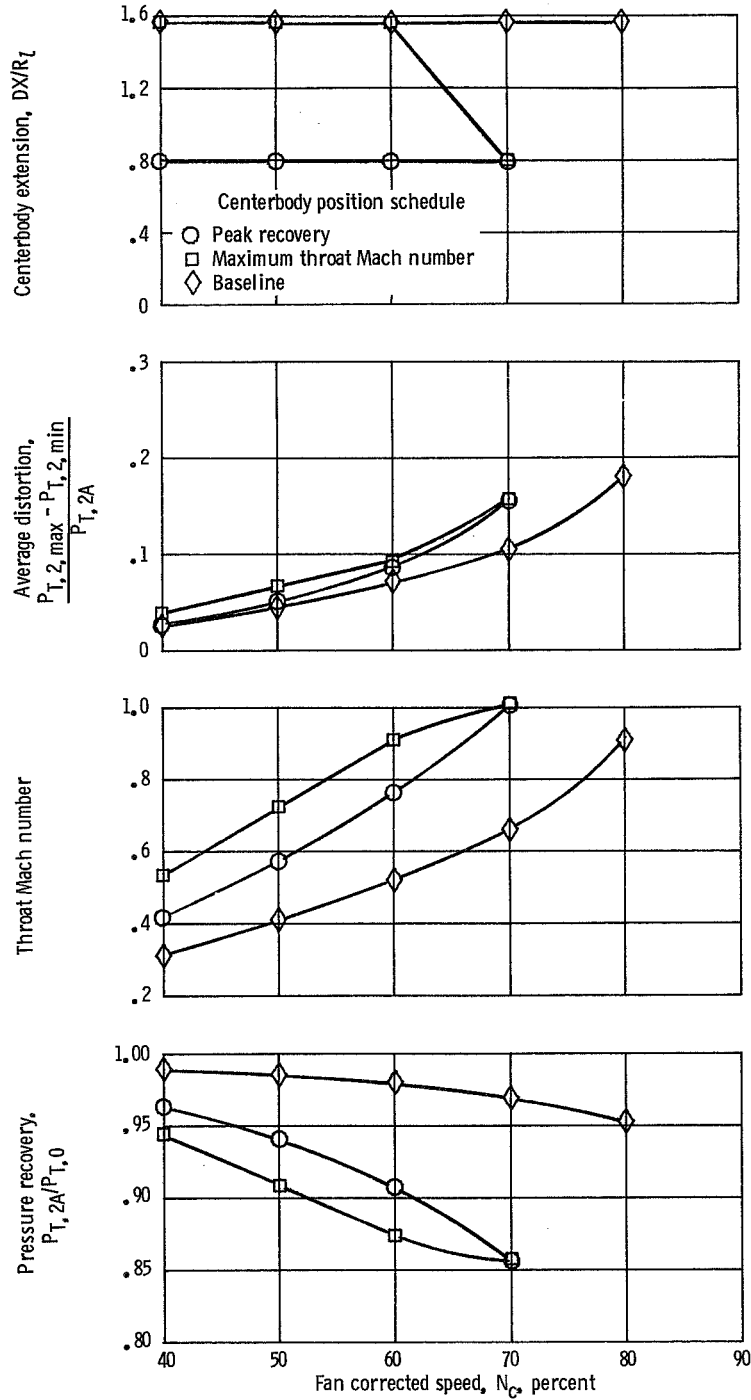
(a) Aerodynamic performance.

Figure 16. — Inlet performance with sharp cowl lip, auxiliary doors closed,  $M_0=0$ , and bleeds closed.



(b-1) Cowl surface.  
 (b-2) Lip rake ( $X/R_l=2.63$ ).  
 (b-3) Throat rake ( $X/R_l=4.30$ ).  
 (b-4) Compressor face rake ( $X/R_l=7.42$ ).  
 (b) Inlet pressure distributions. Fan speed, 60 percent.

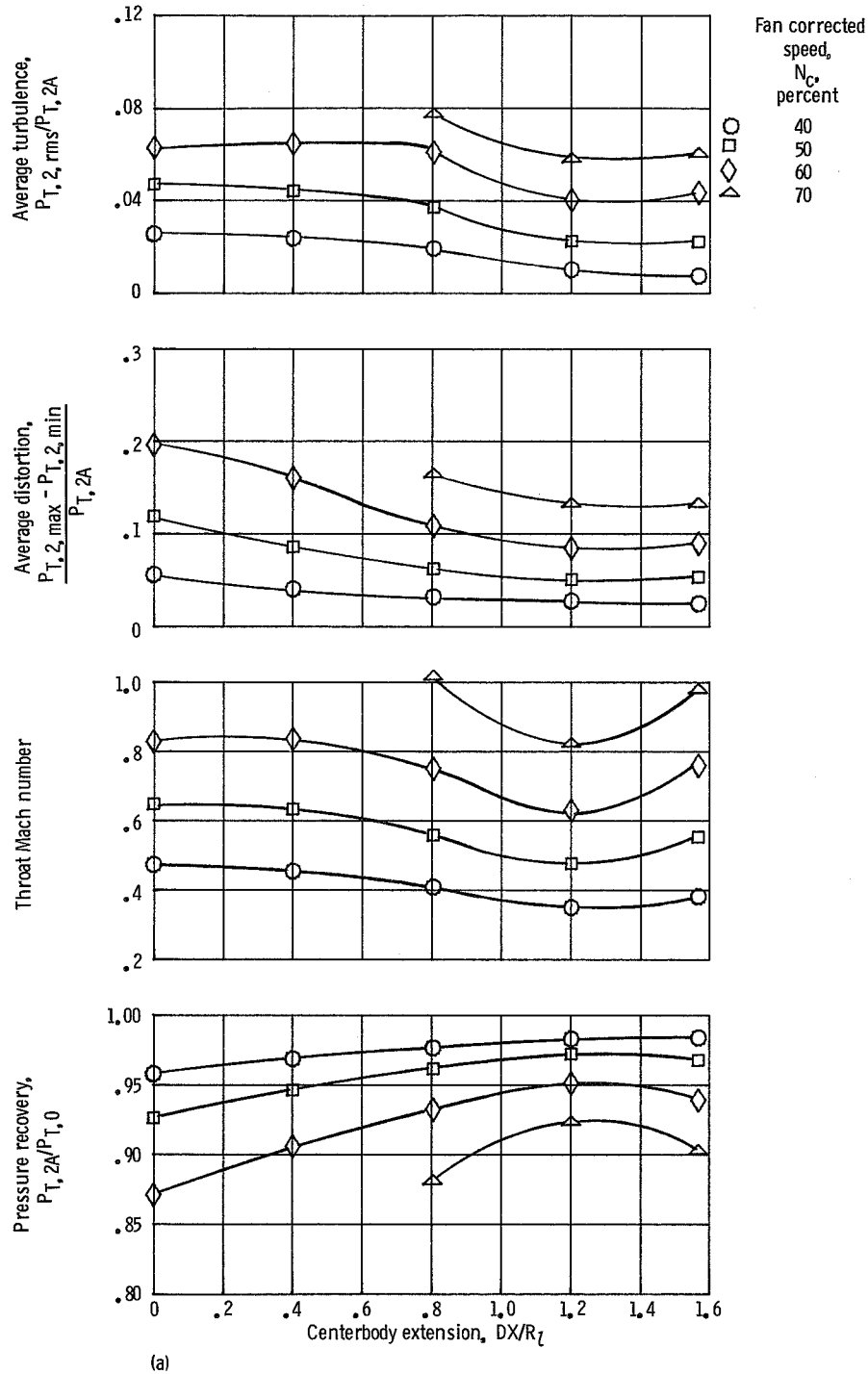
Figure 16. -Continued.



(c)

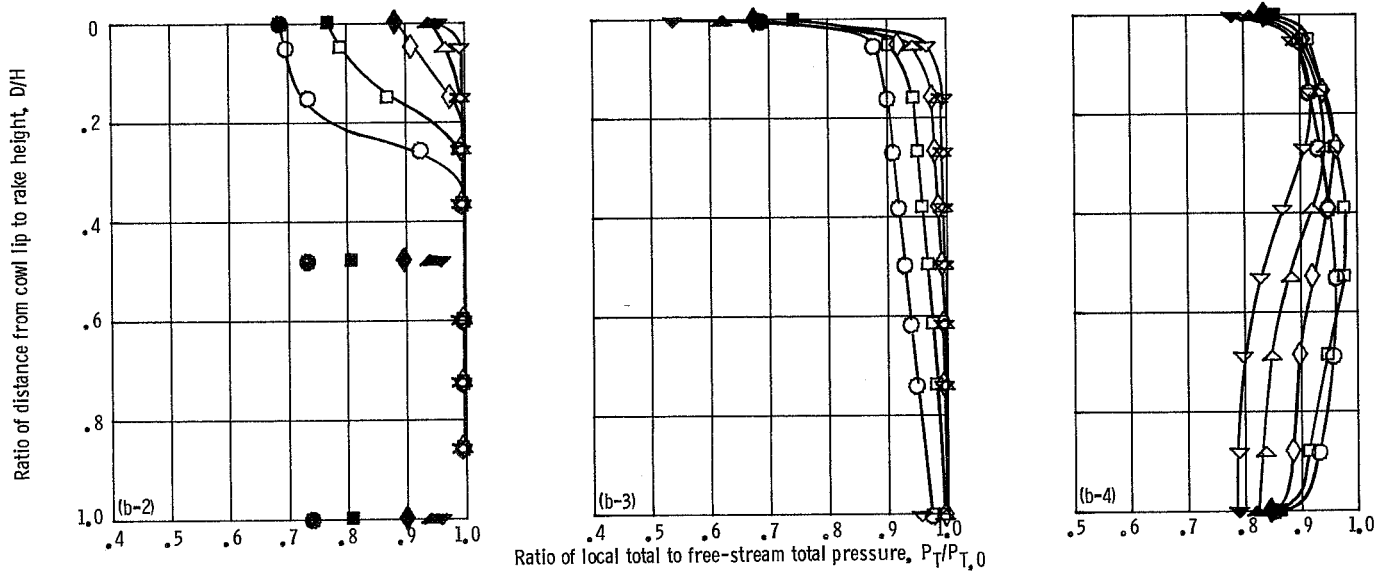
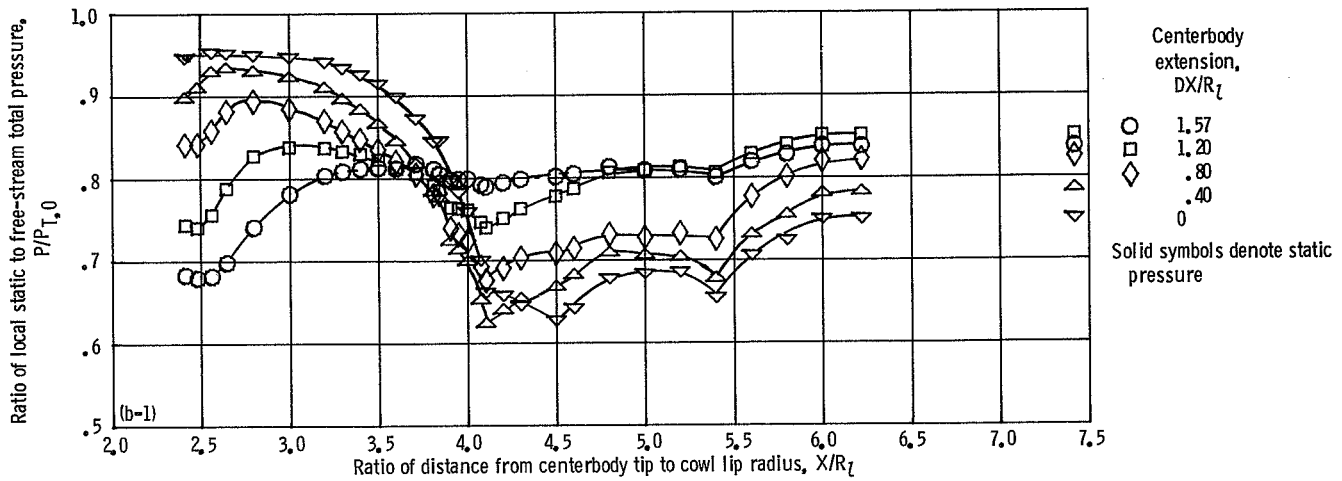
(c) Performance maps/comparison with baseline data.

Figure 16. — Concluded.



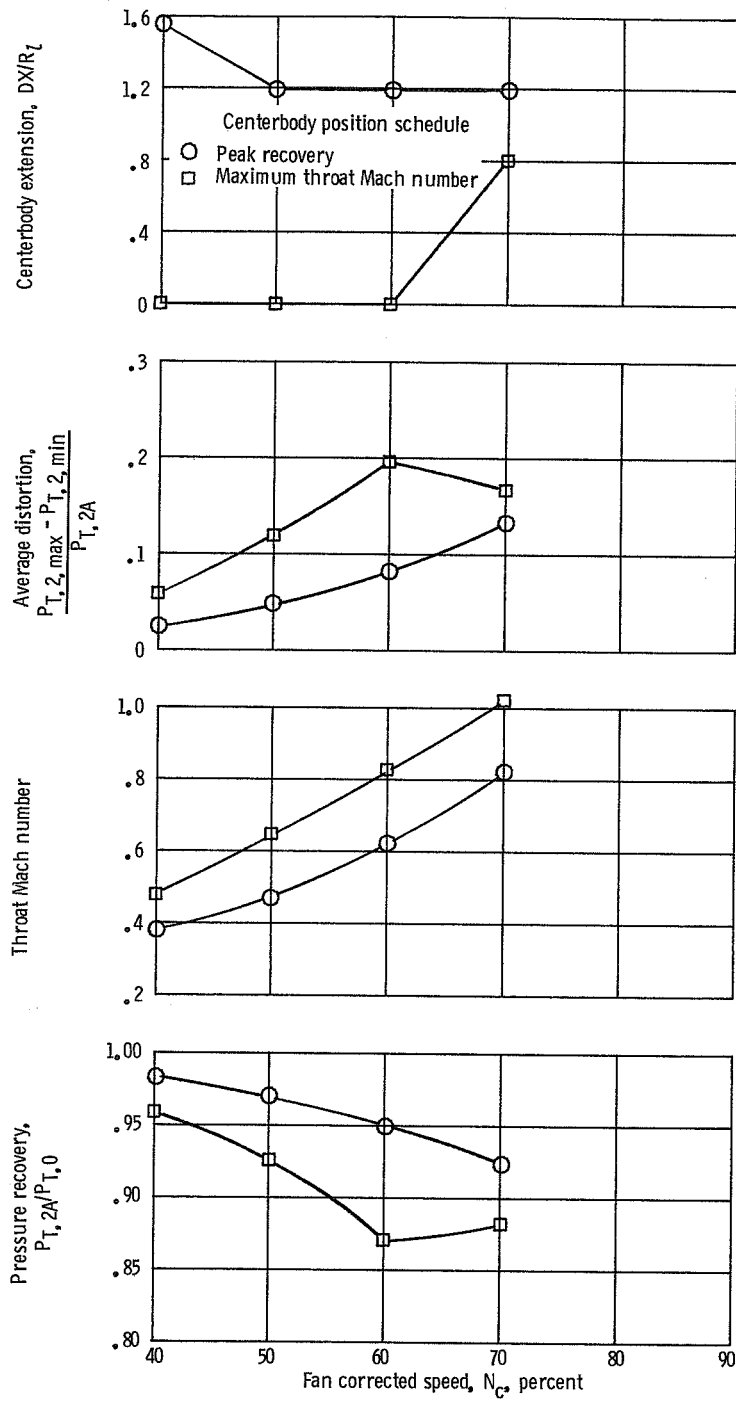
(a) Aerodynamic performance.

Figure 17.—Inlet performance with sharp cowl lip, auxiliary doors closed,  $M_0=0.2$ , and bleeds closed.



(b-1) Cowl surface.  
 (b-2) Lip rake ( $X/R_l=2.63$ ).  
 (b-3) Throat rake ( $X/R_l=4.30$ ).  
 (b-4) Compressor face rake ( $X/R_l=7.42$ ).  
 (b) Inlet pressure distributions. Fan speed, 60 percent.

Figure 17.—Continued.



(c) Performance maps.  
Figure 17.—Concluded.

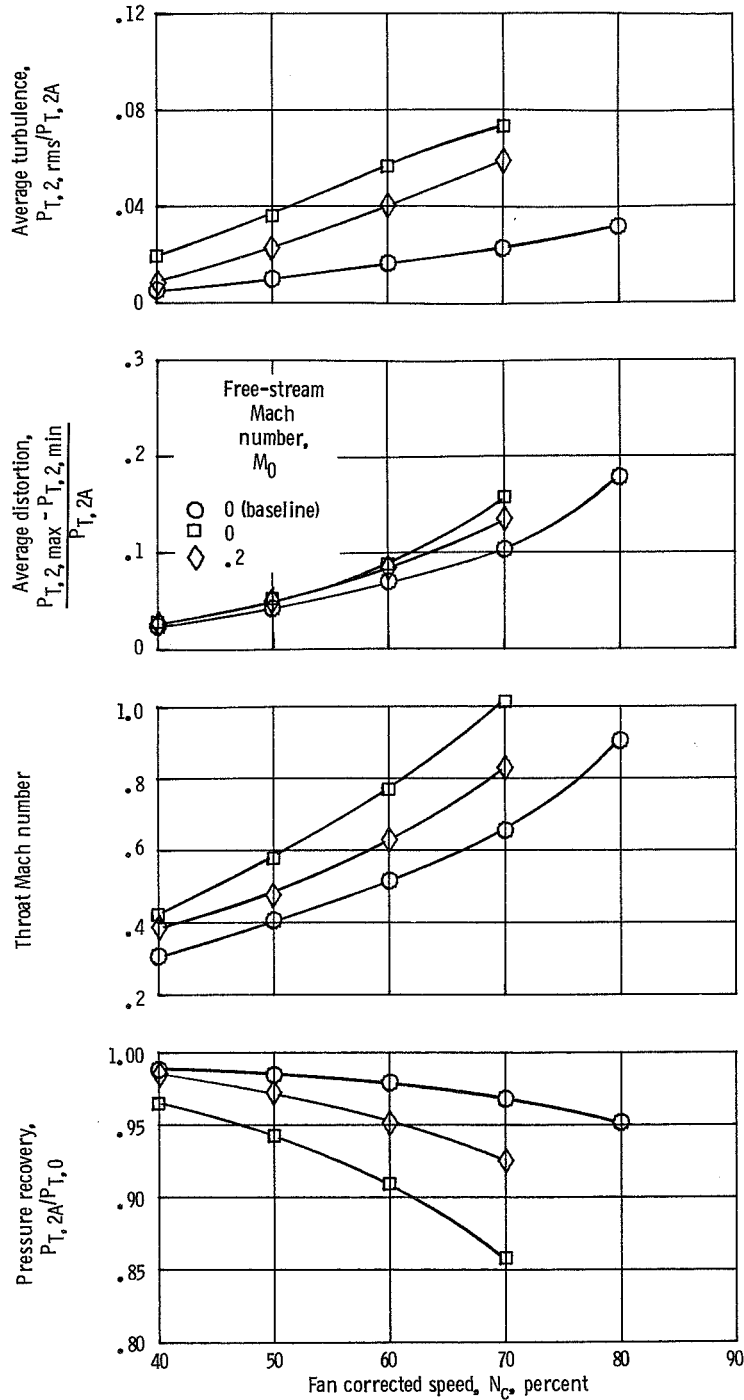
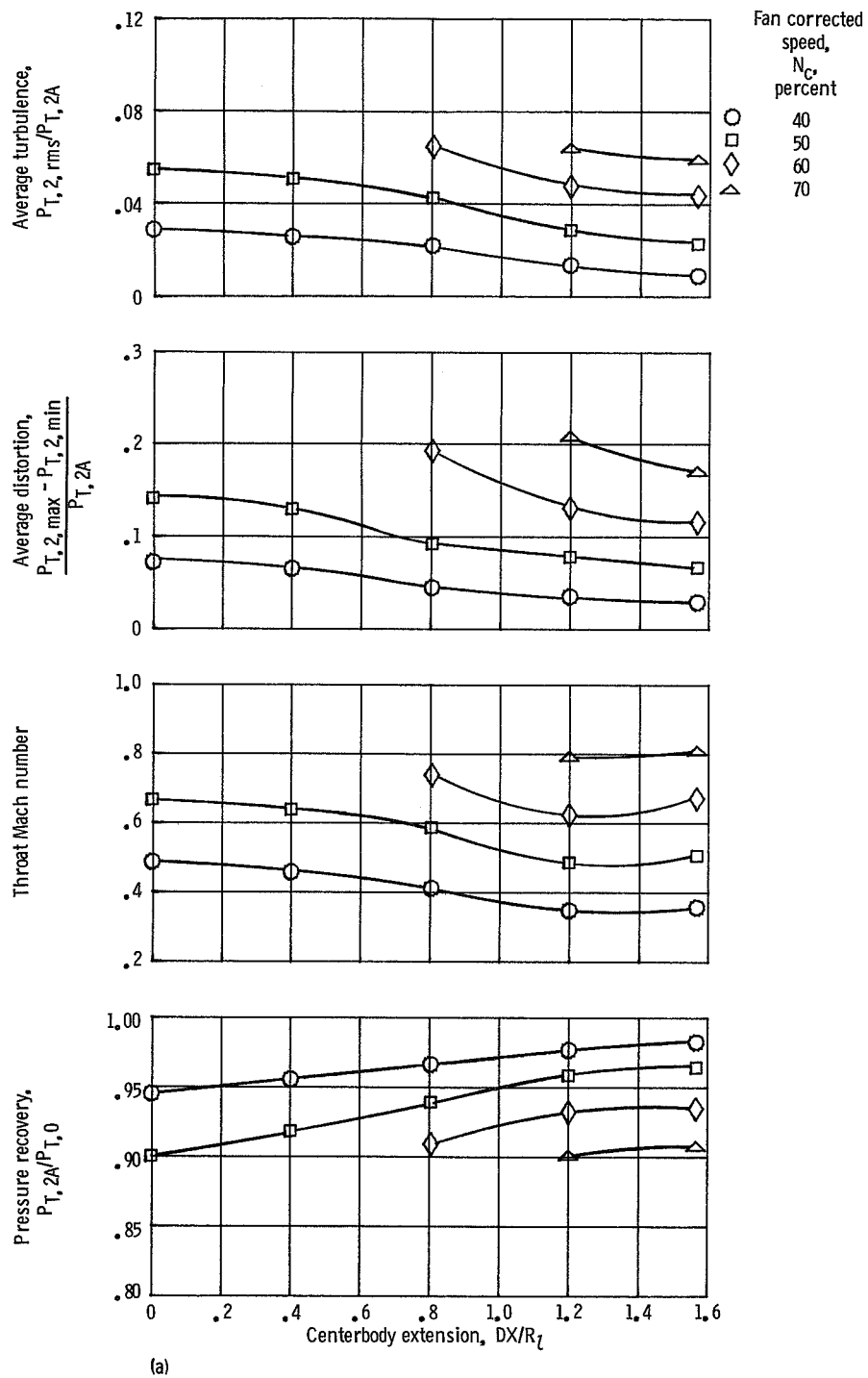
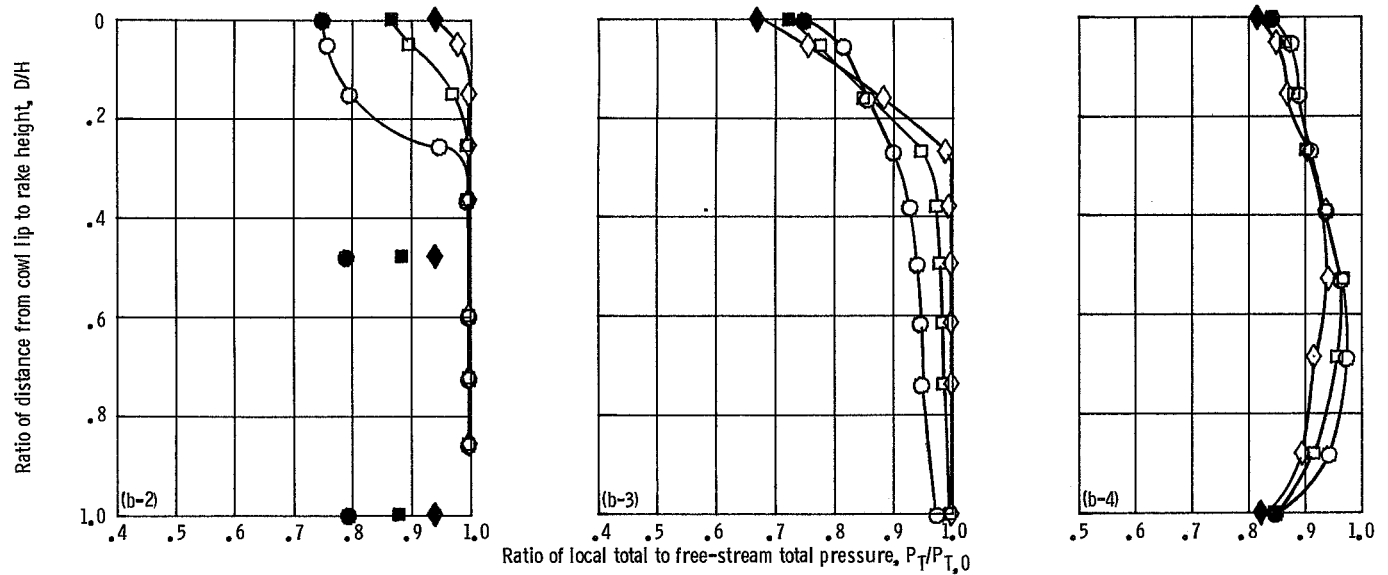
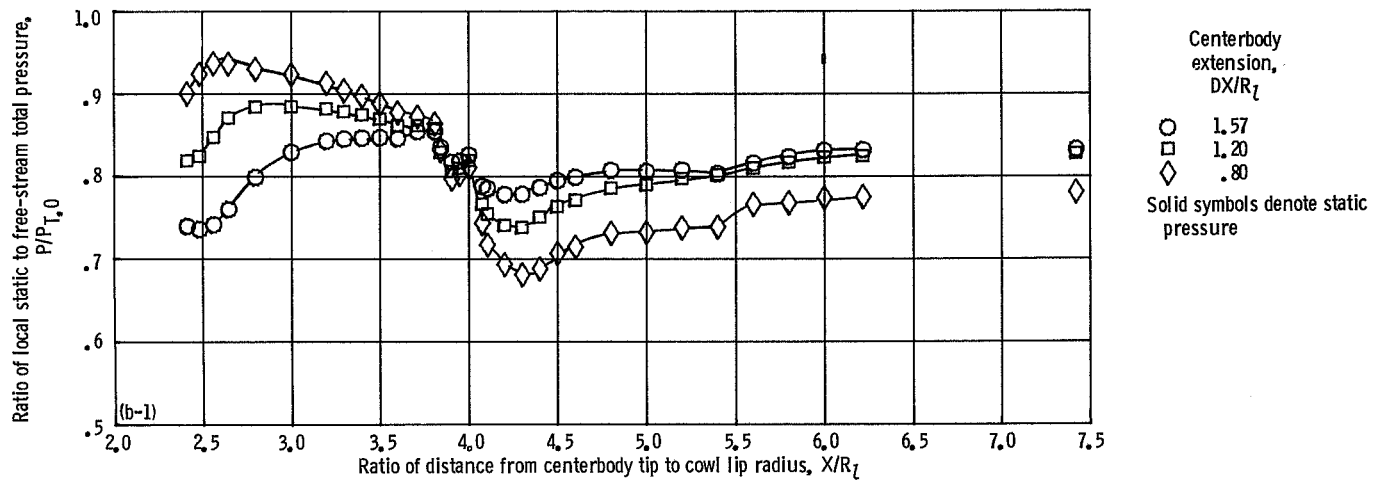


Figure 18.—Effect of free-stream Mach number on inlet peak recovery performance with sharp cowl lip, auxiliary doors closed, and bleeds closed.



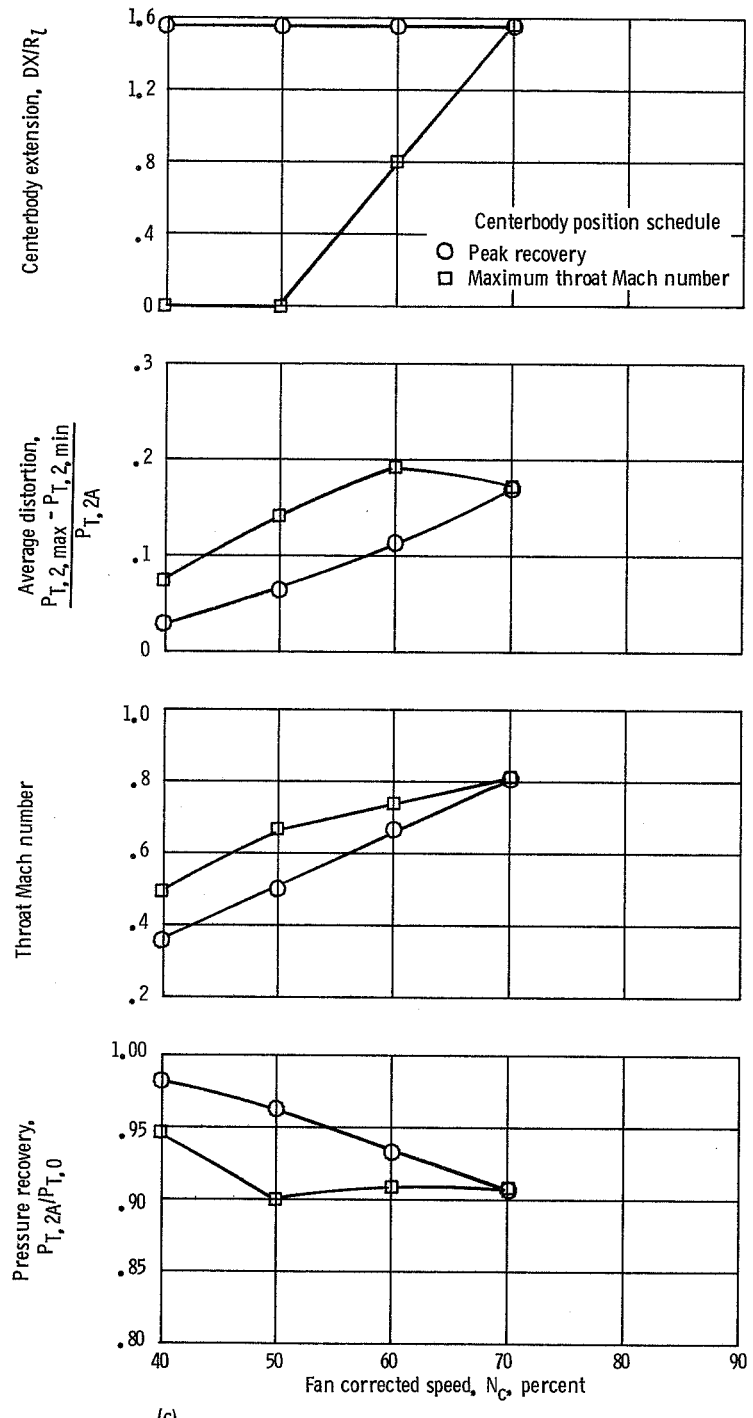
(a) Aerodynamic performance.

Figure 19. -Inlet performance with sharp cowl lip, auxiliary doors closed,  $M_0=0.2$ , and bleeds open.



(b-1) Cowl surface.  
 (b-2) Lip rake ( $X/R_l=2.63$ ).  
 (b-3) Throat rake ( $X/R_l=4.30$ ).  
 (b-4) Compressor face rake ( $X/R_l=7.42$ ).  
 (b) Inlet pressure distributions. Fan speed, 60 percent.

Figure 19.—Continued.



(c) Performance maps.  
 Figure 19. - Concluded.

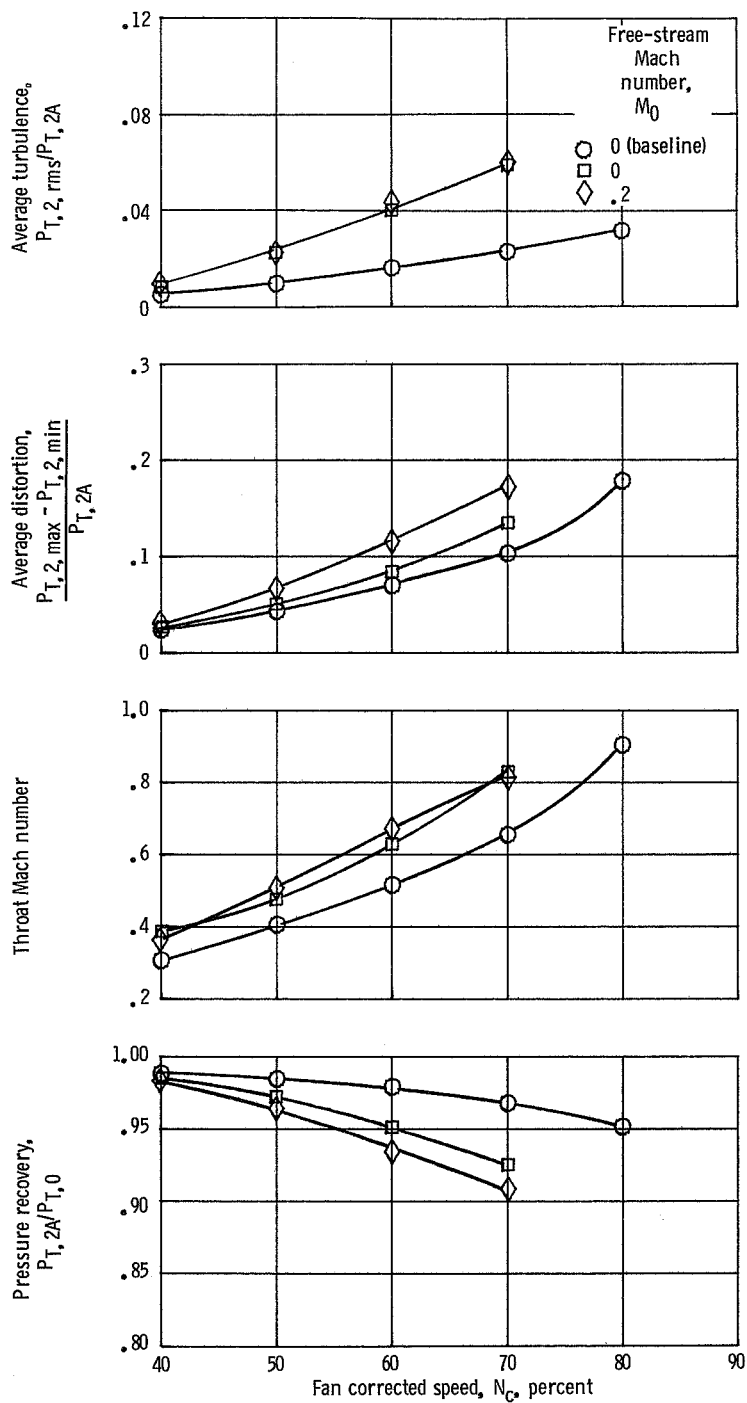
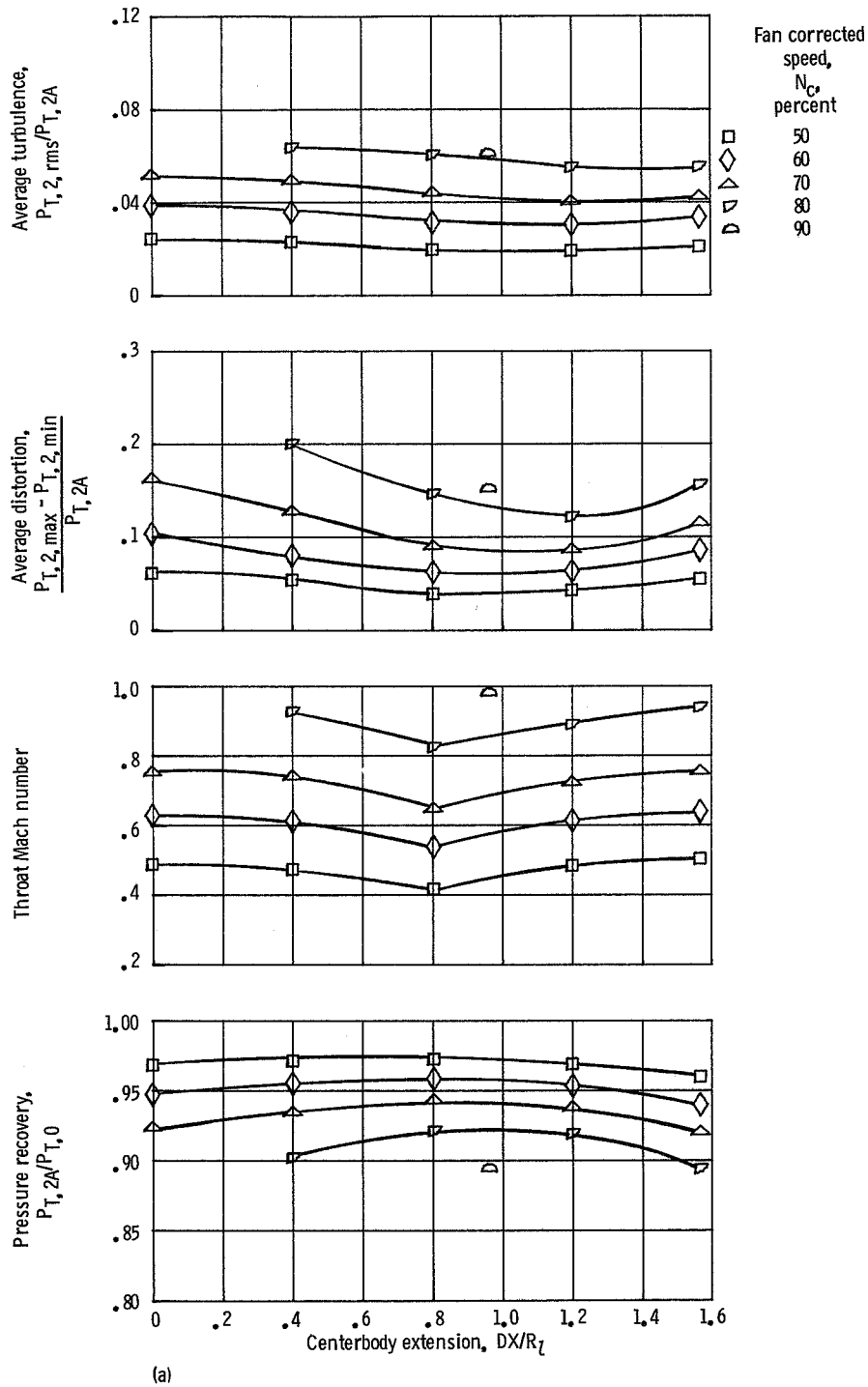
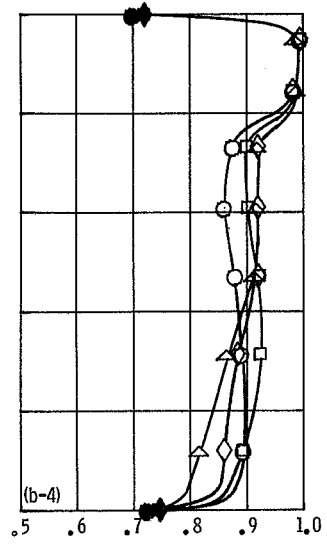
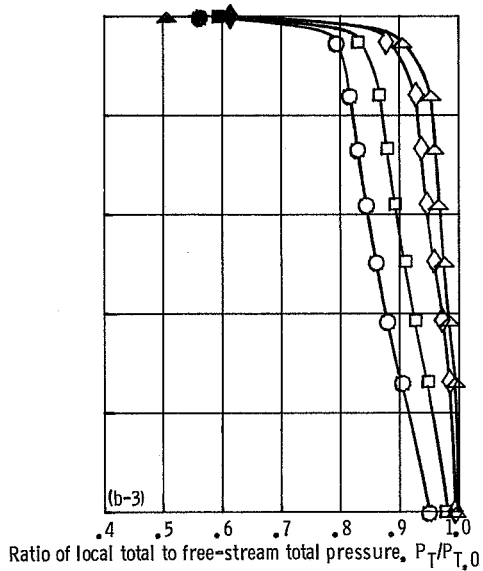
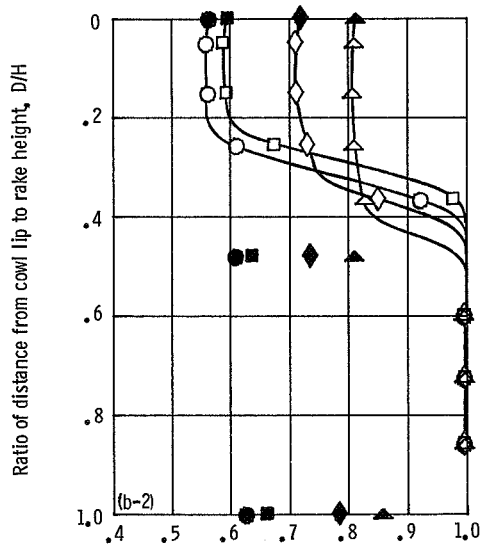
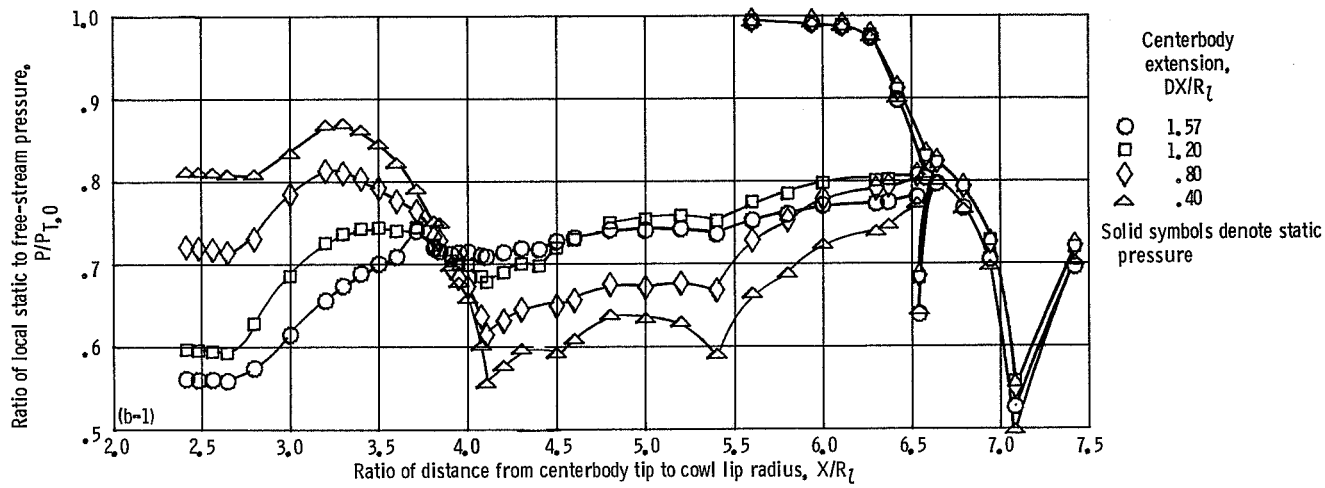


Figure 20. — Effect of bleed inflow on inlet peak recovery performance with sharp cowl lip, auxiliary doors closed, and  $M_0=0.2$ .

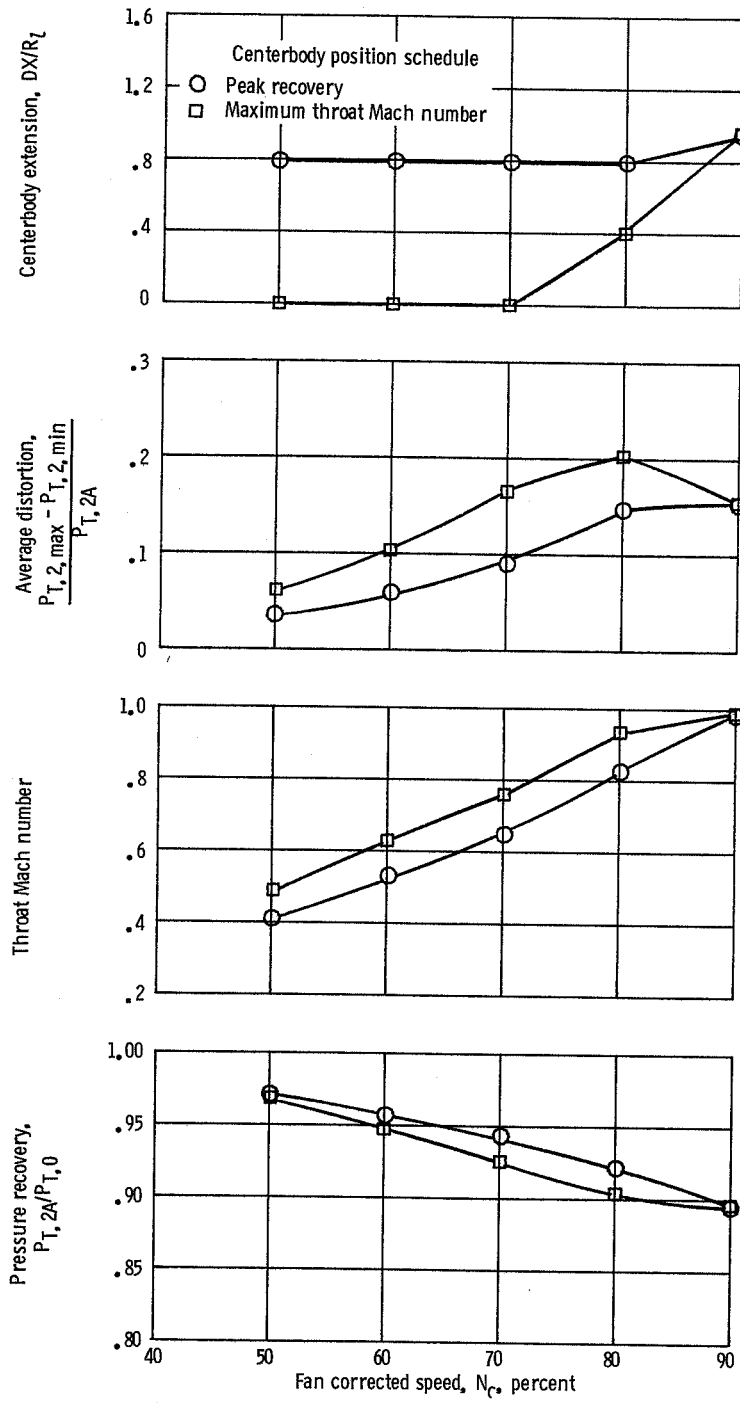


(a) Aerodynamic performance.  
 Figure 21. — Inlet performance with sharp cowl lip, 20-percent auxiliary doors open,  $M_0=0$ , and bleeds closed.



(b-1) Cowl surface.  
 (b-2) Lip rake ( $X/R_l=2.63$ ).  
 (b-3) Throat rake ( $X/R_l=4.30$ ).  
 (b-4) Compressor face rake ( $X/R_l=7.42$ ).  
 (b) Inlet pressure distributions. Fan speed, 80 percent.

Figure 21. -Continued.



(c)

(c) Performance maps.  
Figure 21. — Concluded.

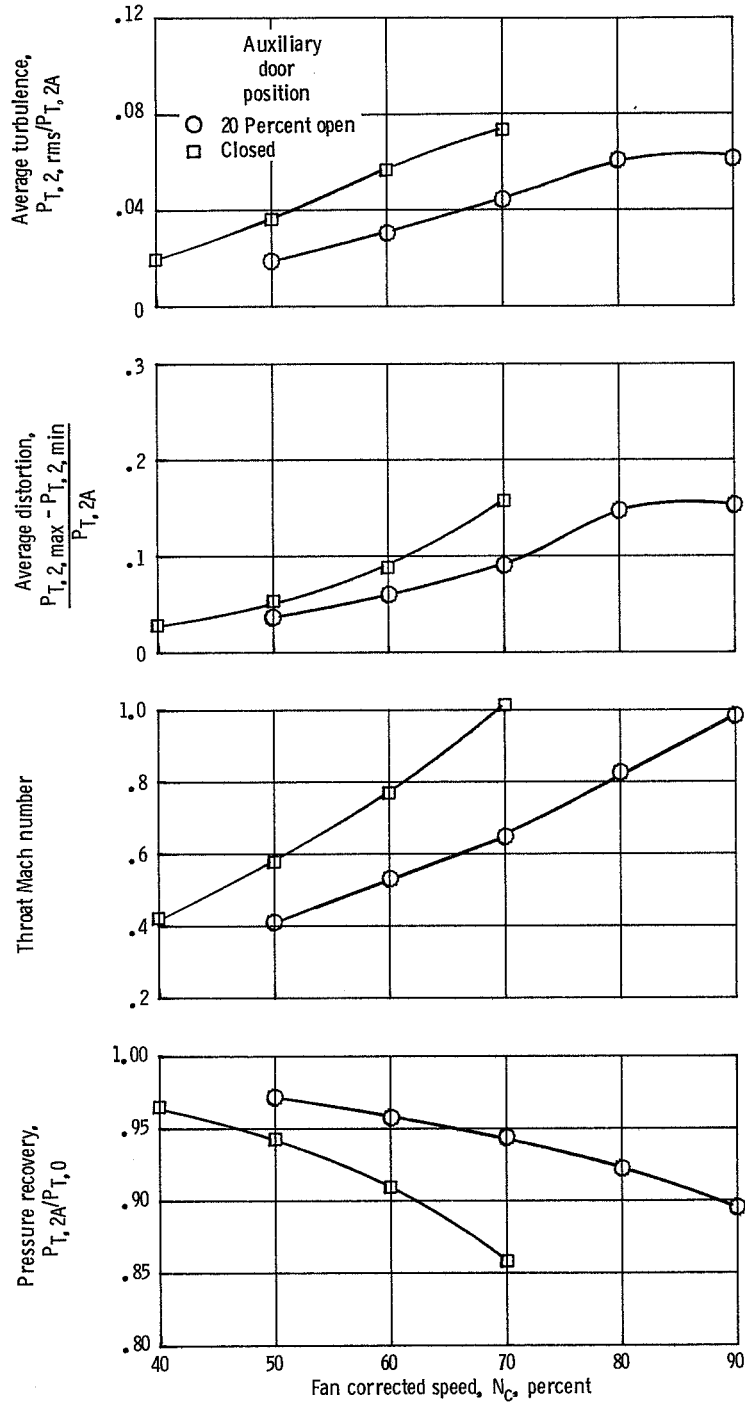
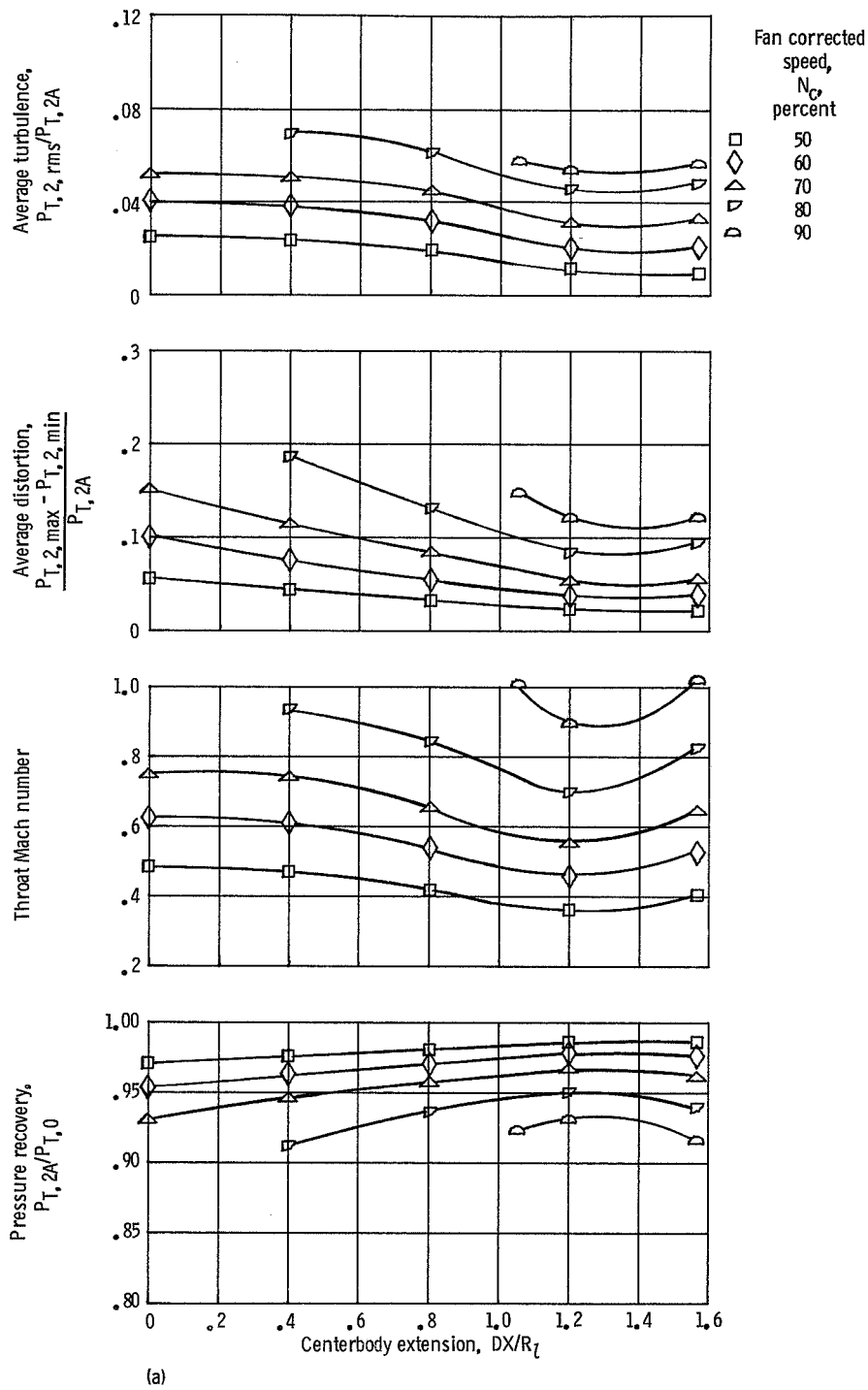
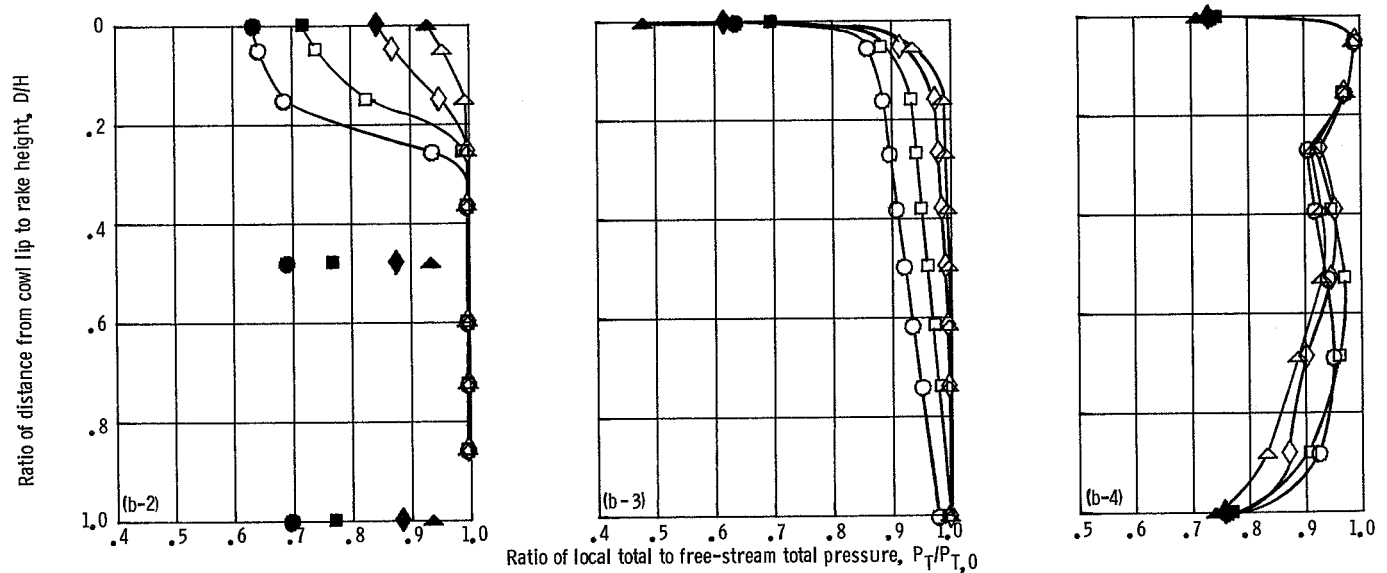
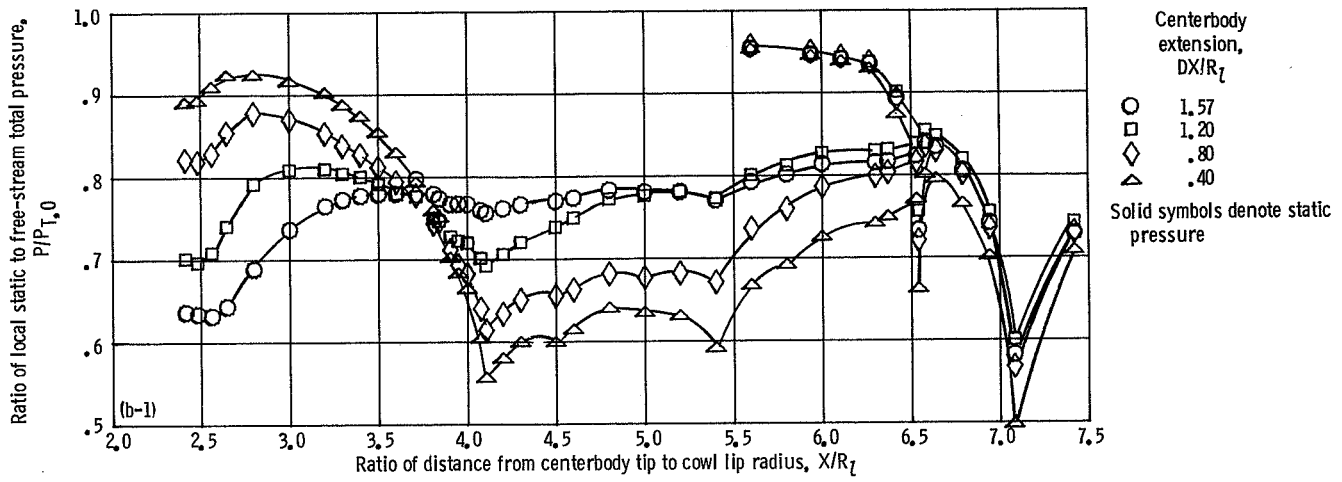


Figure 22. —Effect of 20-percent auxiliary flow on inlet peak recovery performance with sharp cowl lip,  $M_0=0$ , and bleeds closed.



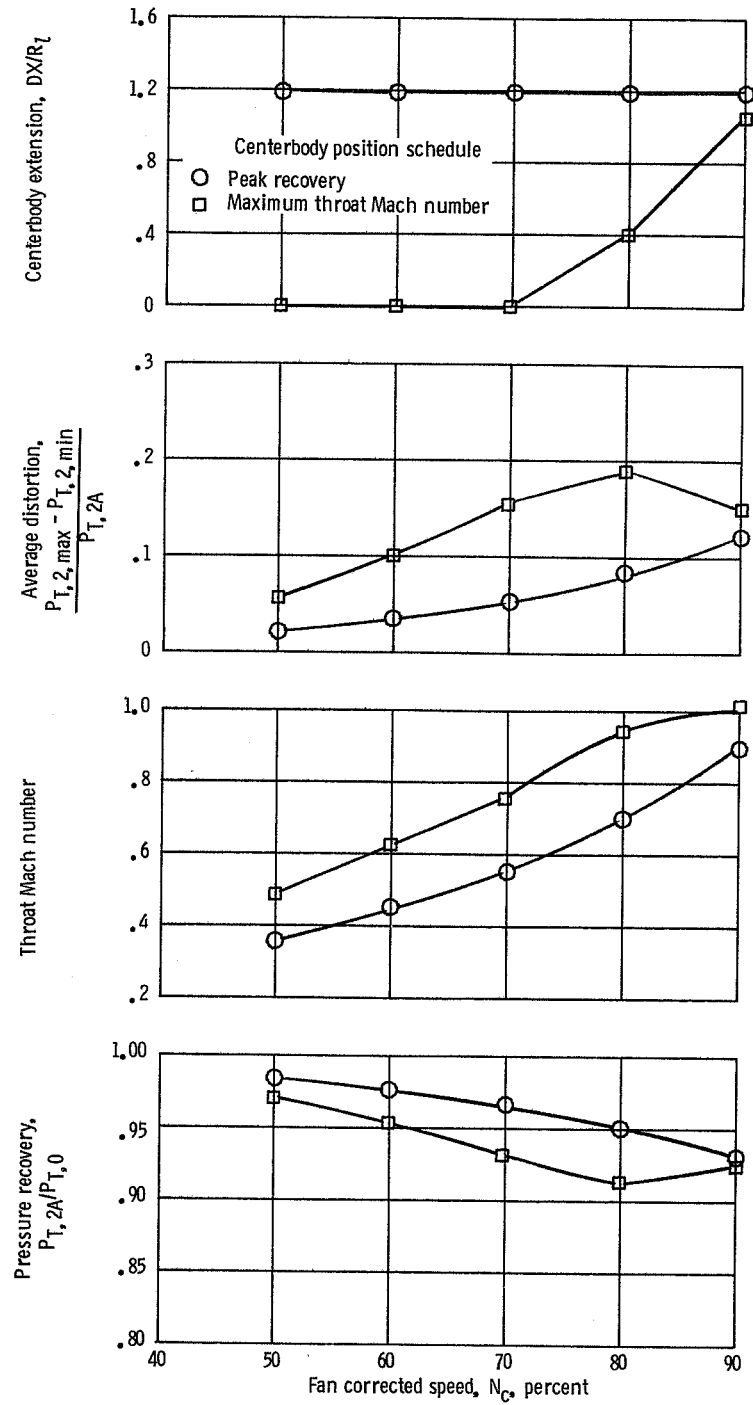
(a) Aerodynamic performance.

Figure 23.—Inlet performance with sharp cowl lip, 20-percent auxiliary doors open,  $M_0=0.2$ , and bleeds closed.



(b-1) Cowl surface.  
 (b-2) Lip rake ( $X/R_l=2.63$ ).  
 (b-3) Throat rake ( $X/R_l=4.30$ ).  
 (b-4) Compressor face rake ( $X/R_l=7.42$ ).  
 (b) Inlet pressure distributions. Fan speed, 80 percent.

Figure 23. -Continued.



(c)

(c) Performance maps.

Figure 23. — Concluded.

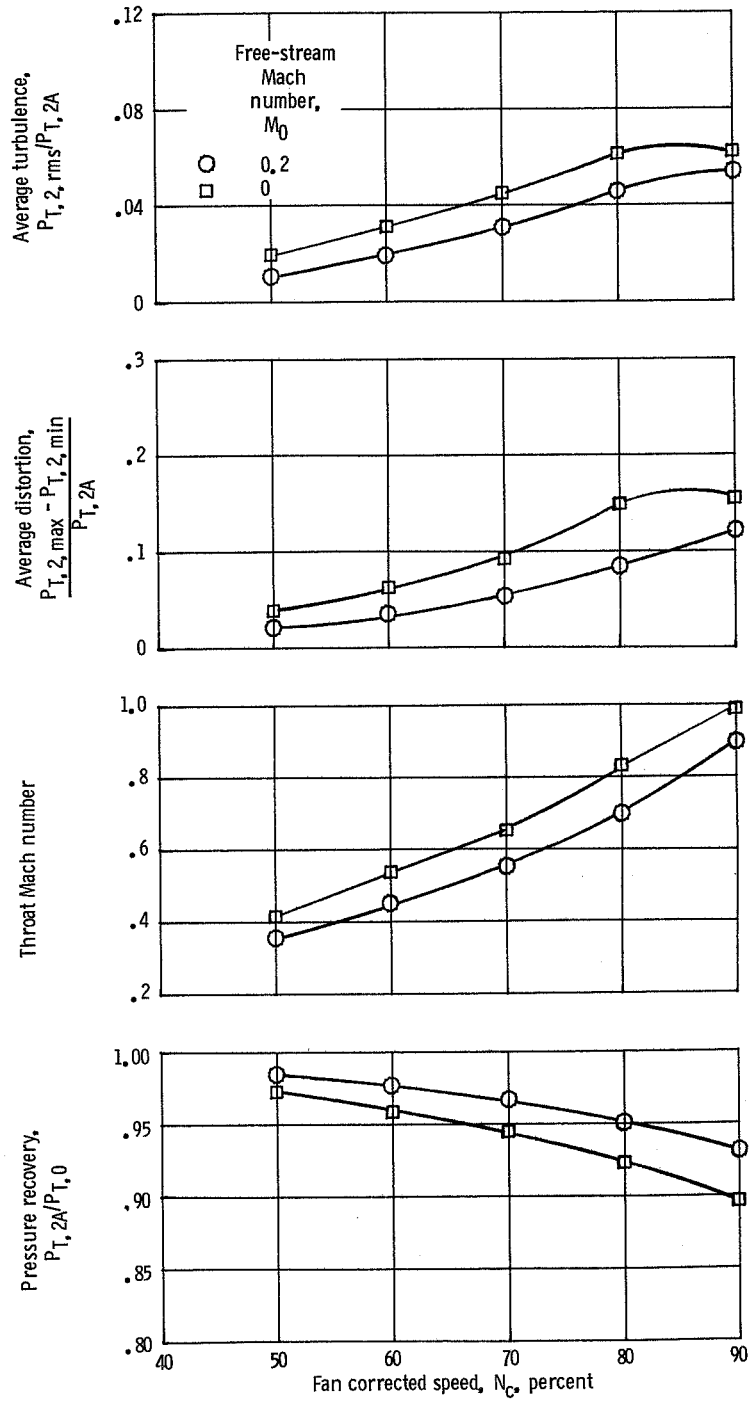
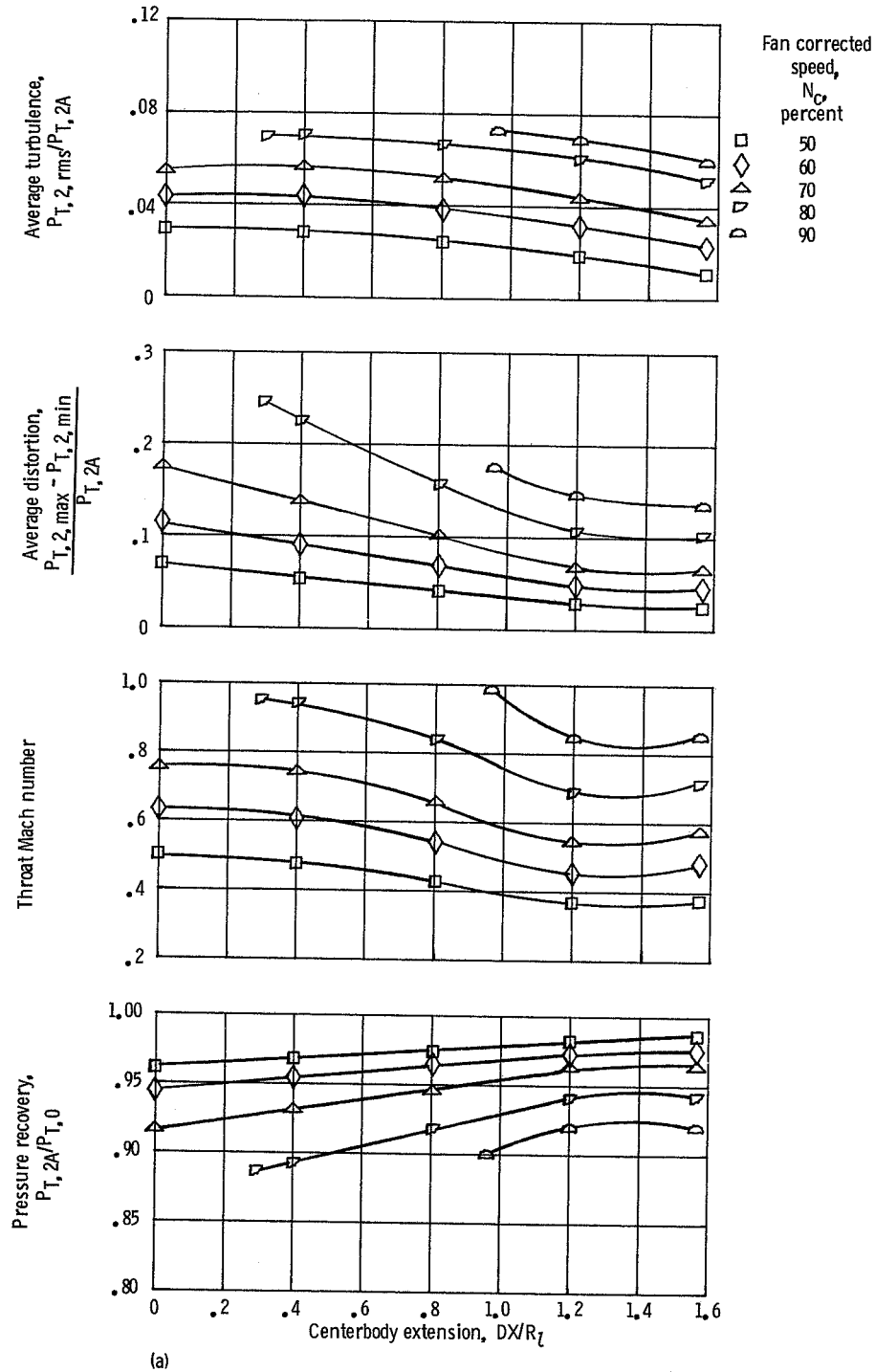
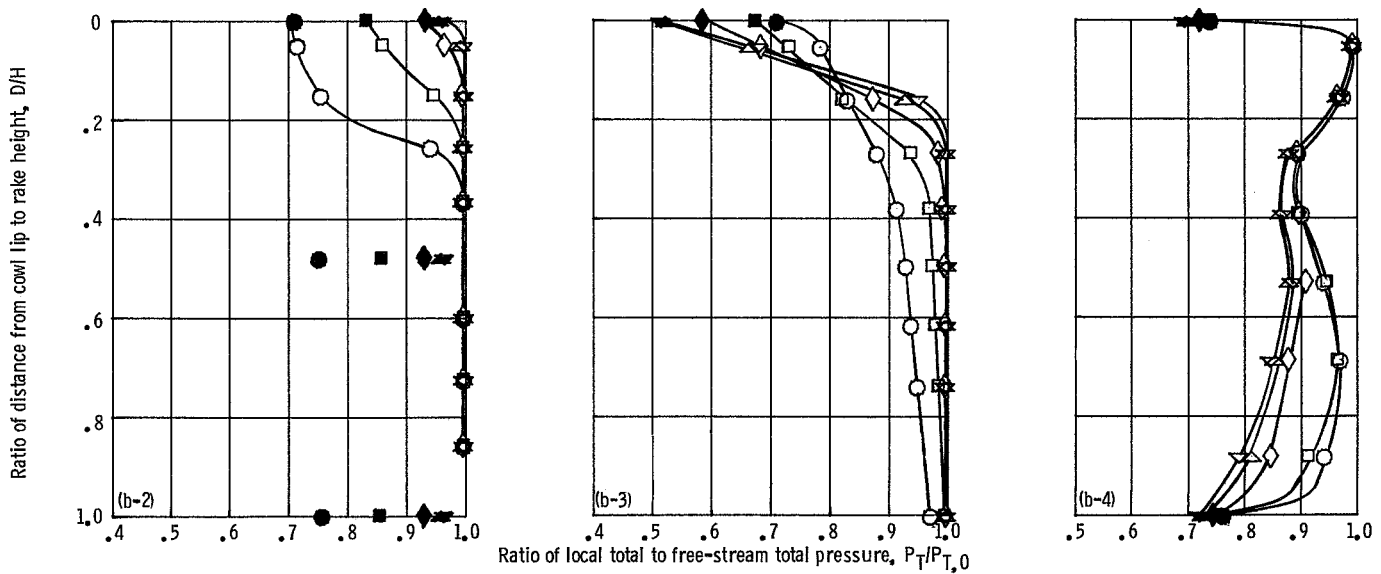
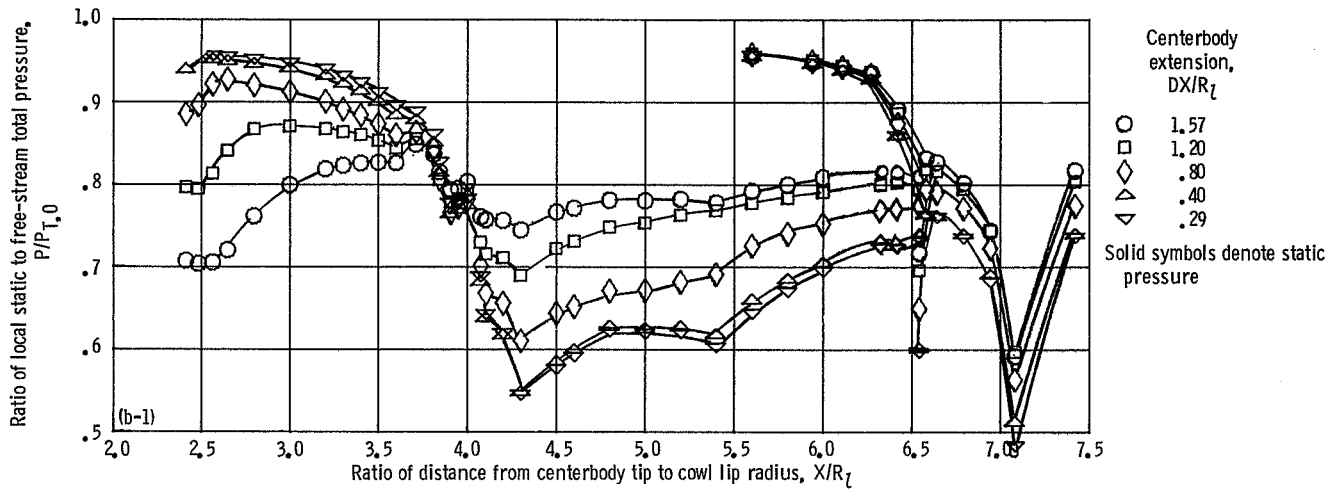


Figure 24. - Effect of free-stream Mach number on inlet peak recovery performance with sharp cowl lip, 20-percent auxiliary doors open, and bleeds closed.



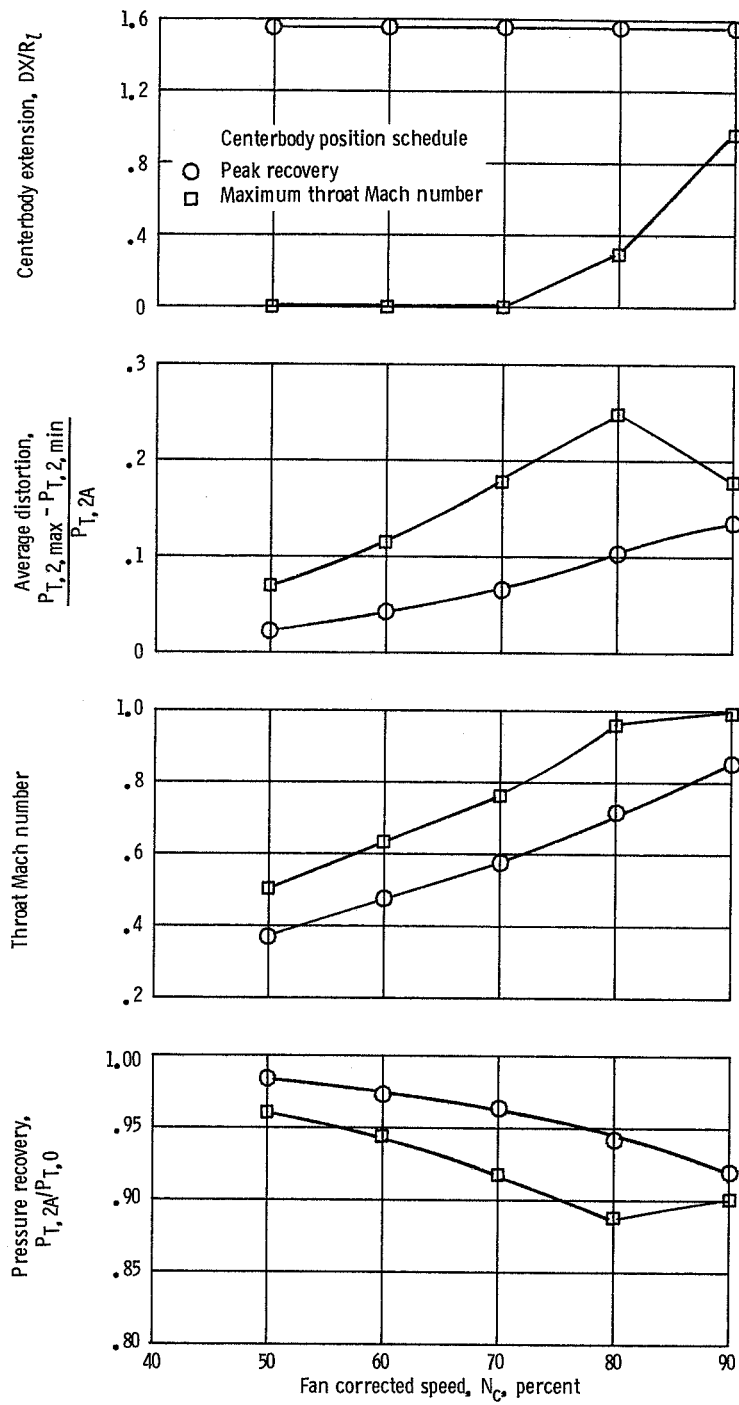
(a) Aerodynamic performance.

Figure 25. —Inlet performance with sharp cowl lip, 20-percent auxiliary doors open,  $M_0=0.2$ , and bleeds open.



(b-1) Cowl surface.  
 (b-2) Lip rake ( $X/R_l=2.63$ ).  
 (b-3) Throat rake ( $X/R_l=4.30$ ).  
 (b-4) Compressor face rake ( $X/R_l=7.42$ ).  
 (b) Inlet pressure distributions. Fan speed, 80 percent.

Figure 25. —Continued.



(c)

(c) Performance maps.

Figure 25. — Concluded.

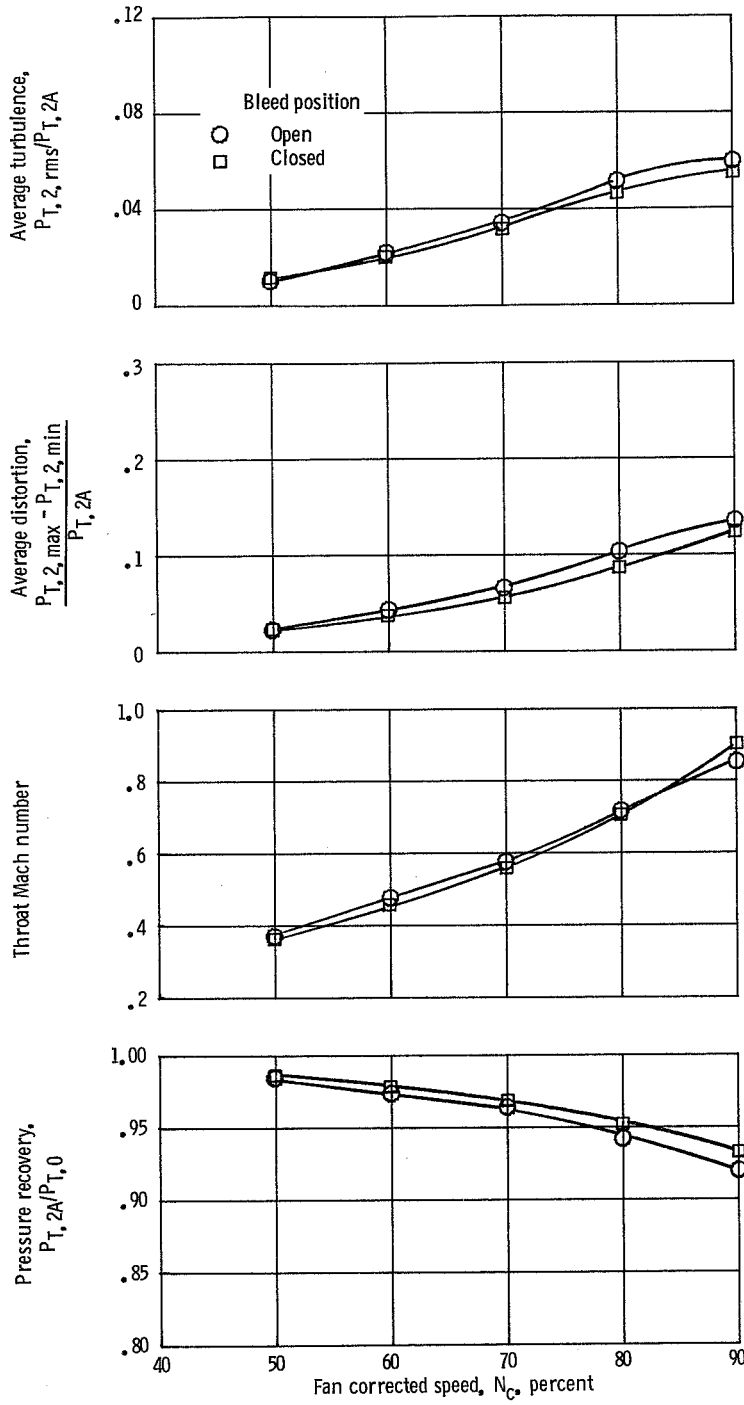
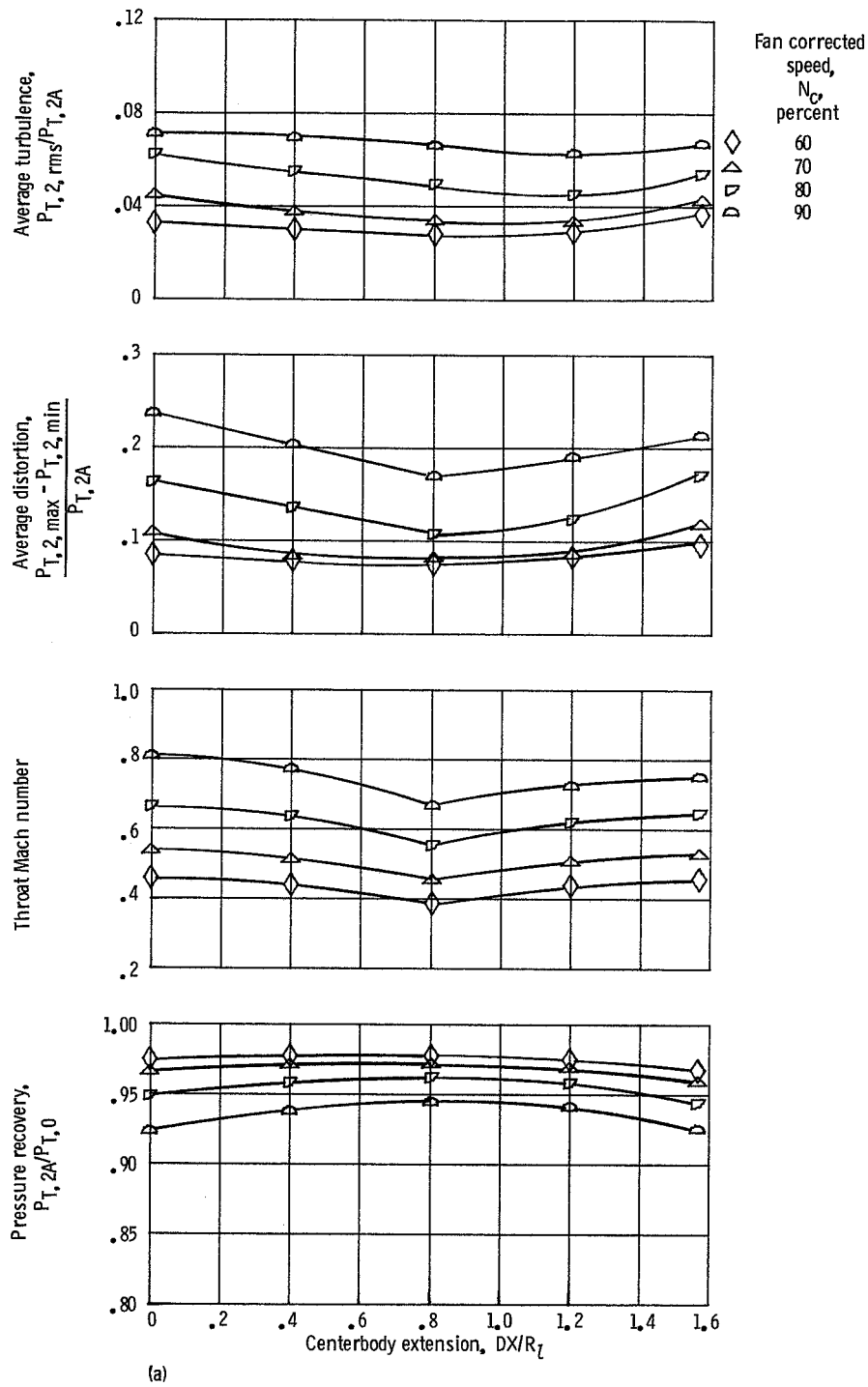
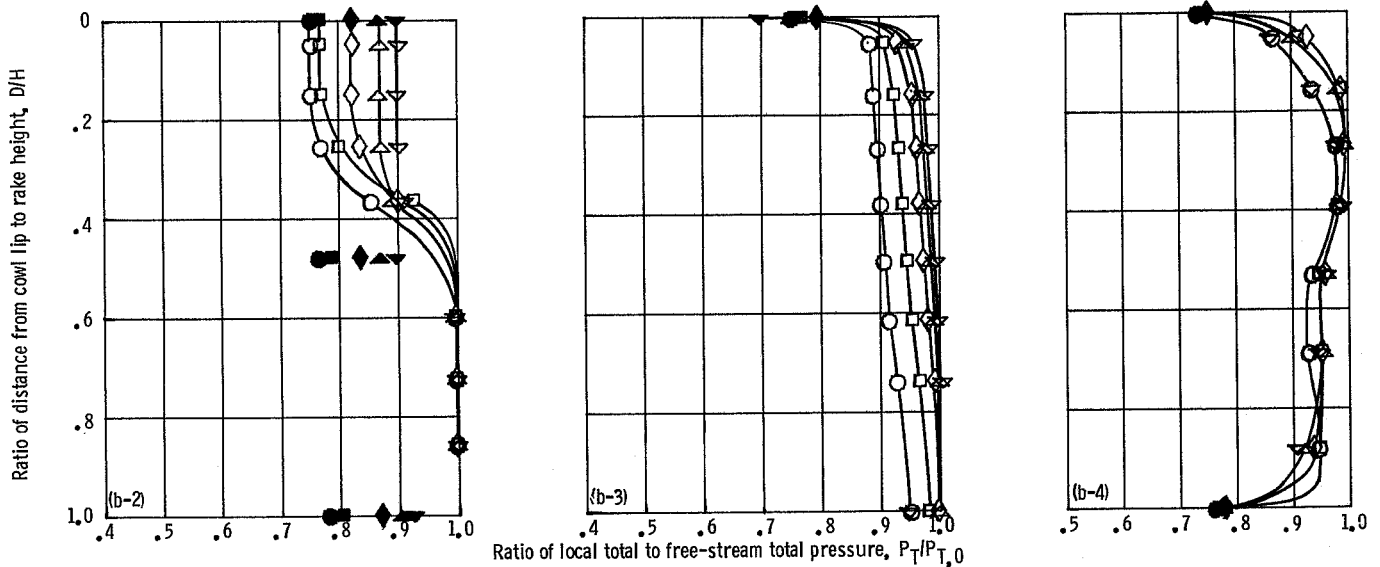
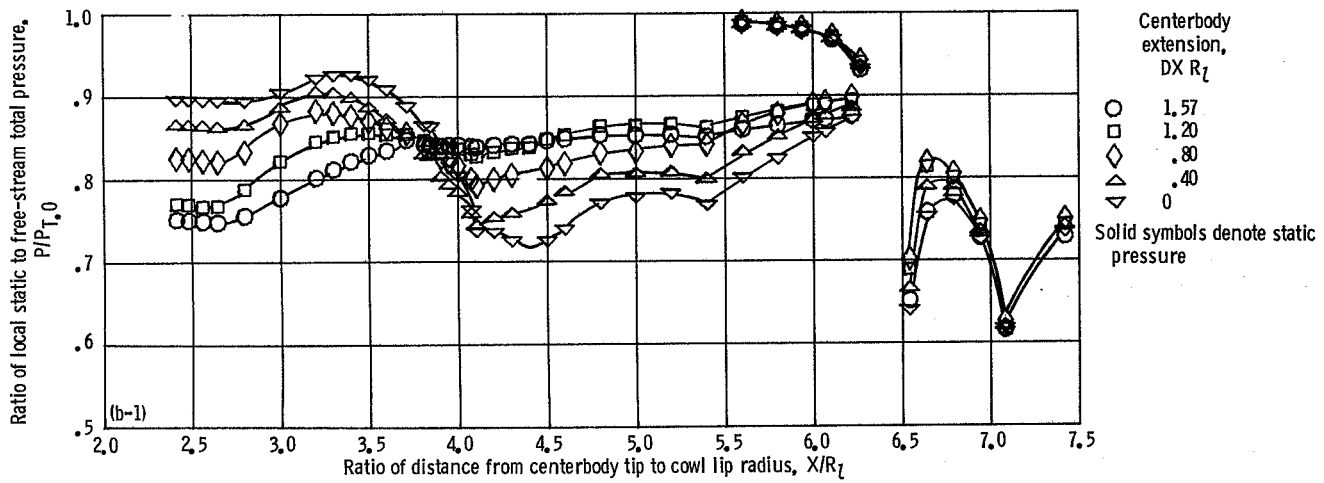


Figure 26. —Effect of bleed inflow on inlet peak recovery performance with sharp cowl lip, 20-percent auxiliary doors open, and  $M_0=0.2$ .



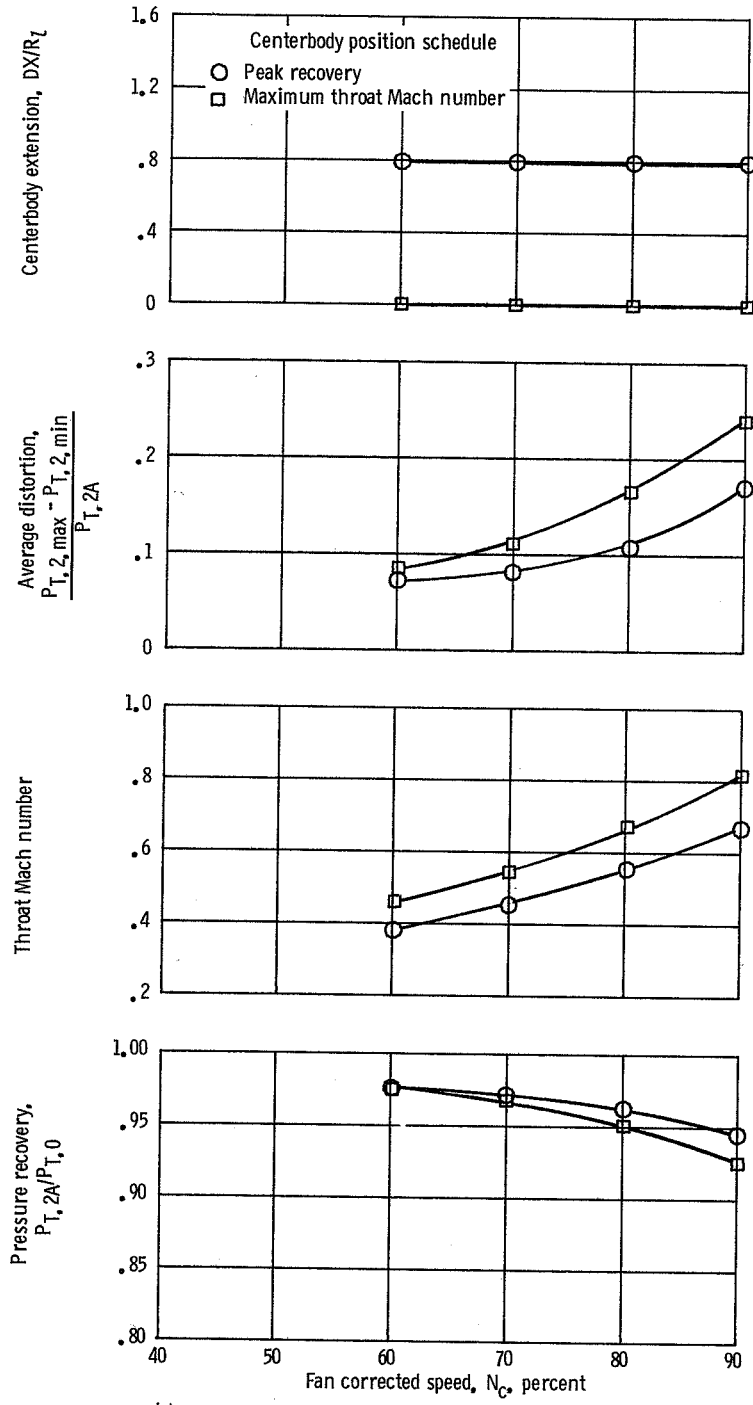
(a) Aerodynamic performance.

Figure 27. -Inlet performance with sharp cowl lip, 40-percent auxiliary doors open,  $M_0=0$ , and bleeds closed.



(b-1) Cowl surface.  
 (b-2) Lip rake ( $X/R_l=2.63$ ).  
 (b-3) Throat rake ( $X/R_l=4.30$ ).  
 (b-4) Compressor face rake ( $X/R_l=7.42$ ).  
 (b) Inlet pressure distributions. Fan speed, 80 percent.

Figure 27. -Continued.



(c)

(c) Performance maps.  
Figure 27.—Concluded.

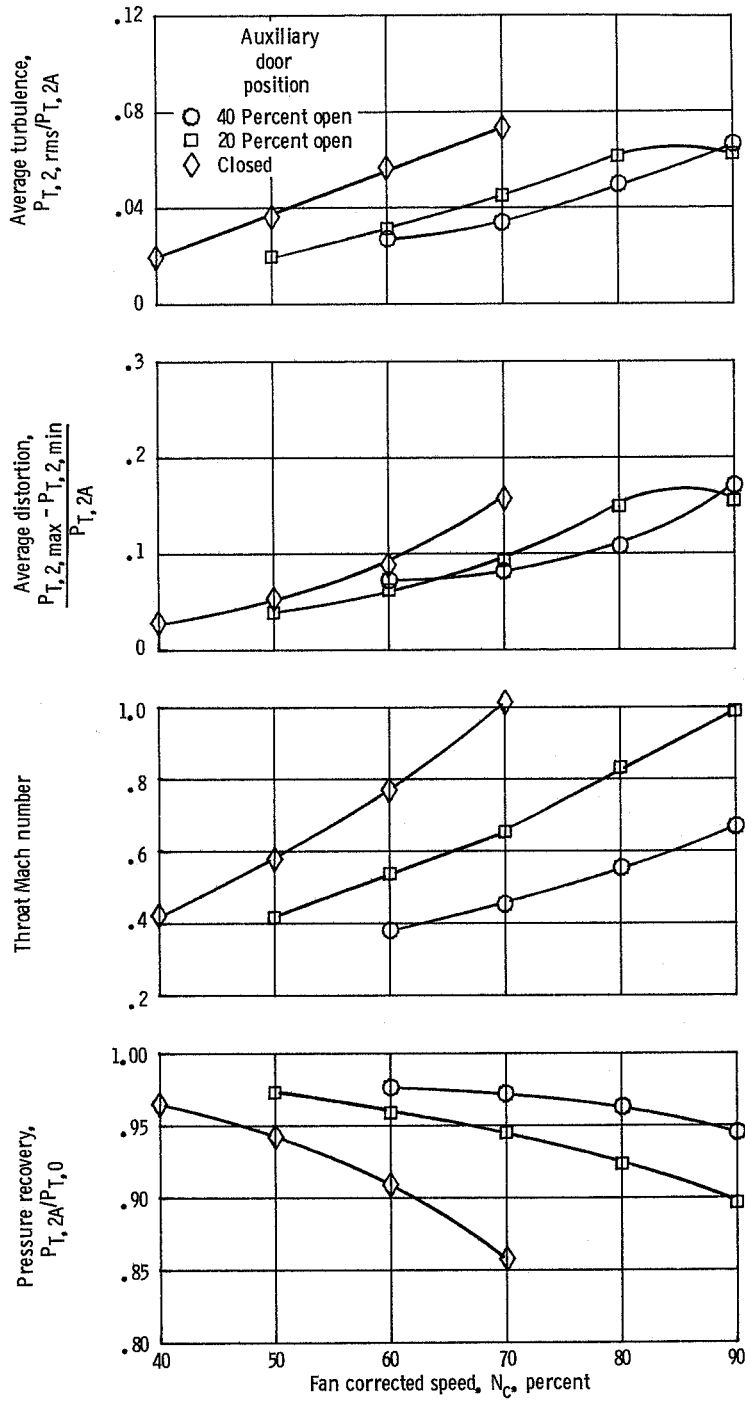
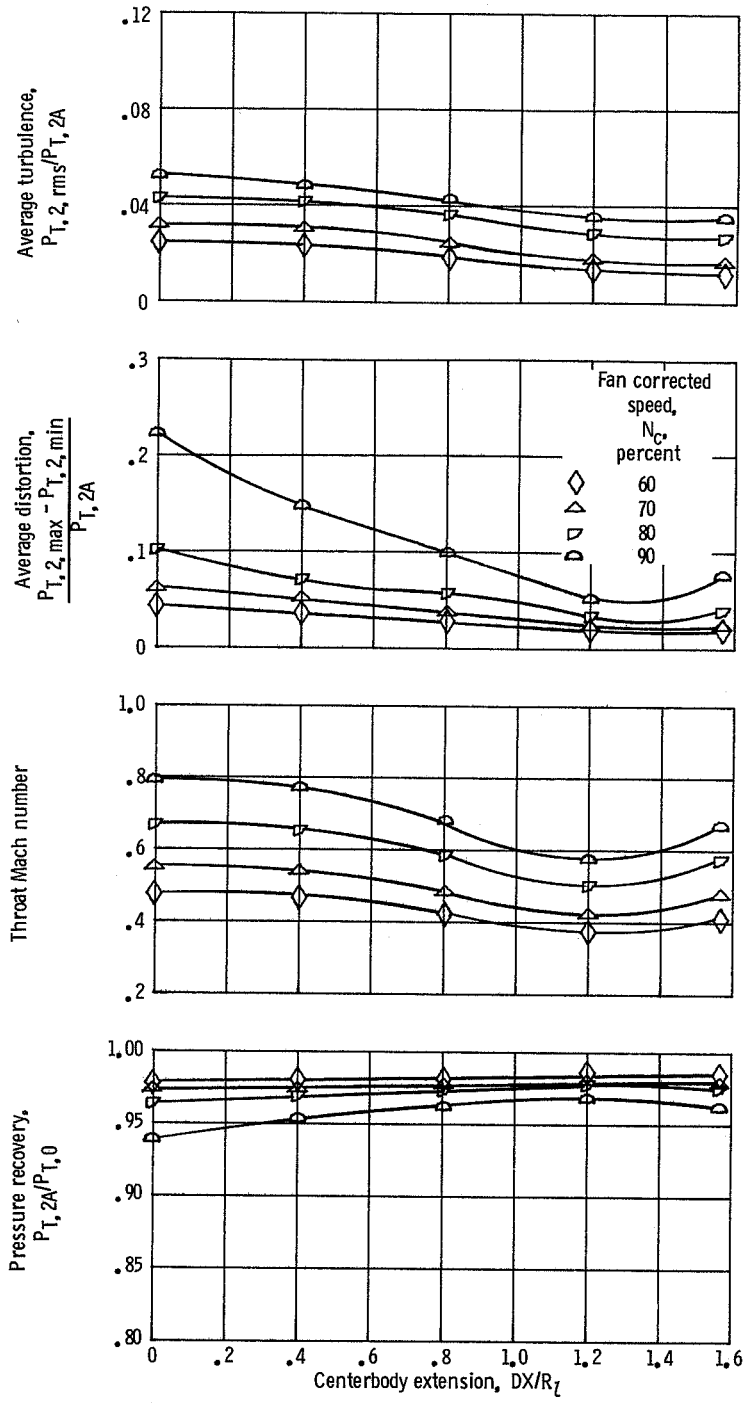


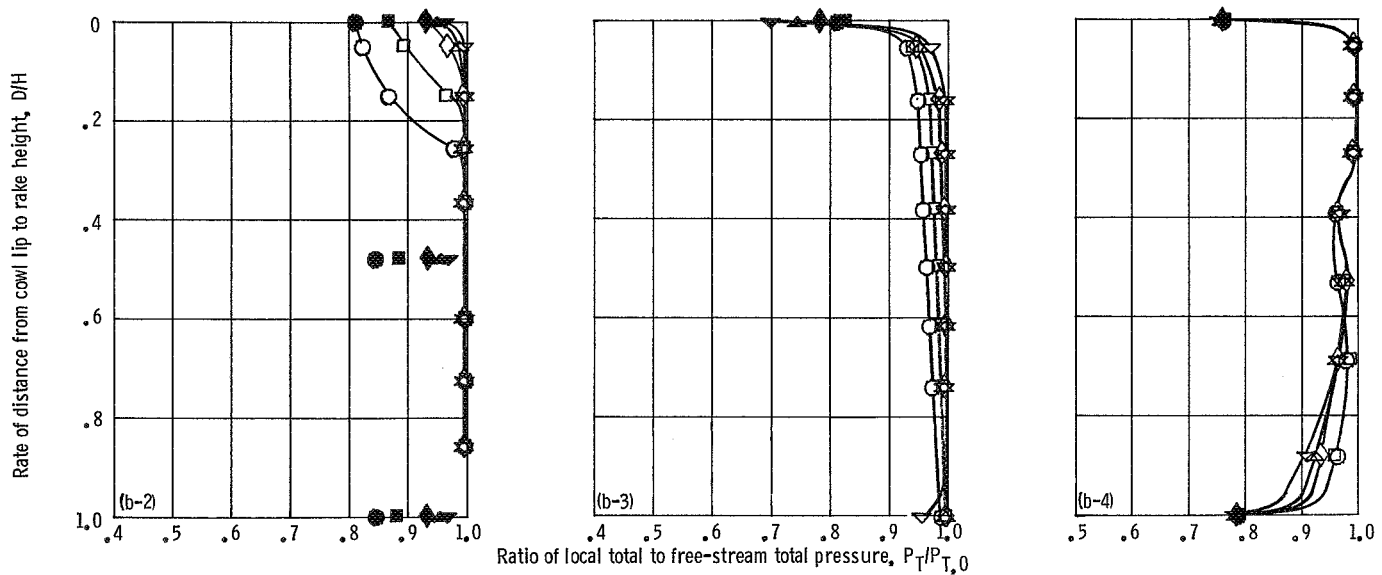
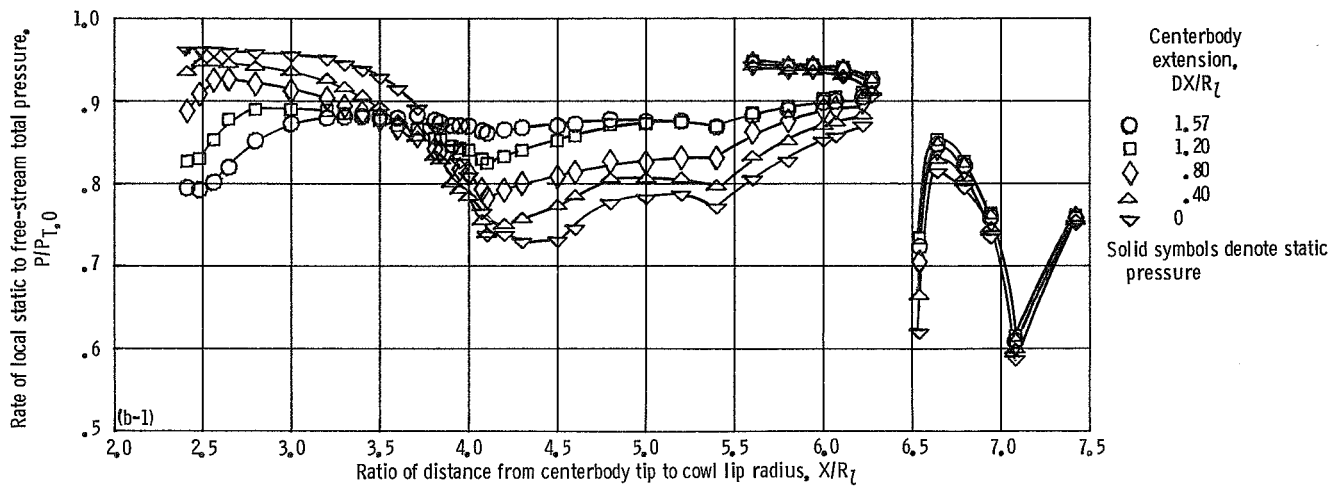
Figure 28. —Effect of auxiliary flow on inlet peak recovery performance with sharp cowl lip,  $M_0=0$ , and bleeds closed.



(a)

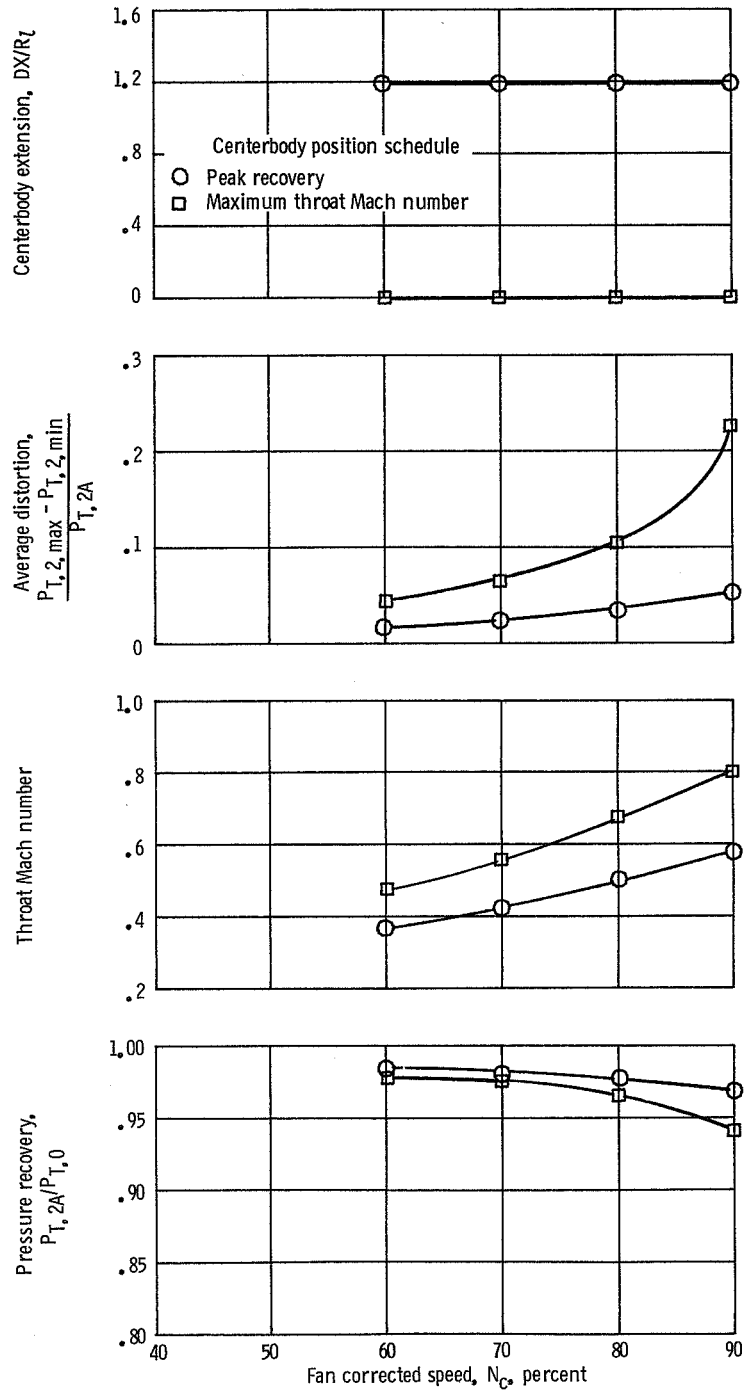
(a) Aerodynamic performance.

Figure 29. -Inlet performance with sharp cowl lip, 40-percent auxiliary doors open,  $M_0=0.2$ , and bleeds closed.



(b-1) Cowl surface.  
 (b-2) Lip rake ( $X/R_l=2.63$ ).  
 (b-3) Throat rake ( $X/R_l=4.30$ ).  
 (b-4) Compressor face rake ( $X/R_l=7.42$ ).  
 (b) Inlet pressure distributions. Fan speed, 80 percent.

Figure 29. — Continued.



(c)

(c) Performance maps.

Figure 29. - Concluded.

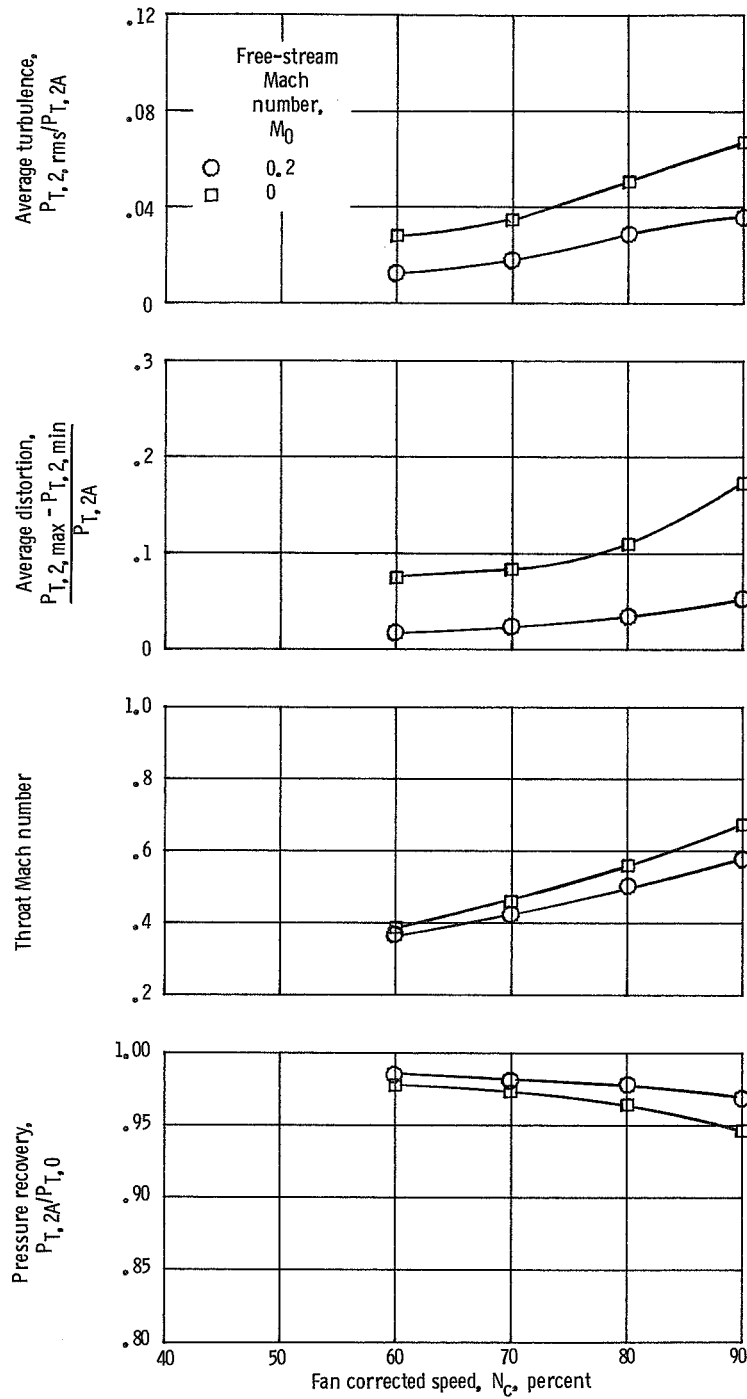


Figure 30. —Effect of free-stream Mach number on inlet peak recovery performance with sharp cowl lip, 40-percent auxiliary doors open, and bleeds closed.

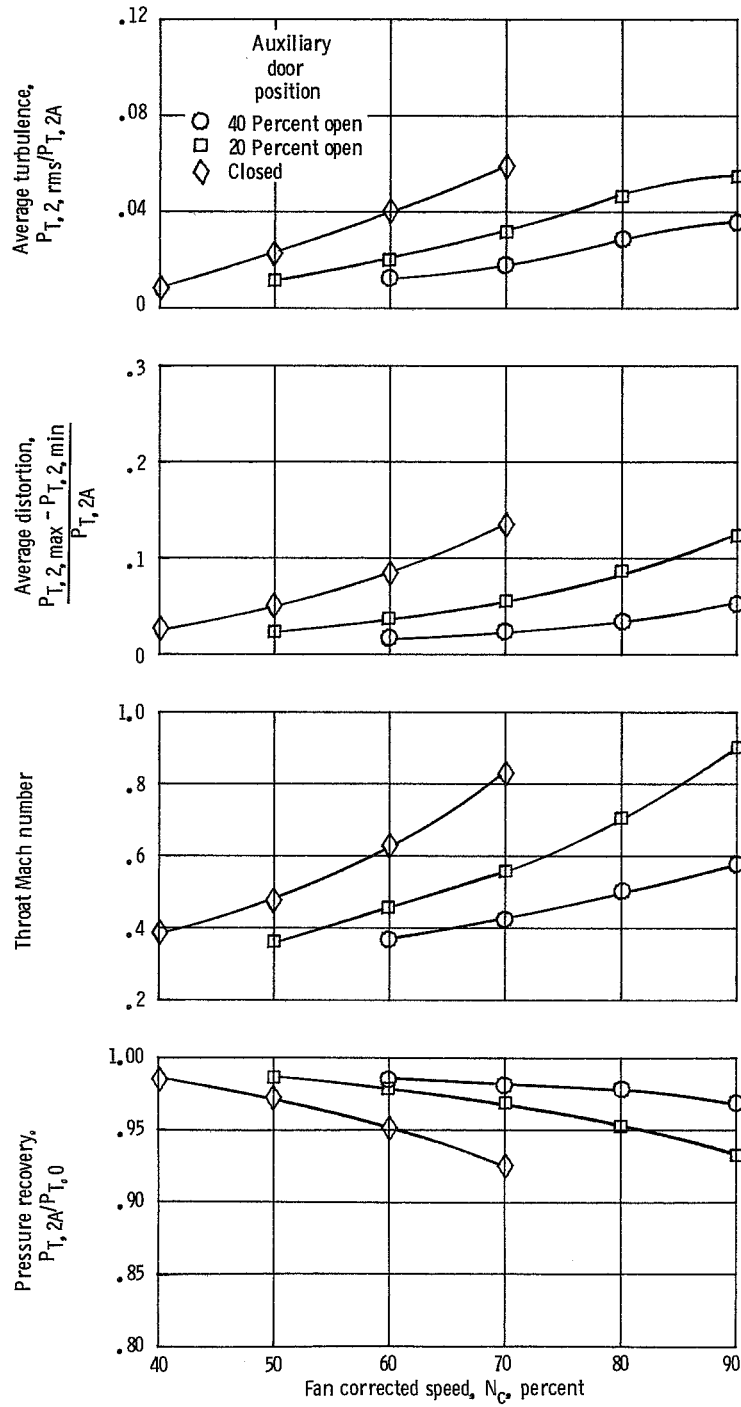


Figure 31.--Effect of auxiliary flow on inlet peak recovery performance with sharp cowl lip,  $M_0=0.2$ , and bleeds closed.

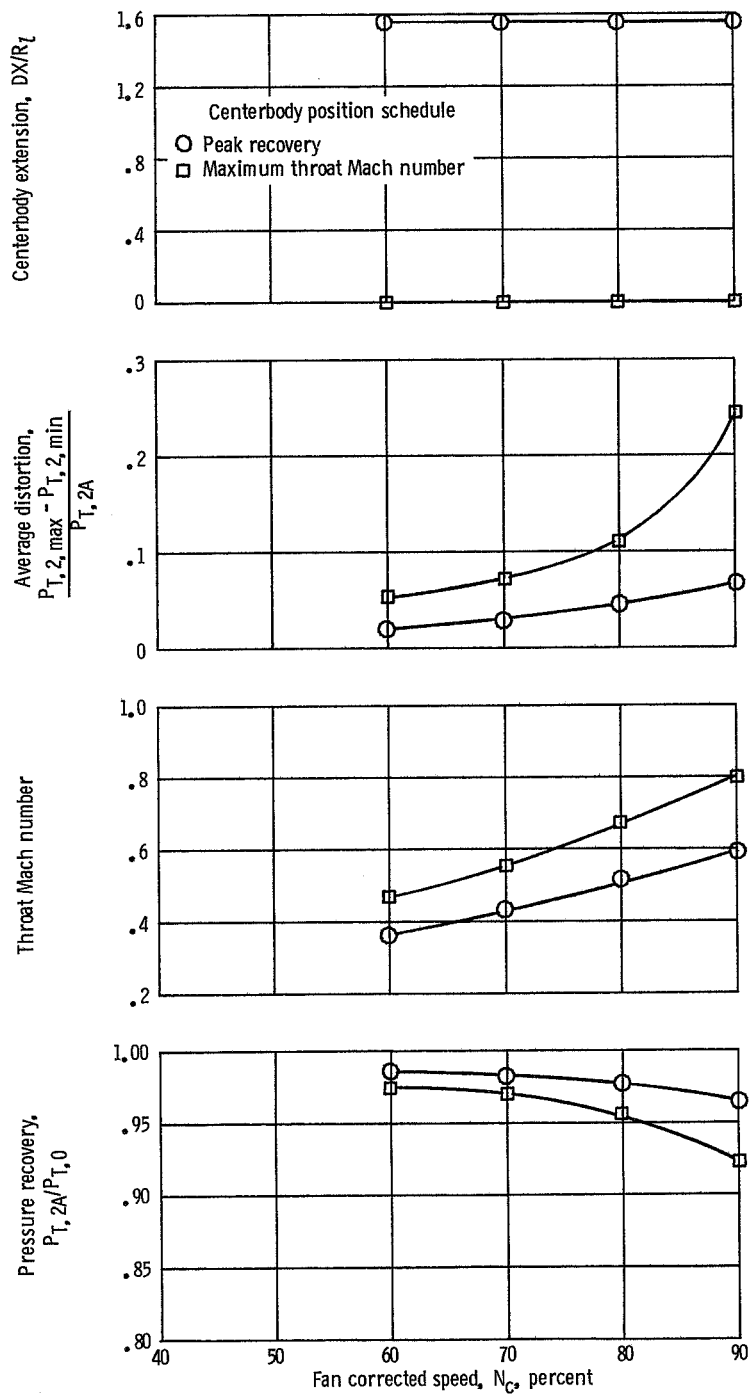


Figure 32. — Inlet performance maps with sharp cowl lip, 40-percent auxiliary doors open,  $M_0=0.2$ , and bleeds open.

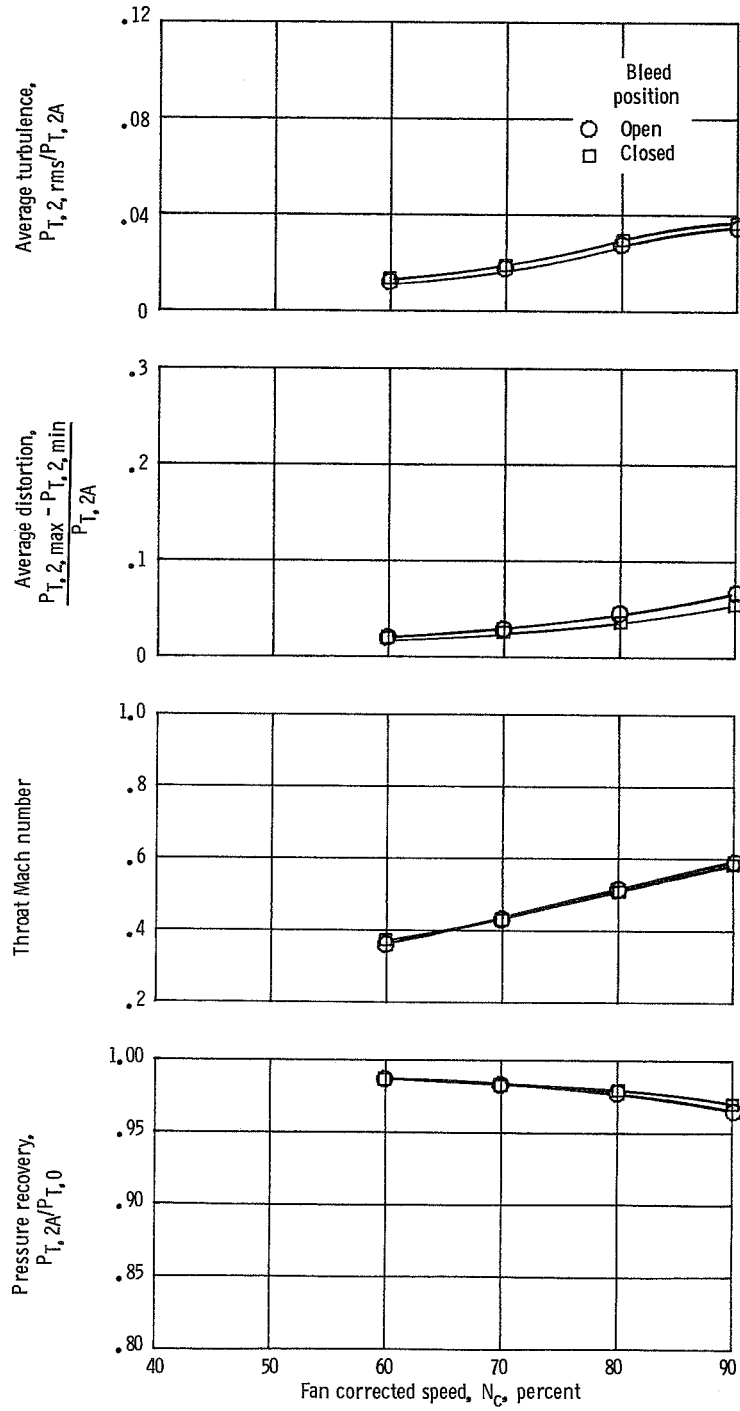


Figure 33.—Effect of bleed inflow on inlet peak recovery performance with sharp cowl lip, 40-percent auxiliary doors open, and  $M_0=0.2$ .



1. Report No. NASA TP-2557		2. Government Accession No.		3. Recipient's Catalog No.	
4. Title and Subtitle  Low-Speed Performance of an Axisymmetric, Mixed-Compression, Supersonic Inlet With Auxiliary Inlets				5. Report Date February 1986	
				6. Performing Organization Code 505-43-52	
7. Author(s) Charles J. Trefny and Joseph W. Wasserbauer				8. Performing Organization Report No. E-2771	
				10. Work Unit No.	
9. Performing Organization Name and Address National Aeronautics and Space Administration Lewis Research Center Cleveland, Ohio 44135				11. Contract or Grant No.	
				13. Type of Report and Period Covered Technical Paper	
12. Sponsoring Agency Name and Address National Aeronautics and Space Administration Washington, D.C. 20546				14. Sponsoring Agency Code	
15. Supplementary Notes					
16. Abstract  A test program was conducted to determine the aerodynamic performance and acoustic characteristics associated with the low-speed operation of a supersonic, axisymmetric, mixed-compression inlet with auxiliary inlets. Auxiliary inlets with areas of 20 and 40 percent of the inlet capture area were tested at free-stream Mach numbers of 0, 0.1, and 0.2. The effects of boundary layer bleed inflow were investigated. A JT8D fan simulator driven by compressed air was used to pump inlet flow. Aerodynamic results are presented for all inlet operating conditions ranging from peak inlet recovery to performance at choked or high throat Mach number conditions. Auxiliary inlets increased overall total pressure recovery of the order of 10 percent. At ratios of cowl lip to free-stream velocity of about 1.6 or less, losses from sharp-lip flow separation were negligible at the compressor face. Losses from boundary layer bleed inflow were insignificant when either the 20- or 40-percent auxiliary inlets were open. Aerodynamic performance was compromised significantly by the high throat Mach numbers required for fan noise attenuation.					
17. Key Words (Suggested by Author(s)) Inlet Supersonic inlet Propulsion				18. Distribution Statement Unclassified - unlimited STAR Category 07	
19. Security Classif. (of this report) Unclassified		20. Security Classif. (of this page) Unclassified		21. No. of pages 62	22. Price A04

**National Aeronautics and  
Space Administration  
Code NIT-4**

**Washington, D.C.  
20546-0001**

Official Business  
Penalty for Private Use, \$300

**BULK RATE  
POSTAGE & FEES PAID  
NASA  
Permit No. G-27**

**NASA**

**POSTMASTER: If Undeliverable (Section 158  
Postal Manual) Do Not Return**

---